THE UNIVERSITY
of EDINBURGH

VARIABLE CAPTURE LEVELS OF CARBON DIOXIDE FROM NATURAL GAS COMBINED CYCLE POWER PLANT WITH INTEGRATED POST-COMBUSTION CAPTURE IN LOW CARBON ELECTRICITY MARKETS

Olivia Errey

THE UNIVERSITY *of* EDINBURGH

Thesis submitted for the degree of

Doctor of Philosophy

The University of Edinburgh

School of Engineering

Year of Submission 2017

Abstract

This work considers the value of flexible power provision from natural gas-fired combined cycle (NGCC) power plants operating post-combustion carbon dioxide (CO_2) capture in low carbon electricity markets. Specifically, the work assesses the value of the flexibility gained by varying CO_2 capture levels, thus the specific energy penalty of capture and the resultant power plant net electricity export. The potential value of this flexible operation is quantified under different electricity market scenarios, given the corresponding variations in electricity export and CO_2 emissions.

A quantified assessment of natural gas-fired power plant integrated with amine-based post-combustion capture and compression is attempted through the development of an Aspen Plus simulation. To enable evaluation of flexible operation, the simulation was developed with the facility to model off-design behaviour in the steam cycle, amine capture unit and CO_2 compression train. The simulation is ultimately used to determine relationships between CO_2 capture level and the total specific electricity output penalty (EOP) of capture for different plant configurations. Based on this relationship, a novel methodology for maximising net plant income by optimising the operating capture level is proposed and evaluated. This methodology provides an optimisation approach for power plant operators given electricity market stimuli, namely electricity prices, fuel prices, and carbon reduction incentives.

The techno-economic implications of capture level optimisation are considered in three different low carbon electricity market case studies; 1) a CO_2 price operating in parallel to wholesale electricity selling prices, 2) a proportional subsidy for low carbon electricity considered to be the fraction of plant electrical output equal to the capture level, and 3) a subsidy for low carbon electricity based upon a counterfactual for net plant CO_2 emissions (similar to typical approaches for implementing an Emissions Performance Standard). The incentives for variable capture levels are assessed in each market study, with the value of optimum capture level operation quantified for both plant operators and to the wider electricity market. All market case studies indicate that variable capture is likely to increase plant revenue throughout the range of market prices considered. Different market approaches, however, lead to different valuation of flexible power provision and therefore different operating outcomes.

Declaration of originality

The composition of this thesis and the work it contains result from my own efforts. Contributing information from published work and interaction with research colleagues have been made explicit through references in the text or the acknowledgements preceding the thesis. This work has not been submitted for any other degree or professional qualification.

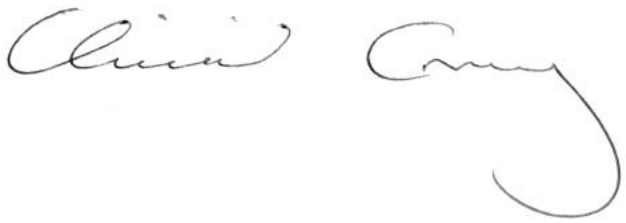

Olivia Errey

October 2018

Acknowledgements

Firstly, I acknowledge the input of my supervision team into the work on which this thesis is based. I have benefitted greatly from conversations with Professor Jon Gibbins, which have given me insight into both the technical and political nature of this research topic. Many of the economic concepts proposed in this thesis stemmed from these conversations. Support and guidance from Mathieu Lucquiaud has been invaluable to me, having come to the field of engineering later in life I had a lot to catch up on and I benefitted greatly from both his technical knowledge and his patience in imparting it. The methodologies for optimising capture levels developed in this thesis originated from his work. Finally, I acknowledge the supervision of Hannah Chalmers who has provided consistent and sensitive support throughout my studentship. I have benefitted greatly from her organized approach and flexibility, as well as her technical guidance. Her prior work on the techno-economics of flexible CCS also informed many concepts presented in this thesis.

I also gratefully acknowledge the support I have received from many internal and external colleagues, in particular Eva Sanchez and Maria Sanchez del Rio Saez who contributed to the Aspen model developed in this work. I would like to thank my colleagues in Edinburgh Bill Buschle, Nacho Trabadela, Laura Herraiz, Alasdair Bruce, Abigail Gonzalez, Paul Tait, Roger Watson, Juan Riaza, also Vivian Scott, Stuart Gilfillan and Mark Naylor.

I am also grateful for my interactions many people working in the commercial industrial sector, in particular I would like to thank David Fitzgerald, Scott Hume and Jeremy Carey for their input during time spent at the Ferrybridge CCPilot plant, and Christina Kandziora and Alexis Alekseev from Linde gas.

I am indebted to the support of my family. This thesis would not exist without them.

Contents

List of tables

List of figures

1 Introduction

1.1 Outline of the problem

Fossil fuel combustion is the dominant source of global energy, historically, currently and also in near term projections (International Energy Agency 2017). Combustion of hydrocarbon fossil fuels produces CO_2 dilute as a waste gas, which has traditionally been released directly into the atmosphere. Atmospheric CO_2 has a greenhouse gas effect, and the accumulation of CO_2 released by unabated fossil fuel combustion implies a high probability of climate and eco-system changes, with uncertain and difficult to control outcomes and an “increasing likelihood of severe, pervasive and irreversible impacts for people and ecosystems” (IPCC 2014).

Global energy demand is set to rise (International Energy Agency 2017). Electricity accounts for almost a fifth of total energy demand, and this proportion is projected to accelerate dramatically in the coming decades due to increased electrification of energy systems (International Energy Agency 2017). There must, therefore, be a shift towards alternative technologies that are able to decouple electricity generation and CO_2 emissions in order that this energy demand will be met without increased atmospheric accumulation of CO_2.

The most developed low CO_2 electricity generation technologies include nuclear power generation and renewable energy options, such as wind, solar, hydro, wave and tidal power. However, these technology types are limited in their ability to offer responsive and flexible electricity generation in the way that fossil fuel plant has traditionally provided. This limitation creates a challenge for electricity system operators tasked with balancing real time demand variations in electricity networks, as electricity must be delivered at the same rate and frequency as it is used. Where periods of high electricity demand do not correspond with windy or sunny weather, for example, alternative electricity sources must be available. There is, therefore, an additional requirement for cost-effective solutions for flexible electricity export with low atmospheric CO_2 emissions.

In this thesis, flexible operation refers to deliberate and controlled changes to the electrical power output of individual plant. Variation of fuel type, switching across a portfolio of technologies or other concepts of operating ‘flexibility’ are excluded from the definition used in this work.

1.2 Outline of the solution

Power generation with carbon capture and storage (CCS) is a further energy technology option that can provide electricity with low atmospheric CO_2 emissions. CCS utilises energy available in fossil fuels or biomass, but the CO_2 stream from their combustion is captured rather than released directly to the atmosphere. The separated CO_2 stream can be stored, or sequestered, in deep geological formations or other inert forms.

CCS can theoretically generate electricity with comparable levels of flexibility to unabated thermal power plant (IEAGHG 2012a). However, CCS applied to large scale power generation is, at the time of writing, a technology in development yet to be commercially operated at scale in real electricity systems. Therefore, this thesis explores technical and economic potential of flexible operation of CCS in low carbon electricity markets, specifically applied to natural gas-fired power generation.

While CCS can be applied to the full range of hydrocarbon fuels, this work focusses on its application to natural-gas fired power generation for the following reasons: In mid-term future energy scenarios, natural gas-fired power generation is projected to be a key power generation technology with continued use and roll-out (International Energy Agency 2017). Natural gas-fired power plant is often used as a flexible generator of choice in current electricity systems, because of technical abilities for rapid response and the economic characteristics of a lower capital to operating cost ratio. As even modern, efficient, gas-fired power plant have CO_2 intensities significantly higher than the power generation average required to limit global warming to 2°C (IPCC 2014), CCS will be necessary if the projected capacity volumes are rolled out. As such, the application of CCS to natural gas power plant is pertinent when considering CCS as an option for flexible electricity generation.

Technologies for capturing CO_2 from fossil power generation can be described in three categories of processes: Post combustion capture, pre-combustion capture and oxyfuel combustion. These processes, in addition to CO_2 capture from other industrial CO_2 sources, are illustrated in Figure 1-1.

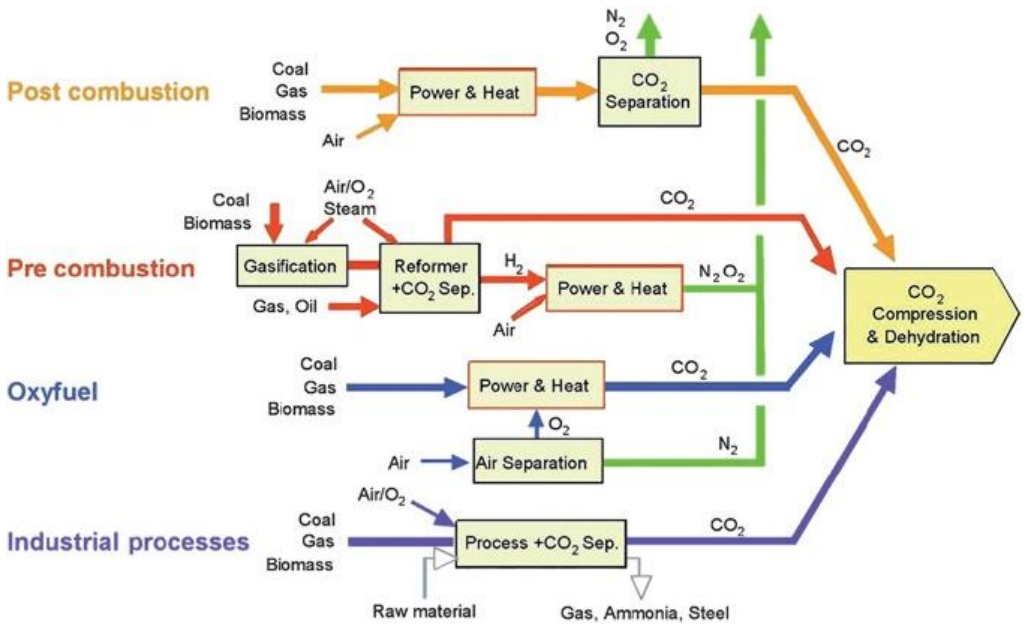

Figure 1-1 Overview of CO_2 capture processes and systems (IPCC 2005)

This thesis considers the techno-economics of flexible operation of natural-gas combined cycle power plant operating with post-combustion CO_2 capture. Specifically, the potential for flexible operation of the capture plant is considered. Variations in the amount of CO_2 captured will correspond to changes in the parasitic energy load associated with capturing and compressing CO_2 under given operating conditions. Subsequently, net plant electricity export can be varied, although relative atmospheric CO_2 emissions will also vary accordingly.

In this work, the relationship between the proportion of CO_2 captured and compressed by the capture plant (the capture level) and the net plant electricity output is determined, through an integrated model of a natural gas-fired combined cycle power plant operating amine-based CO_2 capture. The potential for varying the capture level is ascertained, a methodology for optimized operation is proposed and the value of this operation in a range of low carbon electricity market case studies is examined.

1.3 Novel contributions of this thesis

1. A standard MEA based post-combustion CO_2 capture unit operating with a combined cycle natural gas-fired power plant is described and simulated in Aspen plus. Off-design operation is simulated in all units of the integrated plant, including

the steam cycle, capture unit and compression train, to represent performance under flexible operation.

2. A simulated performance curve, indicating continuous variations in electricity output penalties with capture level in an integrated NGCC power plant operating post-combustion capture (PCC), is presented. This provides indicative relationships between power exported and CO_2 flows either emitted or captured.
3. A methodology for optimal operation of CO_2 capture plant with respect to capture level is described, offering the dual benefit of maximizing plant revenue for the operators and providing additional relatively low-cost grid capacity at times of high demand.
4. Different types of future low carbon electricity markets in which CCS may operate, in addition to a basic price of carbon for CO_2 emissions, are identified and described. Specifically, scenarios where zero-carbon electricity is eligible for a premium tariff, and where the system is constrained by an Emission Limit Value (ELV) are considered. The potential revenues from flexible operation of CO_2 capture plant under each indicative case study are quantified and discussed.
5. Decision diagrams are presented for the range of market scenarios described above. These diagrams enable visual evaluation of optimum operation and can provide information for use by plant operators who can act accordingly to maximize plant revenue in response to market price signals. Dispatch models can also make use of this method to predict the market value of flexible operation, which, when considered with projected lifecycle costs, can provide a clearer picture to investors and policy makers.

1.4 Outline of the thesis

Chapter 2 introduces electricity systems with respect to system balancing. It details the requirement for flexible low CO_2 intensity power generation in future low carbon electricity systems and reviews the current literature on the potential for CCS plant to provide this flexibility.

Chapter 3 reviews the role of natural gas power plant in electricity systems, both currently and under future low carbon constraints. It further provides a technical literature review of the application of post-combustion CO_2 capture to natural gas-fired combined cycle power plant.

Chapter 4 describes the process of CO_2 capture level variation to provide flexible power output from CCS power plant. It goes on to present a methodology for maximizing short run cash flow by optimising capture level operation in response to market signals. Three different low carbon market case studies are defined and considered in the optimisation analysis.

Chapter 5 presents a process model of a natural gas-fired combined cycle power plant integrated with post-combustion capture. The model can simulate off-design conditions to describe changes in plant performance and electricity export with CO_2 capture level. The detailed modelling methodology is described, and simulation results are presented resulting in a relationship describing the variation in specific Electricity Output Penalty of capture with changes in CO_2 capture level.

Chapter 6 presents sets of decision diagrams that illustrate the methodology for optimal capture plant operation for the three low carbon market case studies described in Chapter 4, applying the results of Chapter 5 to ascertain the relationship between plant net electrical output and the proportion of CO_2 captured. This chapter includes analysis of the relative value of the optimal capture level operating decisions. Finally, the implications for optimal flexible operation are discussed for each low carbon market case study.

Chapter 7 concludes with a summary of the findings of this thesis, a discussion of the limitations and recommended areas for future work.

2 Low carbon electricity systems and the value of flexible CO_2 capture

This chapter introduces conventional electricity systems, describing requirements for flexible power provision and outlining relevant financial mechanisms. The chapter goes on to describe options for limiting CO_2 emissions in future low carbon electricity systems, and to discuss the impacts of these options in terms of changes in supply and demand patterns. The chapter clarifies the need for flexible and controllable power provision when operating under low carbon constraints. This work proposes flexible operation of CO_2 capture and storage (CCS) as a potential provider of responsive power in such low carbon electricity systems. The potential of CCS is explored, the technical feasibility and the prospective value of both the generation unit operator and the system operator. This chapter concludes with a critical review of the relevant current literature covering techno-economic aspects of operating power plant flexibility with CO_2 capture, and an outline of the gaps which will be filled by this thesis.

2.1 Electricity systems and the significance of system balance

Given that electricity is a flow of energy, provision for its demand must be met in real time; that is, energy must be converted to electricity at the same rate as it is used. To do this, electricity systems need to enable synchronized generation and provision of electricity, through generators (sources of electrical energy) connected to loads (sinks of electrical energy) by transmission and distribution networks. These networks are managed by System Operators (SOs), with the aim of reliably providing consumers with electricity upon demand, in a safe and economically efficient manner.

Since system synchronicity is essential to reliable electricity provision, SOs must ensure that the generation-provision system remains in balance. They do so by securing appropriate power flows, voltages and phase angles to meet the network specific demand on a second by second basis, maintaining network frequency within strict limits. This is crucial, since any large frequency deviation resulting from mismatched supply and demand may lead to extensive equipment damage on generators or loads designed for a specific frequency. In extreme cases this may lead to network blackouts, and even short outages can be extremely costly. One UK study

of such deviations, for example, estimated losses of up to 10 million pounds per hour long outage across the economy (Walker et al., 2014). Modern economies are highly dependent on a reliable electricity supply and so system balancing is a service of significant importance, and thus, a service with significant value.

2.1.1 Unit commitment processes and the Short Run Marginal Cost of Electricity generation

Demand for electricity varies continually. Typically, it follows daily, weekly and seasonal patterns, with occasional exceptional peaks or drops in system demand. Normally, SOs manage this variability with a 'unit commitment process', where predictions of demand are balanced against projections of potential generator capacity and operability, in discrete time periods (typically 1 hour or 30-minute delivery intervals). To be considered in the electricity system, generation unit operators offer expected capacities over a specified future time-period, covering one or more delivery intervals. Generation operators can be contracted by SOs to commit to providing their expected capacities as a continuous output of electricity into the network. Alternatively, for network balancing purposes, both generation and load units can be contracted to provide rapidly varying output or consumption of electricity within a given delivery interval, or to be on stand-by to provide the network with reserve generation capacity or load reduction at short notice. These latter contracts are known as balancing, or ancillary services.

Unit commitment processes are designed to contract power generation to meet system demand at the lowest feasible cost, through the selective purchase of electricity at the lowest available price. The price of electricity from any one generation unit is related to the unit's marginal cost of electricity provision, defined as "the cost of producing an additional unit of output" (Della Valle 1988). The marginal cost of electricity includes fuel, other variable operating and maintenance (O&M) costs, and any specific emission penalties payable, such as a carbon price. However, this cost does not include fixed costs, such as repayment of capital, which would require payment whether the unit generates electricity or not.

The 'Short Run Marginal Cost' (SRMC) is the marginal cost of electricity provision within the capacity of an existing unit, excluding long term consideration of future electricity demand or generation portfolios. SRMC is typically used as an accepted

basis for efficient pricing in conventional electricity systems[1] (Della Valle 1988). SRMC metrics assume that an existing generation unit has already been financed and built, and therefore that generating and selling electricity at anything above the marginal cost will provide the unit with positive income, even if revenue gained in that time-period does not contribute significantly to fixed or capital costs. This pricing convention relies on the assumption that there will be times when a plant operator exports electricity at prices higher than the SRMC to cover fixed costs.

2.1.2 System merit order

Disparities in SRMC across generation types lead to a system 'merit order': technologies with the lowest marginal costs operate near continuously whereas generation options with higher marginal costs operate only when prices increase. When an electricity system is running efficiently, generation units offering a lower selling price will normally be contracted to operate more often than generation units offering electricity at higher prices. Figure 2-1 provides an illustrative representation of a unit commitment process merit order in a conventional electricity system (conventional in the sense that there are negligible economic incentives for CO_2 emission reductions).

The market price is set by the last unit to be dispatched to meet demand, known as the marginal generator or 'price setter'. All electricity exported to the grid during each delivery period is then sold at this market clearing price. The electricity selling price (y-axis Figure 2-1) is indicative of the SRMC behind the respective marginal generator. As a general trend, in accordance with Green (2008), and Barton & Infield (2004), when demand is low, the wholesale electricity market price is approximately equal to the SRMC of the marginal generator. As demand increases and larger proportions of the network capacity are utilized, wholesale prices are set at a small increment above the marginal generator SRMC. Finally, when demand is close to the maximum system capacity, the introduction of 'peaking plant' will normally lead to an exponential rise in wholesale prices several times higher than their SRMC. This is primarily because the fewer cumulative hours a plant operates, the less opportunity

[1] Electricity systems can be state owned operations or liberalised markets, partially or fully. This work assumes a liberalised market (referring to terms such as contract bidding and market prices). However, as all electricity systems require coordination and use mechanisms for maximising system efficiency that are not dissimilar from the market mechanisms referred to in this work (Stern 2014), the concepts presented in the following chapters are not exclusive to liberalised market systems.

there is to generate income to finance the capital and fixed costs of the plant. The implication is that if marginal peaking plant with the highest SRMC electricity is sold close to its marginal cost, and no units enter the market at a higher price, the unit would never be able to accrue revenue to finance capital. In this way, electricity prices become disproportionately high at times of high demand/supply ratio.

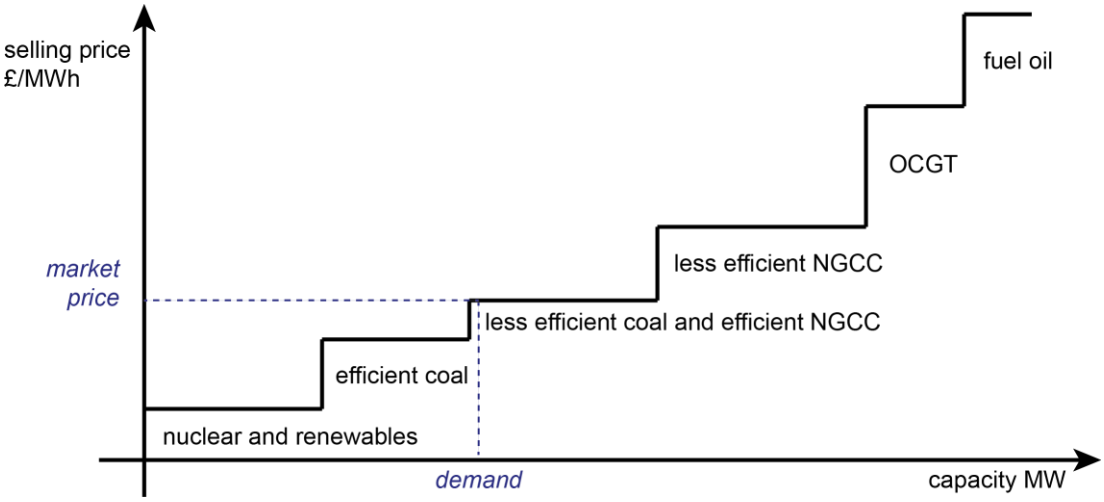

Figure 2-1 Illustrative representation of a unit commitment process merit order in a conventional electricity system

For the purposes of this work, when wholesale electricity prices reach the SRMC of the generating unit (a natural gas plant operating with CO_2 capture), it will be an assumed condition for electricity market entry or exit (i.e. generation plant turn on or off). In other words, the plant will operate as a 'price taker' rather than a 'price maker'. Price takers will accept the market price of electricity, and as such do not influence the wholesale clearing price. The price of electricity at which a price-taker will enter the market will therefore be theoretically equal to the unit SRMC, as higher bidding would increase the likelihood of being undercut, while lower bidding would lead to net revenue losses. In conventional systems, most medium capacity, mid-merit generation units operate as price takers, since there are sufficient similar technology units to provide market competition (Kirschen et al. 2011; Yucekaya 2013). In real world markets there are exceptions to this; for instance, long term bilateral contracts, or distortions from the cost of stopping and starting generation might mean that some units could continue to operate, even if the market price were to drop below the unit SRMC. However, SRMC is an efficient metric for consideration of merit ordered unit

commitment processes, and as such is used as a representative mechanism for electricity market operation here.

Where a power plant can be controlled to respond to market price signals, either by ramping up power export capacity at times of high electricity price, varying output rapidly to provide premium priced ancillary services, or reducing SRMC at times of lower electricity price to enable entry to the market without experiencing negative income, power plant operators will be able to maximize cash flow. This thesis assesses options for natural gas plant operating with CO_2 capture in this light.

2.1.3 Timeframes and response times for electricity provision

To assess the feasibility of flexible operation of a power plant in electricity markets, it is necessary to understand the timeframes within which flexibility is valued.

Electricity markets operate across different timeframes to achieve second-by-second system synchronicity at the lowest price. Contracts for electricity provision can be made months or years in advance of the delivery period, although some non-zero cost provision may be made for amending contracts closer to the time of dispatch as changes in demand and operability arise. An electricity exchange auction then operates close to the delivery period (typically 24 hours before dispatch (IEAGHG & Alie 2008)) where remaining demand is met through short term contracts. In a liberalized energy market, this exists as an electricity spot market. The auction closes shortly (typically one hour) before the delivery period, at a cut-off point known as ‘gate closure’, after which balancing services can still be traded by units able to offer a rapid response. To ensure balancing services remain competitive in price, parallel ancillary services are typically procured in advance by the SO, to accommodate uncertainty in forecasts and to protect against unexpected incidents such as major equipment failure. This contracting process is represented in Figure 2-2. In this way, unit commitment processes ensure increased demand is met through the procurement of remaining available capacity at increasingly premium rates, thereby maintaining system balance.

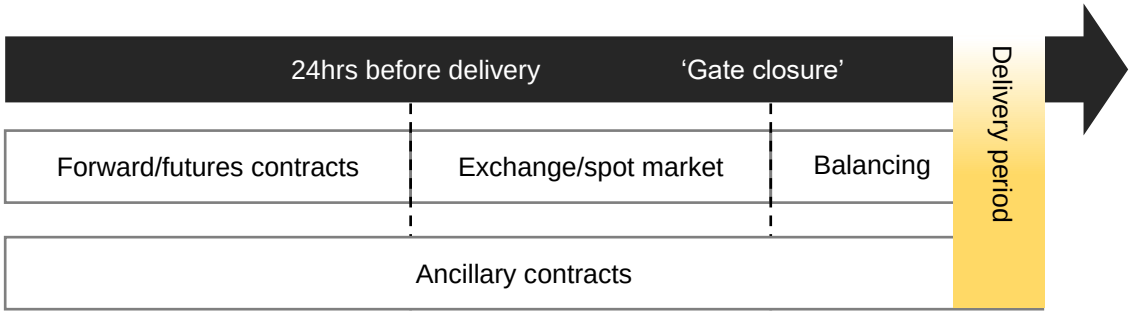

Figure 2-2 Electricity system contracting illustration, adapted from National Grid

Timing requirements for typical ancillary services in Great Britain, Spain and Germany are detailed in Table 2-1 to provide indicative examples of the response times necessary to access these markets.

Table 2-1 Technical requirements for generating units to provide ancillary services in GB, Germany and Spain. Adapted from *Montañés et al. (2016)*

Area	**Primary reserve**	**Secondary reserve**	**Tertiary reserve**
Great Britain	Activated in 10 sec. sustained for 20 sec.	Activated 2 min. after dispatch instruction. Delivery rate >25 MW/min. Sustained >15 min.	Max response <240 min, typically contract for <20 min. Sustained >120 min. Recovery period <1200 min. Deliver >3 times/week.
Germany	Activated within 30 sec.	Activated after 30 sec. Full response <5 min. Sustained 15 min.	Activated in 15 min. intervals. Complete activation <15 min. Sustained >15 min.
Spain	Load change of 1.5% of nominal (0<t<15 sec) Lineal from 15<t<30 sec.	Start ≤ 30 sec and full action in 15 min.	Maximum variation of power within 15 min. Sustained >2 h.

In summary, typical response times necessary for generators to profit from flexible operation are between 30 minutes and 1 hour for wholesale spot market access, and from 10-30 seconds for primary reserve ancillary services (such as frequency response), to between 30 seconds and 15 minutes for secondary reserve and 15 minutes to 2 hours for tertiary reserve services. It is worth noting that SOs also

typically offer holding payment (payment/MW) in addition to response payments (payment/MWh) for plant capable of providing certain ancillary services.

2.2 The economics of low carbon electricity systems

As described in Chapter 1, modern energy systems have the additional challenge of reducing cumulative CO_2 emissions, while continuing to maintain security of supply and cost effectiveness. These electricity systems are referred to as low carbon electricity systems.

2.2.1 Incorporated costs of CO_2 emissions

Low carbon electricity markets must account for the externality of CO_2 emissions. That is, without legislation explicitly limiting emissions, an additional value for CO_2 abatement must exist as an incentive to move away from unabated fossil fuel power plants that are economically favourable in current markets. This incentive could be realised through a carbon price where plant operators must pay a duty on every tonne of CO_2 released. In academic, industrial and political literature that considers economic options for low carbon electricity systems, carbon prices are the most commonly used metric for accounting for the CO_2 emissions from power generation. However, carbon markets have so far proven to be politically difficult to establish and maintain. For example, a carbon price introduced in Australia in 2012 was repealed by the succeeding government administration in 2014 (Teeter & Sandberg 2016) and EU Emissions Trading System (ETS) established in 2006 to introduce an EU wide CO_2 market has seen prices significantly depressed due to a surplus of spare allowances, with CO_2 prices struggling to rise above 4 Euro/tonne at the end 2016[2]. Investment decisions based on unstable carbon markets are problematic, and instead alternative fiscal methods for incentivising low carbon electricity have been introduced by many governments. Alternative incentives include subsidies paid per unit of low carbon electricity generated, for example the Renewable Obligation Certificates issued by the UK Government (Ofgem, 2010), or fixed price contracts that guarantee an income specifically for low carbon generation, otherwise known as Feed-In-Tariffs, which are currently utilised in many countries around the world (Cory et al. 2009)

Carbon prices, which are essentially an embedded cost, are reflected in SRMC calculations and therefore merit order allocation and LCOE estimates. However,

[2] http://www.eea.europa.eu/data-and-maps/data/data-viewers/emissions-trading-viewer

subsidy payments are not well represented in this manner as they do not directly describe expenditure. Indeed, subsidies are often granted based on estimated generation costs, and in the event, this may become problematic if the subsidies do not adequately reflect the amount of CO_2 saved per subsidy payment. If this occurs, there is the risk that more monies might be paid out to one low carbon technology than to others. If such subsidies also do not reflect the requirement for flexible generation, the risk can be exacerbated in low carbon electricity systems, where flexible operation become more valuable.

2.2.2 The increased value of flexibility in electricity systems with intermittent renewables

Low carbon electricity systems that have a higher proportion of renewable power generation will depend on the availability of intermittent energy sources, such as wind or sunlight. Electricity generation from unabated fossil fuel power plant can be adjusted through regulating fuel input rates and is traditionally a major provider of flexible generation. However, given the increase in intermittent power capacity, and the decrease in capacity of more traditional means of system balancing, there will be an amplified requirement for technologies that can offer both flexibility with low CO_2 emissions

A higher proportion of system capacity reliant on variable renewable energy sources increases the requirement for flexible generation in two ways. First, the requirement for rapid variation in power output to provide ancillary services (see Table 2-1) cannot easily be achieved by current renewable technologies. Although there are efforts to improve this ability (Ela et al. 2012), there will likely be fewer generation units on the system that can provide the whole range of these vital balancing services. This increases the value of ancillary services and will likely be reflected in more expensive contracts, as already experienced in countries with high wind penetration (Holttinen et al. 2013). Second, there will be times when renewable energy sources are minimal (e.g. when the wind is not blowing) and ‘back-up’ capacity will be required to ensure system demand is met during such times. Alternative capacity, utilized when renewable options are unable to meet system demand, will therefore be necessary. Renewable electricity technologies reliant on wind, sun or ocean energy sources also have negligible fuel costs and so are therefore typically at the bottom of the merit order (see Figure 2-1), with their electricity purchased before other generation

options. This implies lower operating hours for non-renewable power plant, and therefore higher electricity prices during operating hours to cover investment costs.

By way of illustration, a Poyry modelling study (2011) of electricity systems in NE Europe with high wind and solar penetration, found that there would be periods when wind displaced all other forms of generation, while during other periods wind power would produce negligible output and almost a full system back-up capacity would be necessary. Figure 2-3 illustrates their findings for an indicative January and July in 2010 and 2030, when wind and solar make up approximately a quarter of the system generating capacity. Prices can be seen to spike with increased magnitude and frequency in the later simulation.

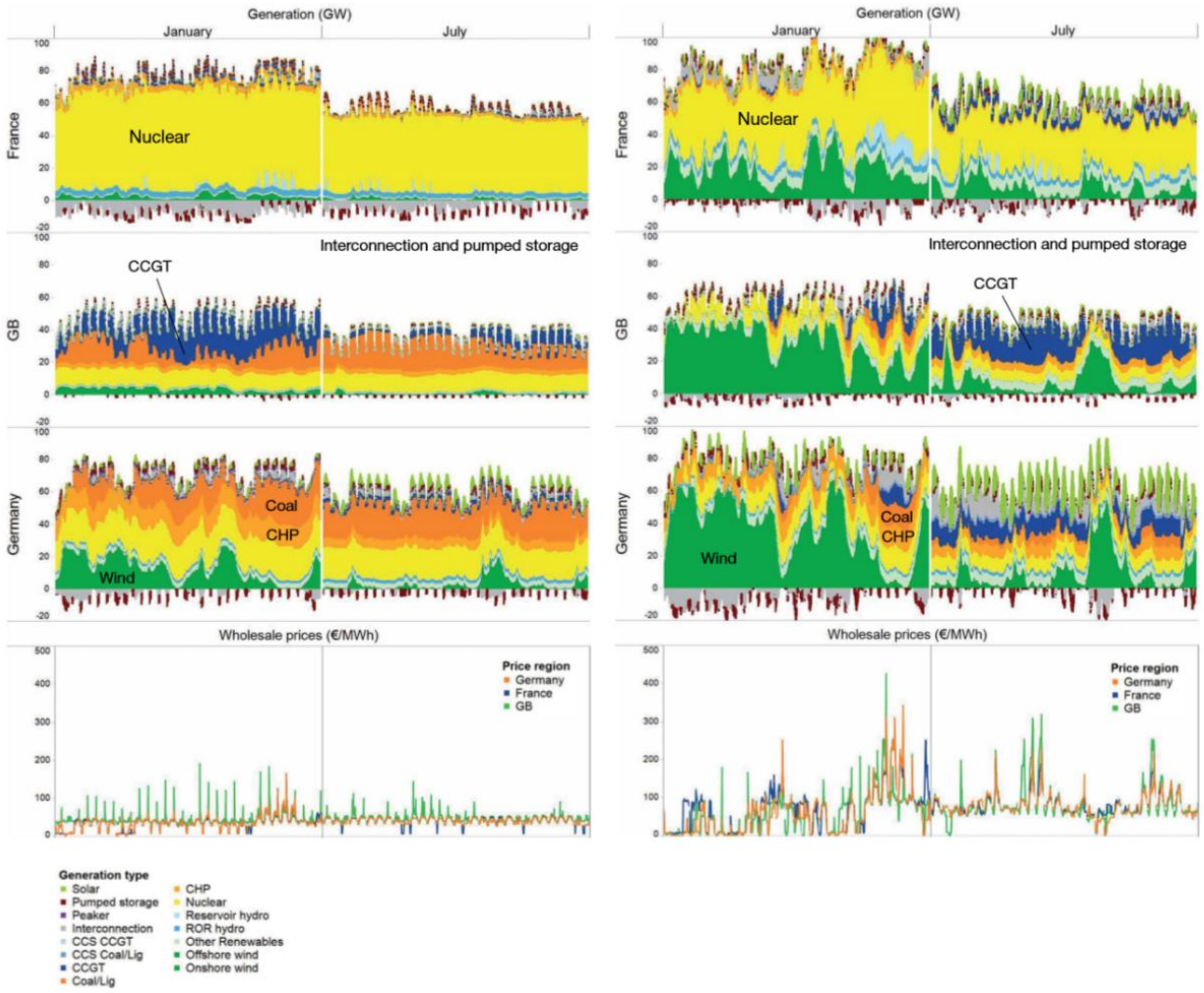

Figure 2-3 Demand and generation profiles compared with electricity prices in 2010 (left) compared with projected profiles and prices for 2030 (right) for simulated scenarios if wind and solar renewable targets are met in Germany, France and Great Britain *(Poyry 2011)*

In the work by Poyry (2011) shown in Figure 2-3, renewable generation technologies with variable output are shown to operate whenever they are available, while other generation types are shown to fill in the demand/supply difference accordingly. The generation types projected to provide this flexible output will depend on the system.

Low carbon options for flexible generation include energy storage or demand side management options as well as low CO_2 generation. Energy storage retains energy from low carbon sources for later release, effectively smoothing the export profiles of intermittent renewable sources. Energy storage technologies include, among others, pumped hydro, compressed or cryogenic gas energy storage, flywheels, various types of thermal energy storage and rechargeable batteries. Demand side management reduces demand in response to electricity availability, typically offering premiums to large, transmission connected energy users to turn down their demand following a signal from the system operator. Advanced demand side management is a further option, where demand from smaller distribution grid connected energy users can be manipulated by system operators to increase the volume of available demand response, for example automating electric vehicle charging times to respond to electricity availability. However, both energy storage and advanced demand side management remain areas of research and development. The technologies are currently expensive and cannot provide sustained output during long wind/sun free periods without very high levels of storage capacity in the system. Current literature studies suggest that alternative options for managing electricity demand, including energy storage and demand side management, are likely to be more expensive than responsive generation if used exclusively (Brouwer et al. 2015; IEAGHG 2012a).

Low carbon generation options that do not rely on intermittent energy sources include nuclear, biomass and fossil fuel with CCS. Nuclear power can provide responsive output, as indicated in the French profile in Figure 2-3, but this is economically inefficient due to low fuel costs and technical challenges associated with managing heat within the power plants (Nuclear Energy Agency 2009). The availability of biomass to provide sufficient back up capacity for a whole electricity system faces challenges where land use for food supply and biodiversity are competing and necessary obligations.

This thesis explores CCS as a potential provider of flexible electricity output. However, it is recognised that both demand management and energy storage technologies can also contribute to balancing a low carbon electricity system, and

should be considered on a level playing field with their specific associated costs taken into account. Effective system planning for transitioning to low carbon energy systems will enable different technology options to together provide sufficient and flexible output that can reduce system costs most effectively. Price signals to indicate the most efficient way to achieve both capacity and flexibility therefore must, therefore, include consideration of the levelised electricity costs, **and** further valuation of flexibility to meet system balancing demand at the lowest available costs.

This thesis aims to address the assumptions of levelised cost of electricity (LCOE) as a single metric used to consider the 'cost effectiveness' of low carbon technologies. The following section examines LCOE comparisons in this light.

2.2.3 Levelised costs of electricity in low carbon electricity markets

Presently, policy makers and investors use the Levelised Cost of Electricity (LCOE) as a metric for comparing low carbon electricity generation technologies. LCOE is the ratio between the net present value of costs and the net present value of electricity generated, or the income from electricity sales. In other words, the LCOE provides an indication of the average electricity price that must be attained to cover all initial and ongoing costs over an assumed plant economic lifetime, given projections of the total volume of electricity that would be generated within that time. This definition is detailed in equations 2.1 – 2.3.

$$LCOE = \frac{Net\ Present\ Value\ of\ costs}{Net\ Present\ Value\ of\ electricity\ generated} \quad (2.1)$$

$$LCOE = \sum_{t=1}^{n} \frac{\frac{CAPEX_t + fixO\&M_t + SRMC_t}{(1+r)^t}}{\frac{(Capacity \cdot CF)_t}{(1+r)^t}} \quad (2.2)$$

$$SRMC_t = FuelCost_t + varO\&M_t + £CO_{2_t} \quad (2.3)$$

Where:

t	Years	Time period (typically 1 year)
n	Years	Assumed plant lifetime
r	%	Discount rate
$Capacity$	MW_e	Full load electrical output of unit
CF	%	Capacity factor
$CAPEX$	£	Cost of capital
$fixO\&M$	£	Fixed operating and maintenance costs
$varO\&M$	£	Variable operating and maintenance costs

$FuelCost$	£	Fuel costs
$£CO_2$	£	CO_2 emission costs
$SRMC$	£	Short Run Marginal Costs

LCOE can be a useful method for indicative comparisons of dissimilar electricity generation options that differ in output, costs, operating procedures and life spans. However, LCOE projections of yet unbuilt units rely on assumptions over the course of the expected plant lifetime. In particular, assumptions are necessary for a projected capacity factor, and for SRMC values (see Eq. 2.2), which are dependent on assumptions of fuel price and CO_2 emission costs over the plant lifetime (see Eq. 2.3). Given uncertainties in markets and legislative structures, these costs are unlikely to remain constant, or to change predictably over the decadal periods at which plant lifetimes are assumed (typically 25 years for a natural gas power plant). Moreover, as described in detail by Joskow (2011), calculation of LCOE - a levelised, annualised cost - requires that electricity is considered as a single priced homogeneous product rather than a service with a range of values depending on when and how it can be dispatched. The associated profitability of a responsive, dispatchable power generator is generally not fully represented by this single value.

Therefore, while measures of LCOE and CO_2 intensity provide some understanding of options for cost effective, low carbon energy technologies, these metrics alone are inadequate when applied to integrated electricity systems.

The following paragraphs describe the assumptions contained in LCOE calculations, exploring how flexible operation impacts the weighting behind each assumption, and with a focus on the implications of these assumptions for the techno-economics of flexible CCS on natural gas.

Figure 2-4 provides a range of expected LCOE values for major conventional and low carbon technology electricity generation options. Corresponding CO_2 intensities are also shown. There are numerous sources that provide indicative LCOE values for low carbon electricity technologies (e.g. IEA, GCCSI, EIA, DECC) so the LCOE values presented in Figure 2-4 are taken from the most recent IPCC WG3 report (2014), which aims to compile different ranges into rational global averages.

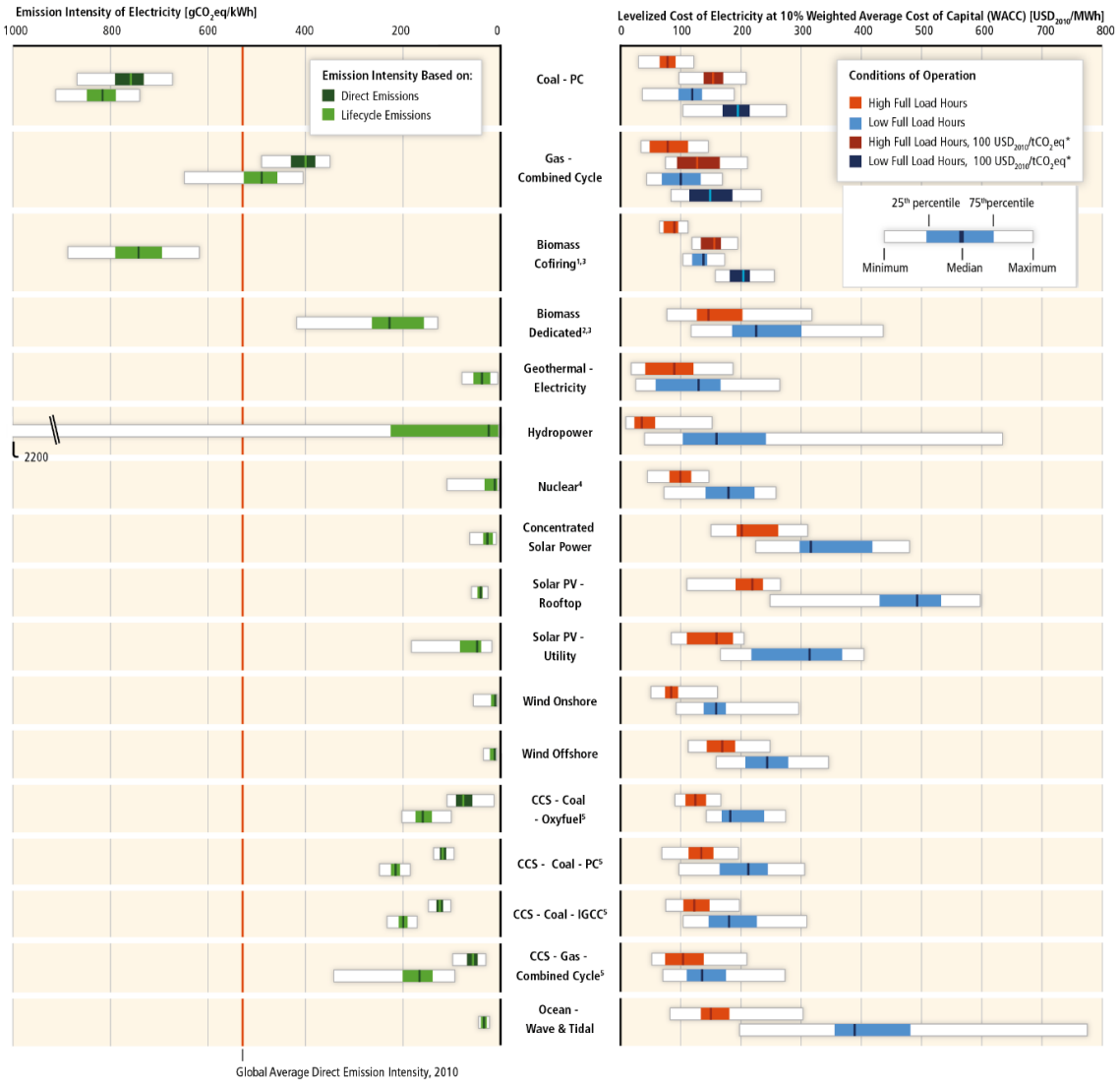

Figure 2-4 Levelised Costs of Electricity and corresponding emission intensities for a range of conventional and low carbon electricity generation technologies *(IPCC 2014)*

Figure 2-4 illustrates the range of LCOE estimates, in terms of uncertainties (illustrated by the full width of the bars) and in terms of the inclusion of CO_2 pricing and the impact of operating hours. Generation types with higher CO_2 intensities will be more affected by CO_2 prices than those with lower intensities.

Generation units projected to operate more frequently (high full load hours) have lower LCOE values than those with lower operating hours. This impact on LCOE is greater for generation options with higher capital costs, as can be seen for ocean and solar technologies. Operating hours are represented in an assumed capacity factor on which the net present value of electricity generated depends (see Eqs 2.1 and 2.2).

The capacity factor is the ratio of actual power output to the theoretical output if a unit were operating continuously at full load. Capacity factors are estimated from the projected availability of a unit to generate (based on technical capacity and projections of expected environmental conditions, i.e. average temperature, wind/solar availability) and the expected demand placed on the unit to operate within projected market conditions (i.e. the unit's place in a merit order). Any capacity factor estimate, therefore, contains inherent uncertainties related to the technology specific capacity for flexibility.

Indicative capacity factors for some technology generation options are shown in Figure 2-5 to provide an indication of expected variance between different technology options.

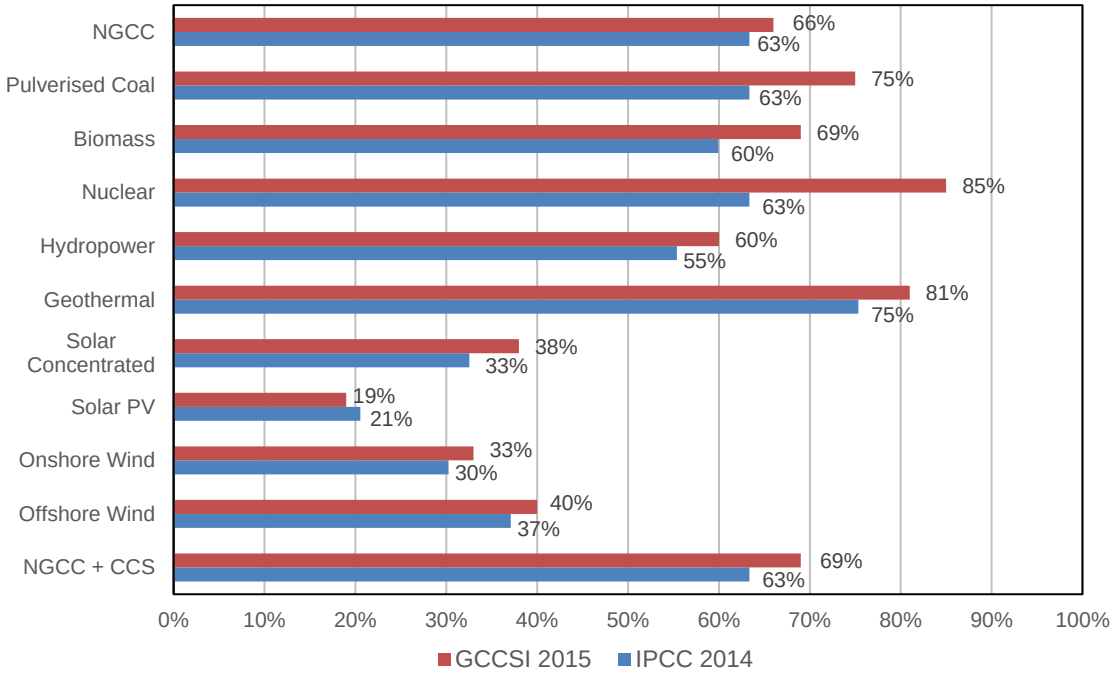

Figure 2-5 Assumptions of capacity factors for different technologies from two major review reports *(Irlam 2015; IPCC 2014)*

Figure 2-5 illustrates that renewable technologies reliant on intermittent energy sources have the lowest capacity factors, primarily because they have the lowest availability factors. There will be significant periods of time when the energy intensity of the sun or wind is low or negligible (or potentially too high) reducing the unit output. Nuclear and geothermal power, operating as base load technologies, typically have

the highest assumed capacity factors, while fossil fuel plant, operating as mid-merit providers, are assumed to have medium to high capacity factors in most modern electricity systems. Capacity factors do not approach 100% for any technology as there will always be outages for scheduled maintenance, and efficiency (and therefore output) reductions over the lifetime of a plant.

Importantly, capacity factor assumptions within the LCOE do not provide a correlation between operating hours and electricity price, i.e. the LCOE metric *provides* an average electricity price with the inherent assumption that electricity can be sold at the LCOE price (on average) whenever electricity is generated by the unit, ignoring the technical ability to take advantage, or not, of available market prices. This overlooks the fact that a plant with availability to respond to higher prices will have a higher revenue than a plant which is unavailable to generate during these periods. A generation unit able to operate at maximum output during all times when then electricity price is higher than the unit LCOE projection, will pay off capex faster and will ultimately see an effective LCOE decrease over the plant lifetime. Taking the example of wind power, a capacity factor of 30-40% implies there will be significant periods of time that the unit is unable to operate at full generation capacity. If many of these periods of low or minimal output arise during times of higher electricity prices, then it is possible that wind generation will sell electricity for lower than the estimated LCOE, without the opportunity to increase this average at other times. This scenario is not unlikely, as at times of low wind across an electricity system, the supply of electricity with respect to demand drops and it is at these times that the electricity price increase (see Figure 2-3).

Higher capacity factors, all else being equal, lead to lower unit LCOE values. Technologies that are not reliant on intermittent sources are constrained by electricity system economics rather than availability; these units can technically operate at very high capacity factors where sufficient incentives are provided. Subsequently, a scenario with high intermitted penetration results in an electricity system with lower capacity factors across the board for all but the intermittent plant, which are limited only by their availability so maintain constant capacity factors regardless of the technology portfolio. Operating at lower capacity factors will lead to the mid-merit, and to an even greater extent the peaking plant, seeing an increase in relative LCOE. Electricity prices, or ancillary service costs if used as a buffering mechanism against inflated prices, will therefore become even more valuable in these times, and plants

that can respond during these periods will further benefit from the variance. This can lead to system wide price increases which fail to provide the best value to society.

Further assumptions inherent in LCOE estimates are based on fuel and CO_2 costs, both of which are unlikely to be stable, or predictable. By way of illustration, historical variance in both natural gas values (BP 2014) and emergent carbon markets (IPCC 2014) has seen prices rise and fall by up to 600% in the first 15 years of this century alone. As these prices will impact on the short run marginal costs for any given generation unit, their variability will impact on the merit order, and potentially impact the assumed capacity factor.

In summary, important factors describing the cost or value of a low carbon electricity technology as part of an electricity system are not well represented currently in Levelised Cost of Electricity (LCOE) calculations. Long term assumptions of operating loads, efficiencies and costs are made to provide an indication of average revenue necessary to return investment. In this way, LCOE projections are unable to account for the ability of a generation unit to respond to price signals. LCOE cannot, therefore, account for flexibility and system wide pricing to reflect the true value of an electricity generation technology. The use of LCOE in technology comparisons is therefore limited and should be used with complementary system specific pricing analysis.

This thesis provides a methodology for additional pricing analysis for fossil fuel power plant operating with CO_2 capture, specifically on the flexible operation in response to the parallel price signals of wholesale electricity prices and CO_2 abatement.

2.3 Flexible operation of CO_2 capture and storage

To summarize an assessment by IEA Greenhouse Gas R&D Program (IEAGHG 2012a) that reviewed the potential for operating flexibly with CCS power plant, there are three main ways in which power plant operating CO_2 capture can provide flexibility:

- Variation in load with CO_2 capture processes following plant ramp rates accordingly.
- Internal energy storage options in the CO_2 capture system.
- Variations in the amount of CO_2 vented, thereby varying the parasitic energy load and subsequent net plant output.

These options are discussed in turn below.

The first option allows for ramping to provide flexible operation like traditional plant, but with lower CO_2 emission intensities. However, according to IEAGHG (2012a), there will likely be additional technical constraints and also efficiency penalties for part load operation with the addition of CO_2 capture. This option, therefore, leads to reduced flexibility than on the equivalent plant operating without CCS.

The latter two options decouple plant output from CO_2 capture levels; capture units operate in response to market price signals rather than according to power plant operation alone. This relies on manipulating the internal energy penalty of CO_2 capture and compression. In this way CO_2 capture can enhance the flexibility of fossil plant, rather than limiting it.

The energy penalty incurred by operating with CO_2 capture is a significant percentage of the net plant output. Taking the example of modern amine capture technologies used in a post-combustion capture, a 7-11 %-point penalty reduction is typical after 90% of the flue gas CO_2 is captured and compressed (NETL 2015), which equates to approximately 15% of output for an efficient NGCC. If capture related processes are temporarily turned down or off, then that energy penalty can potentially be converted to electricity exportable to the grid. Some examples of internal energy storage in the CO_2 capture system, describing the second option above, are solvent storage in post-combustion capture plant, and liquid oxygen storage in oxyfuel plant. Solvent storage describes a process where solvent rich in captured CO_2 is stored during peak electricity prices. CO_2 regeneration is stopped or decreased so the electrical penalty for CO_2 compression is reduced and steam previously diverted to regenerate the solvent can be expanded to instead generate additional electricity for export. When electricity prices are low, the additional solvent can then be regenerated by extracting additional steam from the steam cycle. Similarly, liquid oxygen storage makes use of intermediate stores of liquid oxygen within the cryogenic air separation unit (ASU) of an oxyfuel plant. Oxygen produced surplus to requirement during low electricity prices can be stored for later use, so that oxygen production can be switched off or down, releasing the parasitic load required for the ASU compressors, thereby increasing net plant output while meeting requirements of the oxyfuel combustion process.

The third option, CO_2 venting, describes a CCS power plant operating at a lower capture level, or bypassing capture operations completely, e.g. venting flue gas prior to a post-combustion capture unit, or air-firing and venting flue gas prior to a CPU in oxyfuel plant. Steam from the power cycle previously diverted to the reboiler is then

rerouted to the LP turbine to mitigate the majority of capture energy penalties. The electricity output penalty associated with CO_2 capture can be directly converted to exportable electricity.

There are capital costs associated with internal energy storage options; storage vessels and higher inventories are necessary, and larger equipment would be required for additional flows during times of regeneration. However, CO_2 capture levels can be maintained, and so such techniques could be valuable in highly carbon constrained systems which do not allow for residual CO_2 venting. Venting CO_2 has fewer capital cost requirements but would incur further CO_2 emission penalties for any additional CO_2 release. All these flexible capture plant options are operable on the condition that the plant has been designed to accommodate this change in operation, for example changes in steam flow and electricity output. Also, these operations must keep within the technical limits of the full CCS chain, including downstream limitations on CO_2 flow or pressure variation.

This thesis focuses on the techno-economics of CO_2 venting with partial capture, specifically applied to the example of post-combustion capture with NGCC power plant. However, the principles described could apply to other CCS power plant technologies, including plant operators working with additional internal energy storage options.

2.3.1 Literature review of the techno-economics of flexible post-combustion CO_2 capture

Previous work on the techno-economics of flexible operation of CO_2 capture levels primarily explores full bypass of the capture unit (Rao & Rubin 2006; Chalmers & Gibbins 2007; Chalmers et al. 2008; Chalmers, Leach, et al. 2009; Chalmers, Lucquiaud, et al. 2009; Lucquiaud et al. 2009; Delarue et al. 2012) or binary shifting between minimum and maximum capture levels (Ziaii, Cohen, et al. 2009; Ziaii, Gary T Rochelle, et al. 2009; Ziaii et al. 2011; Cohen et al. 2012; Cohen et al. 2013; Oates et al. 2014). Chalmers & Gibbins (2007) carried out an early assessment of the potential for flexible CCS power generation through a set of decision diagrams based on carbon and electricity prices, assuming a fixed energy penalty for full capture and a small residual energy penalty at bypass. These decision diagrams illustrate a method for ascertaining the more profitable operation (capture or bypass) based on the balance of short run marginal costs (which include fuel and carbon prices) and income from sales of electricity, given wholesale market prices of carbon and

electricity. Chalmers, Lucquiaud et al. (2009) use a similar methodology to further suggest that using solvent storage options may allow a lower maximum CO_2 price for bypass optimisations.

Studies by Cohen et al., (2012) and Ziaii et al., (2008, 2011) expand on the work of Chalmers to explore the value of capture plant bypass in an illustrative grid and electricity market. Both studies implemented a model of an ERCOT grid to create a dispatch order which incorporates the marginal cost of electricity production and the likelihood of the plant being used. Annual operating profits were used as a decision criterion for operating bypass or capture, rather than short run net operating cash flow. Marginal costs of electricity were calculated and a dispatch order that allowed modelling of plant turn on or off. Historical electricity prices were used to assess likely operation given a CO_2 price, and decisions were made to maximise profits to the plant operator. Capture was assumed to operate at 90% and 20% load, with performance taken from a dynamic model. CO_2 that was not captured was vented. In this case, prior knowledge of dispatch is assumed and so all plants with capture either operate at 100% or 20% capture.

Ziaii et al. (2008) found that flexible operation increased profits over steady capture levels of 90%, with solvent storage being profit advantageous. Later, Ziaii et al. (2011) presented a dynamic model of a stripper that determined the switch between 20% and 90% capture was feasible. Ziaii et al. (2011) explored the response of the plant to minimise operating costs versus maximising annualised profit, indicating that a flexible operating cost scenario could see higher reductions in emissions than a flexible profit simulation, but slightly lower annual profits at mid carbon prices than a flexible profit scenario. Additional annual profits from flexible operation were estimated to be between $10–100 million.

Oates et al. (2015) employed a method similar to Cohen et al. (2012), utilising an electricity market model to assess the value of bypass or solvent storage operation of post-combustion CO_2 capture plant under different electricity and CO_2 prices. Their modelling considers natural gas plant as well as coal, and uses first order approximations for the energy penalty of capture. Oates et al. concluded that in conditions where a plant operates capture profitably, i.e. where CO_2 prices were sufficiently high to incentivise capture, flexible operation would not be profitable. However, this conclusion is on the basis of net present value calculations rather than

incoming cash flow calculations responding to electricity price spikes. This analysis therefore doesn't reflect the potential value available for flexible operation.

Delarue et al. (2012) also consider a binary bypass or capture option with a fixed capture penalty, but build on previous work by considering NGCC as well as coal plant, and considering the yearly profit potential in a hypothetical electricity system using a MINLP optimisation model. Their findings indicate that in their electricity system model, flexible bypass would be profitable compared with fixed capture only at CO_2 prices below 30 Euro/tonne, corresponding to conditions when bypass was optimal. Furthermore, in this study the short run marginal cost of flexible operation was compared with open cycle gas turbines (OCGT) for comparison, finding that OCGT became cost competitive at moderate higher CO_2 prices. This is primarily because the additional electricity released from the capture plant as a proportion of total plant output has a very high specific emission intensity compared with OCGT. However, this analysis did not describe lifetime costs, which would be impacted, since capital costs for OCGT would need to be covered in fewer operating hours. The authors conclude:

"if the option of turning off capture plants avoids the need to invest in additional back up capacity (e.g., gas turbines), this [flexible operation with bypass] *could be a relevant strategy also at higher CO_2 prices."*

Other studies consider the full range of possible capture levels, rather than binary operating points (Wiley et al. 2011; Ho & Wiley 2015; Brasington & Engineering 2012; Coussy & Raynal 2014; Luo & Wang 2015).

Wiley et al. (2011), and later Ho and Wiley (2015) assess variable and partial capture levels versus fixed capture, or capture with full bypass alone, in response to demand scenarios based on market data from NSW, Australia. First order energetic assumptions are assumed for set point capture levels (90%, 40%, 20%, 10% and 0% capture). Both studies conclude that flexible capture will be economically beneficial, and that a greater overall amount of CO_2 is captured when variable capture levels are considered versus full bypass alone. However, their conclusions are limited by the high-level nature of their modelling of plant response to flexible operation.

Coussy and Raynal (2013) consider a continuous range of capture levels to calculate operating costs related to capture level. On this basis the authors make an argument for the plant to reduce the capture level to the point at which the cost of CO_2 emissions is higher than the operating cost; Optimum capture is determined by the point at which

the cost of emissions outweighs savings. A limitation of Coussy and Raynal's study is that the metric of electricity price is not considered. Instead of matching income versus outgoings, these authors minimised outgoings alone, and therefore like Oates et al. (2015) they also do not adequately value flexible response in electricity systems.

Luo and Wang (2015) carry out a sensitivity study of LCOE values based on flexible operation of an NGCC plant integrated with post-combustion capture. Their findings indicate that while LCOE increases with capture level, this can be offset by higher CO_2 pricing scenarios. This study is based on a rate-based integrated model of the NGCC-post-combustion capture (NGCC-PCC) system, however it is not clear in the article how off-design characteristics are accounted for, particularly in the steam cycle and compression train. Additionally, LCOE is apparently calculated without consideration of load factors, which would be impacted by flexible operation of the capture unit and therefore affect the outcome of this study.

Zaman & Lee (2015) and Khalilpour (2014) present numerical optimisations of capture plant operation where continuous variation in capture levels are considered. Zaman and Lee (2015) consider reboiler duty response to continuously variable capture levels through rigorous mass and energy balances of the amine plant. However, modelling of the power plant or compression train is not attempted, and the optimisation instead uses simple constant parameter correlations for compression and power plant energetic response, which do not account for the part load behaviour of these units. The optimisation considers cost minimisation over a hypothetical 24-hour pricing period and finds that optimum (lowest cost) capture levels vary from over 90% down to 40% with some step changes in between these times of high and low pricing. Khalilpour (2014) considers a revenue maximisation function, but does not implement plant modelling, instead relying on proportional correlations to describe energetic performance at partial capture. Interestingly, Khalilpour (2014) assesses several different CO_2 mitigation scenarios in addition to a simple CO_2 price (cumulative emission reduction targets and government subsidy per unit of low carbon electricity). They conclude that the available prices of electricity are more important than the CO_2 mitigation incentive for the net value of flexible operation.

Brasington (2012) on the other hand considers a continuous energy relationship between capture level and energy penalty, and goes on to consider the implications of both wholesale electricity price and carbon price on the net plant revenue as a function of capture level. Importantly, his work stops short of proposing a methodology

for optimising the capture level, a gap which is intended to be filled and presented in this thesis.

2.4 Thesis contribution to the literature

This thesis builds on the above studies in three ways:

1 A detailed integrated model of an NGCC plant with post-combustion capture is developed to simulate the relationship between capture plant turn down and electricity output penalty more rigorously than those currently published in the literature. The model accounts for integrated, off-design behaviour of the steam cycle, the steam extraction line, the capture plant and the compression train.

2 An analytical methodology for optimising operating capture level is presented, which optimises capture level through maximising short run net operating cash flow, rather than minimising costs or maximising LCOE. Plant operators will fundamentally look to maximise revenue, and so minimising cost alone will not maximise overall plant revenue where peak electricity prices could justify operating cost increases by subsequent enhanced income. Optimisations based on maximising LCOE will have many inherent assumptions which require detailed system profiling. Instead, this analytical methodology can be used by plant operators in response to real time price signals alone, without the need for market foresight or complex numerical optimisation.

3 The optimisation methodology is considered under three different low carbon market case studies that go beyond carbon price as a mechanism for valuing CO_2 abatement. Specifically, scenarios where zero-carbon electricity is eligible for a premium tariff, and where the system is constrained by an Emission Limit Value (ELV) are considered. The potential for revenues under each indicative scenario are quantified and discussed.

3 The role of natural gas power plant in low carbon electricity systems and the application of post-combustion CO_2 capture

This chapter begins with a high-level introduction to the techno-economics of natural gas-fired power generation, describing inherent characteristics that influence its operation in electricity systems. This chapter goes on to quantitatively detail the likely constraints on unabated natural gas-fired combined cycle (NGCC) plant that will be experienced in low carbon electricity systems and describes the potential application of CO_2 capture on NGCC plant in this light. A general overview of post-combustion CO_2 capture is described, followed by a review of the literature on options for application of post-combustion capture specific to NGCC power plant. The chapter concludes with a summary of published studies on the performance of MEA based post-combustion on NGCC plant specifically.

3.1 Techno-economic introduction to natural gas-fired power plant

Natural gas-fired power plants most commonly exist as Brayton cycle systems (Global Energy Observatory, 2016[3]), wherein natural gas is compressed, combusted, and then expanded through a gas turbine. A standalone simple cycle is referred to as an Open Cycle Gas Turbine or OCGT. Combined Cycle Gas Turbines (CCGT) or Natural Gas Combined Cycle systems (NGCC) add a bottoming cycle to utilize heat from hot exhaust gases exiting the gas turbine to generate pressurized steam (or, less commonly, an alternative working fluid) for expansion through additional turbines. The inclusion of a bottoming cycle in NGCC increases fuel efficiency significantly, although this also increases the plant capital costs.

OCGTs have lower fixed costs and can start up and shut down very rapidly, and are therefore still commonplace in energy systems, albeit in fewer numbers typically operating as peaking plant. Smaller engine-generators that burn natural gas to generate electricity also exist, but these are relatively small scale with lower efficiencies than gas turbines, and are frequently off-grid outside the management of

[3] http://globalenergyobservatory.org/list.php?db=PowerPlants&type=Gas

energy system operators. Neither of these simple cycles has the capability to be effectively integrated with a post-combustion capture plant due to the lack of a steam cycle. Therefore, they are outside the scope of this work, which instead focuses on post-combustion capture integrated with NGCC.

Gas turbines have the lowest capital investment cost of all available major power generation technologies, including renewables, nuclear and coal or biomass plants (IEA 2014; Irlam 2015). Capital costs are low compared with other thermal plant because NGCC are smaller than advanced boilers and need only to rely on simple pipeline access for fuel handling. Moreover, the relative lack of impurities occurring in natural gas as compared to solid fuels means less need for complex and expensive clean up units. NGCC are also increasingly fuel efficient, with turbine manufacturers' published performance figures indicating over 61% fuel efficiency in most recent models (see Table 3-1). However, natural gas fuel prices have historically been more expensive per thermal unit compared with other fuels, leading to high short run marginal costs (SRMC), even for high efficiency NGCC. SRMCs are therefore usually higher for natural gas plants than for coal plants and are consistently higher than those for nuclear plants and renewable generators.

Gas turbines are controlled by fuel injection into the gas turbine, so can be turned on or off and ramped up and down as required (subject to fuel availability), with the capacity to offer part load and rapid response in ways that renewables and nuclear find challenging (as detailed in Chapter 2).

Table 3.1 illustrates the modern OCGT and NGCC plant design point efficiencies, ramp rates and turn down abilities are provided in Table 3-1 for some major turbine manufacturers. F-series turbines are the current modern standard for large scale power gas turbine applications. H- or J-series are the state-of-the-art.

Table 3-1 Modern gas turbine performance indicators from major manufacturers

	GE		Siemens		MHI	
	F-series[1]	H-series[2]	F-series[3]	H-series[4]	F-series[5]	J-series[6]
Simple cycle LHV efficiency %	37.8 - 38.7	41.5 - 41.8	39.8	41	38.2 - 40.0	41
Combined cycle LHV efficiency %	58.4 - 60.4	61.6 - 62.1	58.5	>60	57.0 - 61.2	61.5 - 61.7
Ramp rate MW/min	44 - 48	120 - 140	75	>15	18 - 36	40
Minimum load %	23	24	13	20	45 - 75*	50*

*Referring to GT only - information not found on combined cycle ability

NGCCs commonly fill mid-merit or higher order roles in traditional energy systems due to these economic and technical characteristics; controllability, lower capital costs and higher operating costs. For the same reasons, NGCC are also often employed to provide balancing services to electricity systems.

3.2 The role of natural gas-fired combined cycle gas turbines in future low carbon electricity systems

The IEA World Energy Outlook 2017, along with other projections (Birol et al. 2015; British Petroleum 2014), indicate that natural gas usage will surge over the coming decades, with power generation being the dominant sector in which natural gas usage will increase. These projections are based on the increasingly competitive prices of natural gas due to unconventional gas sources and the growth in global LNG trade, in addition to greenhouse gas targets. With around half the CO_2 emissions associated with modern coal plant, NGCC are increasingly considered as an alternative to large coal plant for reducing the CO_2 intensity of electricity systems (Seebregts 2010; Parliamentary Office on Science & Technology 2015). However, there is a limit to

1 https://powergen.gepower.com/content/dam/gepower-pgdp/global/en_US/documents/product/gas%20turbines/Fact%20Sheet/9f03-04-05-fact-sheet-april-2015.pdf
2 https://powergen.gepower.com/products/heavy-duty-gas-turbines/9ha-gas-turbine.html, https://powergen.gepower.com/content/dam/gepower-pgdp/global/en_US/documents/product/gas%20turbines/Fact%20Sheet/9ha-fact-sheet-oct15.pdf
3 http://www.energy.siemens.com/us/pool/hq/power-generation/power-plants/gas-fired-power-plants/combined-cycle-powerplants/scc5-4000f-1s/A96001-S90-B328-X-4A00.pdf, http://www.energy.siemens.com/us/pool/hq/power-generation/power-plants/gas-fired-power-plants/FlexPlant-Brochure-LR.pdf, http://www.energy.siemens.com/hq/pool/hq/power-generation/gas-turbines/SGT6-5000F/gasturbine-sgt6-5000f_poster.pdf
4 http://www.energy.siemens.com/hq/pool/hq/power-generation/gas-turbines/SGT5-8000H/gasturbine-sgt5-8000h-h-klasse-performance.pdf
5 https://www.mhps.com/en/products/thermal_power_plant/gas_turbin/lineup/pdf/mhps_gas_turbine_m501f_m701f.pdf, https://www.mhps.com/en/products/thermal_power_plant/gas_turbin/lineup/m701f.html
6 https://www.mhi-global.com/products/pdf/H480-48GT28E1-B-0.pdf

which natural gas power can provide increasing power demand while meeting greenhouse gas reduction targets. The most recent IPCC assessment report indicates that for average warming to be limited to 2C (on a probabilistic scale), the total atmospheric CO_2 equivalent concentration should not exceed the range of 430 – 540 ppm, which is the equivalent of further cumulative global emissions being limited to approximately 1000 $GtCO_2eq$ (IPCC 2014; SPM 10). These targets correspond to decreases in emissions of approximately 4% per year until beyond 2050, considering a predicted emission peak in 2020 (Allen et al. 2009), with total emissions targeted as being close to zero or negative by the second half of the century (IPCC 2014) These projections imply that electricity systems must rapidly decarbonize and emit below 50 $kgCO_2/MWh_e$ on average by the middle of the 21st century, see Figure 3-1.

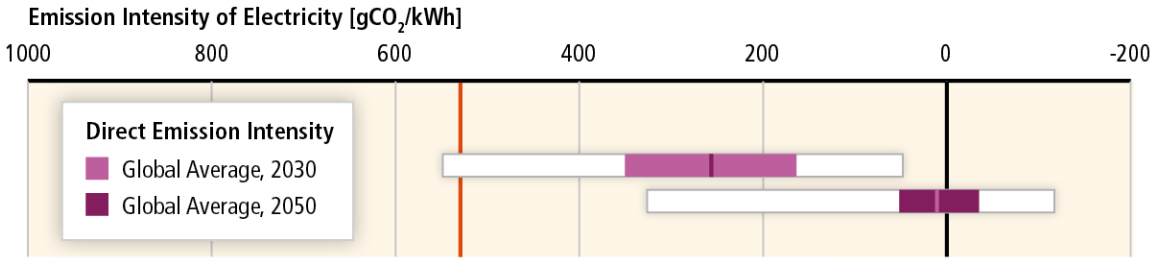

Figure 3-1 Electricity system CO_2 intensities necessary to limit cumulative atmospheric CO_2 to 430-530 ppm CO_2 eq (IPCC 2014, WG3, Ch 5)

Currently, even the most efficient natural gas fired power plant will not enable these CO_2 intensity targets without restricted hours or without the application of CO_2 capture. NGCC operating with fuel efficiencies between 58 and 62% will generate electricity at full load with a CO_2 intensity between 348 and 337 $kgCO_{2eq}/MWh_e$ respectively, assuming an average natural gas fuel CO_{2eq} intensity of 56.1 kg/GJ (Gómez et al. 2006). This is around seven times higher than the maximum recommended CO_2 intensity required for electricity generation by the middle of this century. Moreover, operating NGCC at part load reduces thermal efficiencies, leading to further increases in CO_2 emission intensity. At reduced load, less fuel is injected into the combustor, affecting temperature and pressure ratios in the gas turbine and leading to fluid velocity profiles different from the engineered optimum. The reduction in available heat from the turbine exhaust gas also leads to reduced steam temperatures and flow rates in combined cycles, with subsequent further efficiency losses. A resultant decrease in efficiency as the plant moves away from design-point operation is experienced until a minimum achievable load is reached. Figure 3-2

provides an illustration of the effect of turndown on efficiency in modern standard turbines and the corresponding CO_2 intensity of the electricity generated. When operating NGCC at a minimum 20% load, CO_2 intensities could be closer to 500 $kgCO_{2eq}/MWh_e$.

It should be noted that there have been recent design efforts by major manufacturers to develop turbines specifically for flexibility with better performance at part loads (e.g. Siemens FAst CYcling (FACY) concepts; the GE 7FA; fully-cooled MHI H-class turbines). Still, the trend of reduced efficiency at part loads holds true.

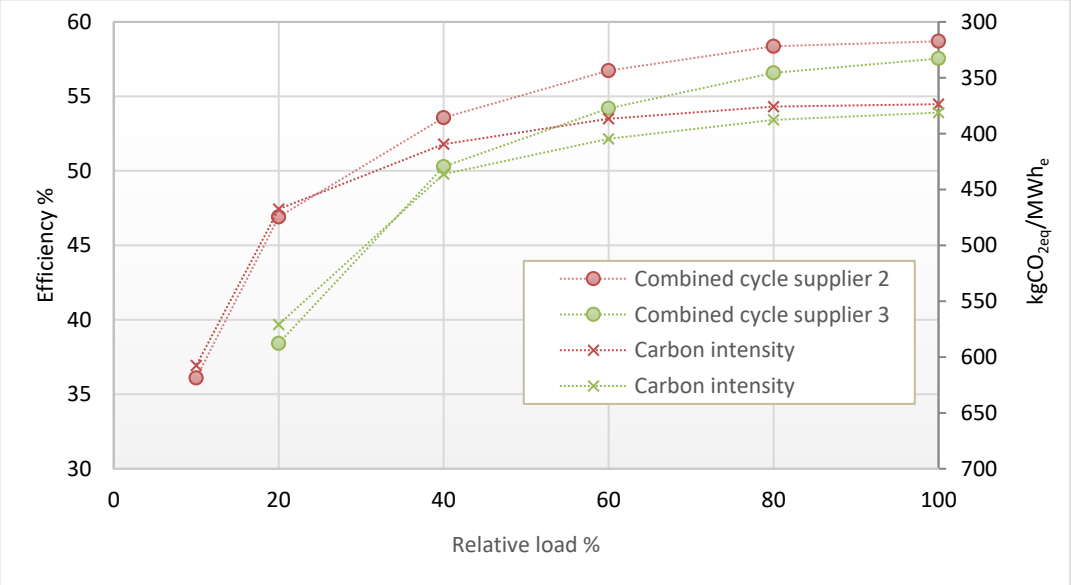

Figure 3-2 Overall plant efficiency versus load for two illustrative CCGT manufacturers (data from industrial sources and IEAGHG 2012)

NGCC undergoing frequent hot and cold start-ups also emit more CO_2 than during steady operating conditions. Bass et al. (2011) present experimentally measured data indicating that during a hot start an additional 240 $kgCO_2/MWh$ are emitted, with an additional 120 $kgCO_2/MWh$ emitted during a cold start. NGCC operating as flexible plant with part load operation and multiple start-up and shut down cycles will therefore emit more CO_2 per kWh generated than the necessary system emission limits. Continued use of unabated natural gas for balancing low carbon electricity systems will therefore be limited.

The application of post-combustion capture CO_2 Capture and Storage (CCS) technology can reduce CO_2 emissions by over 90%. This has been technically demonstrated for natural gas fired power plant (e.g. MHI 2002) and also commercially,

given the right market conditions (e.g. Reddy et al. 2003). The flexibility of post-combustion capture systems to ramp up and down has also been demonstrated on several pilot scale plants (e.g. Fitzgerald et al. 2014; Bui et al. 2016). Therefore, post-combustion CO_2 capture application to NGCC could allow for CO_2 targets to be met while continuing to provide flexible, efficient power provision.

3.3 NGCC with post-combustion CO_2 capture

3.3.1 Natural gas fired combined cycle (NGCC) process description

A natural gas combined cycle contains a gas turbine operating a Brayton cycle and a secondary Rankine cycle formed of a heat recovery steam generator (HRSG) and steam turbines. In summary:

- The gas turbine draws in air through a large air inlet, where it is filtered, cleaned and compressed. Natural gas is then injected into the air and combusted, before expanding the hot fuel-air mixture through gas turbine blades, spinning the turbine to drive an electricity generator. Hot gases exiting the turbine are passed to the HRSG.
- The HRSG captures exhaust heat from the gas turbine, passing the hot exit gases through a bank of heat exchangers to generate steam. Heat exchangers are a series of hot water economisers, evaporator drums and steam superheaters to maximize heat transfer efficiency, and often at more than one pressure so to reduce the temperature pinch and utilise the full range of temperatures available from the cooling gas.
- The steam generated passes to steam turbines, operating at multiple pressures according to the steam pressures generated in the HRSG. Steam is expanded and cooled through the turbine blades driving a generator shaft for conversion to additional electricity. Steam exiting the turbine is condensed and fed back into the HRSG completing a Rankine cycle.

In a typical NGCC plant, roughly two thirds of the power generated comes from the gas turbine, with one third generated by the steam turbines (Winterbone & Turan 2015). When integrated with a post-combustion capture unit, steam can be extracted from the steam cycle to provide heat for solvent regeneration, leading to a reduction in electricity generated by the steam turbine, but leaving the output of the gas turbine unchanged

3.3.2 MEA based post-combustion CO_2 capture process description

There are several existing technologies for post-combustion capture: CO_2 absorption using liquid solvents, for example aqueous alkanolamines, ammonia, and ionic liquids; CO_2 adsorption using solid materials; gas separation with membranes; and cryogenic processes among some other novel concepts.

This study specifically considers solvent based post-combustion capture by absorption, using aqueous mono-ethanol amine (MEA), a primary alkanolamine. A strong argument for focusing on capture with aqueous MEA is that at time of writing, post-combustion capture using aqueous amines is the most established method for operating CO_2 capture projects both on coal and natural gas fired plant, and MEA specifically is most commonly used for baseline studies in current literature (e.g. Fout et al. 2015). Other technologies can offer lower regeneration energies and higher CO_2 capacities compared with MEA (Boot-Handford et al. 2014) with the potential for efficiency and cost savings. However, these are either at earlier stages of development or else commercially proprietorial, and so harder to compare to baseline studies in terms of performance and operability. Post-combustion capture with MEA is therefore selected as the most viable and useful for the purposes of this techno-economic study.

In a typical amine absorption process, a gaseous process stream and an aqueous amine solution are passed counter-currently through a packed column where CO_2 in the process stream is removed by selective chemical absorption of CO_2 into the solvent. Pure MEA is highly corrosive and viscous; undiluted MEA would challenge both the material resistance and the hydrodynamics of a gravity-based absorption column. As a result, aqueous MEA is typically used with around 30% by weight MEA to H_2O. The CO_2 rich amine is then passed into a stripper column where CO_2 is subsequently re-released by boiling the solvent to generate steam, hot concentrated CO_2 lean solvent, and free CO_2 gas. The steam is condensed out of this exiting gas, and an almost pure stream of CO_2 produced. The CO_2 can then be treated and compressed for transport and storage. A typical flow sheet of the process is shown in Figure 3-3.

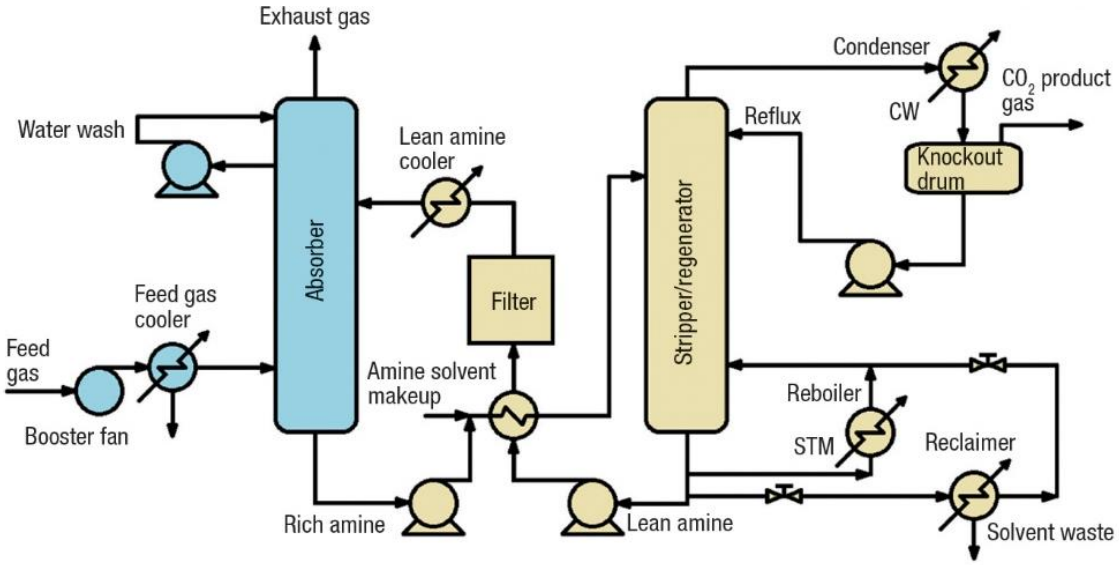

Figure 3-3 Process flow diagram for CO_2 recovery from flue gas by chemical absorption with aqueous MEA (IPCC 2005)

Flue gas from NGCC power plant enters the absorption process loop after exiting the HRSG, typically at atmospheric pressure and approximately 100-120°C, as dictated by turbine exit pressures and the dew point of the flue gases. The vapour liquid equilibrium for CO_2-H_2O-MEA at 30 wt% MEA determines that temperatures around 40°C are required for effective CO_2 absorption, therefore flue gas requires cooling prior to entering the absorber. The large volumes of flue gas are typically cooled with direct contact coolers (DCC), packed columns where falling water counter-currently contacts rising flue gas. To overcome pressure drops associated with packed columns, a booster fan is included in the process loop to enable flue gases to pass through the DCC and the absorber. If the flue gas pressure is slightly above atmospheric exiting the HRSG, the fan can be located after the DCC, an economic option as cooled flue gas will be energetically easier to pressurise and have lower volumes. However, in this work it is assumed that flue gas will exit the HRSG close to atmospheric pressure and the booster fan is therefore located prior to the DCC, as in the diagram provided in Figure 3-3, taken from the IPCC Special Report on Carbon Dioxide Capture and Storage (2005). This is a reasonable assumption for an NGCC plant as standard gas turbines discharge at atmospheric pressures to obtain the maximum work.

After cooling, flue gas enters the packed column absorber, which provides a large contact surface area for CO_2 and MEA to react. Cool, lean (low CO_2) amine enters

from above the main absorber packing section, to counter-currently contact with the rising flue gas. CO_2 is absorbed into the solvent and CO_2 rich amine exits the bottom of the column. The treated, CO_2 depleted, flue gases then pass through a counter-current water wash section to reduce amine losses to the atmosphere and manage the process water balance, before exiting the top of the absorber.

Rich amine exiting the absorber is pumped towards the stripper/regenerator column, by way of a cross heat exchanger, where the cool solvent is heated against the hot, regenerated lean solvent exiting the stripper. Before entering the absorber, the lean amine is further cooled to around 40°C to facilitate CO_2 absorption, as described above. The stripper, also a packed column, degasses the rich solvent of CO_2 by counter-current contact with rising stripping steam, creating hot, pressurised conditions that favour the reversed MEA-H_2O-CO_2 equilibrium. Stripping steam is generated in the reboiler through partial evaporation of the solvent. The CO_2-H_2O vapour product exits the stripper and is cooled in an overhead condenser, where the water is removed and routed back to the stripper column by way of a reflux knockout drum. The CO_2 gas product continues to a multi-stage compressor where it is typically compressed to between 80-200 bar, dependent on the specific transport and storage application. Amine reclamation equipment and a corresponding amine make-up stream can be included in the process loop to manage amine performance and losses resulting from solvent degradation.

3.3.3 Application of post-combustion capture to NGCC

There are technical differences between post-combustion capture when applied to flue gas from natural gas combustion and from coal combustion, gas sweetening or other industrial processes. Natural gas is combusted in excess air to regulate turbine inlet temperatures, producing large volumes of atmospheric pressure flue gas, dilute in CO_2, but relatively high in oxygen. Subsequently, flue gas from gas turbines has approximately 50% greater volume than flue gas from coal plant, with lower CO_2 concentrations of around 3-4% compared to 12-15%. These differences impact absorption based post-combustion capture processes as follows:

- CO_2 separation is driven by CO_2 phase equilibrium; The lower the concentration of CO_2 in the gas phase, the harder to remove the CO_2. This can lead to increased energy penalties per mole of CO_2 captured. Dilute CO_2 gas streams require leaner solvents to provide the adequate driving force for

mass transfer. Solvent is regenerated by boiling the CO_2 out of the liquid, with a corresponding energy penalty. It is increasingly energetically expensive to remove CO_2 from lean solutions, so where very lean solvents are needed to absorb CO_2 from dilute gas streams, more energy is required to boil the solvent per molecule of CO_2 separated.

- Dilute CO_2 flue gas with lower potential for absorption can require longer columns to allow for longer contact time for equivalent capture levels.
- The lower concentrations of CO_2 lead to lower exit flow rates of CO_2 per MW of power generated, leading to relatively smaller, cheaper, CO_2 treatment equipment, including compressors.
- Larger flue gas volumes can require larger, more expensive equipment, including wider separation columns and larger, more energy intensive flue gas booster fans and gas cooling equipment.
- Solvents used for CO_2 capture can experience degradation when exposed to oxygen (Goff & Rochelle 2004). Additives and inhibitors may therefore be further required for high O_2 flue gas.
- Flue gas impurities such as heavy metals, chlorine, SO_2 and NO_2 affect the absorption process by forming heat stable salt with MEA. Natural gas does not contain the same levels of these impurities, therefore much of the pre-treatment required for coal flue gases prior to separation processes is not required for post-combustion capture applied to NGCC.

3.4 Literature review of post-combustion capture applied to NGCC

3.4.1 Simulation of integrated amine based post-combustion with NGCC

Early synthesis reports on amine based post-combustion CO_2 capture from power plants typically included detail on flue gas from combined cycle gas turbines in addition to coal (IEAGHG 1999; Rochelle 2000; MHI 2002; Rao & Rubin 2002; Reddy et al. 2003; International Energy Agency 2004). However, these early studies did not integrate the capture plant with the power plant and focussed on ancillary boilers for solvent regeneration. Integration of the power plant steam cycle with the amine reboiler, through extraction of lower grade steam from the crossover between the Intermediate Pressure (IP) turbine and the Low Pressure (LP) turbine (the IP-LP crossover), enables significant energetic and cost efficiencies compared to using an external boiler. This integration option has since become a standard baseline in mainstream technical literature.

Other options for integrating amine-based post-combustion CO_2 capture with NGCC plants have been investigated in the literature, typically examining the effect on either efficiency or cost. These can be categorised into three types:

1. Flue gas recycling: Flue gas recycling (FGR), otherwise known as exhaust gas recycling (EGR) is a process whereby a proportion of the exit flue gases are recycled into the gas turbine to reduce the excess air content in the combustor in order to increase the CO_2 content and therefore the driving force in the absorber, and also to reduce the overall volume of flue gases from a GT unit (see Elkady et al. 2008; Evulet et al. 2009 for example). Several studies have simulated the impact on FGR on an integrated NGCC plant (Biliyok & Yeung 2013; Li et al. 2011; Lindqvist et al. 2014; Hu et al. 2017; Luo et al. 2015). These studies indicate the potential for reduced energy penalties from the post-combustion capture unit, which offers the potential for reduced equipment sizing and downstream costs. However, gas turbines modified in such a way as to offer FGR are expensive, and there is reduced flexibility and operability of systems with FGR in place.
2. Advanced integration takes place within the post-combustion capture unit. For example, Amrollahi et al. (2011) carried out an exergy analysis on integrated post-combustion capture with NGCC, finding the main irreversibilities to be in the absorber and stripper. Amrollahi et al. (2012) used the same model to analyse CO_2 capture process configurations including split solvent flows to the stripper, absorber intercooling, and lean vapour recompression, finding these latter options together to increase efficiency by 0.8%- points. Sipöcz and Tobiesen (2011) found that absorber intercooling with lean vapor recompression combined with exhaust gas recirculation (EGR) increased efficiencies by 1.2%-points. However, these have not been used in benchmarking literature which makes it harder to compare these data with general benchmarks, and therefore render them less relevant for this techno-economic study.
3. Alternative steam extraction points: HRSG units in NGCC plant operate at different pressure and steam conditions, offering additional opportunities for steam extraction for the capture unit. For example, Botero et al.(2009) simulated direct integration of the reboiler in the HRSG, suggesting up to 1%-point efficiency gain compared with standard IP/LP cross-over integration but offering potentially 20-30% costs reductions. Biliyok et al. (2015) find efficiency gains from partial integration with the LP drum.

Although the above integration options show promise in terms of cost and efficiency savings, this work uses a typical IP-LP integration with the basic amine loop. While this basic configuration may offer lower performance than more novel configurations, the techno-economic argument in this thesis proposes a generalizable model that can be applied to any of these systems, and so the basic configuration is used as an example for simplicity and ease of comparison.

3.4.2 Off design point studies of post-combustion capture with NGCC

Off-design operation in post-combustion CO_2 capture on power plant can refer to the process of allowing the capture unit to ramp up or down in response to changes in load of the power plant. It may also refer to varying the operation of the capture plant, either turning it off or on, or else varying capture levels, as is indeed the focus of this work.

Several studies have been published on the response of an MEA based post-combustion capture unit applied to part load operation of an NGCC. Mȍller et al. (2007) simulated three off-design operations, with part-load strategies, concluding that steam availability at part load should not be an obstacle to operation. However, this study only considers variations in solvent circulation, while assuming a constant regeneration temperature and a reboiler heat demand. Jordal et al. (2012) later carried out a more detailed modelling study to describe the response of an integrated post-combustion capture NGCC plant down to 40% load, finding tolerant conditions in the absorber and stripper, sufficient steam for the reboiler to maintain 90% capture and an efficiency drop of just 0.4%-points at full turndown. Karimi et al. (2012) and Rezazadeh et al. (2016) carry out similar studies to 50% and 60% load reductions respectively, reaching the same conclusions as Jordal et al. with respect to steam availability and capture plant operational stability.

Lucquiaud, Chalmers and Gibbins (2008) evaluated steam cycle configurations for flexible operation with assessing options for a clutched low pressure turbine, a throttled low pressure turbine and a floating pressure system. A throttled LP turbine maintains constant steam temperature into the LP cylinder and therefore maintains constant steam pressure and temperature to the capture plant reboiler, providing flexibility at relatively low cost, although throttling losses will be experienced. The floating crossover pressure configuration has the potential to provide the same

flexibility as a throttled low-pressure turbine, and offers the best net plant integrated efficiencies.

3.4.2.1 Variable CO_2 capture levels

Further studies have technically assessed impacts of variable capture levels on the behaviour and output of an integrated post-combustion CO_2 capture plant. Although these studies focus on coal, and do not account for the full integrated plant, they are useful by way of comparison with the patterns observed in this work's simulation.

Ziaii et al. (2009) developed an integrated CO_2 compression and steam power cycle in Aspen Custom Modeller. An optimisation for set capture level points is simulated under two dynamic scenarios. The work lost is calculated by a given equation based on a relationship between the reboiler duty and the steam requirement, rather than on a detailed integrated model. Ziaii's simulation work indicates that there is a 1:1 linear relationship between variation in reboiler duty and solvent flow rate, which implies a constrained model that does not parametrically assess the options for turndown. The simulation assumes little change (less than 2%) in lean loading with a change in load and as a result, an almost constant specific heat duty/kg CO_2 in the reboiler with capture level. Lower capture levels therefore have a much flatter design minimum for lean loading to reboiler duty than higher capture levels. Consequently, Ziaii's work finds that optimum lean loading changes significantly at higher capture levels and shifts rapidly towards higher capture levels given a specific CO_2/electricity price ratio.

Lucquiaud et al. (2009) detail that changes to steam flow for partial capture or bypass can be realised by placing a valve at the LP turbine inlet to vary the steam diverted to the reboiler unit, while ensuring that the temperatures at the inlet of the LP turbine experience relatively small temperature changes. This study asserts that bypass operation is only technically feasible on a retrofitted plant or a plant designed with overcapacity of the LP turbine, generator and compressor for this specific purpose, or sized with future demand considered.

Sanpasertparnich et al. (2010) carried out set-point simulations of capture level turn down in a coal plant operating post-combustion capture with MEA. The relationship between power loss in the power cycle, and reboiler heat duty is estimated with a polynomial, but not simulated in an integrated model. Stripper pressure and solvent

flow are varied. The study indicates that below a capture level design point, the electricity output penalty per tonne of CO_2 captured reduces only slightly with capture level. A flat relationship is observed until the efficiency of compression significantly increases below around 40% capture. The effect of capture efficiency reduction is simulated for all levels of flue gas load. The simulation indicates that flue gas bypass experiences a much lower reduction in electricity output penalty than the full flue gas load. As flue gas load is decreased, plant efficiency is seen to decrease and the energy penalty per tonne of CO_2 to increase, although the overall energy penalty on the system decreases. This is the result of bypassing the ID fan and solvent flow rate compressors.

Arce et al. (2012) assess cost minimisation of solvent regeneration through a dynamic model for process control. A second-order polynomial is used to approximate reboiler duty to CO_2 flow rate rather than an integrated model. By optimising CO_2 flow rate in response to CO_2 and electricity prices in a larger minimisation model, they found a 4.7% saving per month on operating costs.

Alhajaj et al. (2016) carried out a modelling study with an equilibrium based MEA capture plant model with NGCC investigating variable operation of capture levels in response to economic stimulus. They report:

"*the reboiler duty and liquid circulation rate per ton of CO_2 captured against degree of capture are constant and do not change with the flue gas bypass option. In fact, the solvent circulation rate per ton of CO_2 captured is observed to be linked to the optimal amine lean loading and the amount of CO_2 captured, which were similar at varying flue gas bypass ratio"*.

The stripper pressure and steam conditions however were fixed parameters in this study, which limits their findings.

3.4.3 Dynamic simulation

Further studies have examined the dynamic response of NGCC operating with post-combustion capture. These studies are important in ascertaining the likely response of the types of partial capture operation focused on in this work, and discussed in the above studies. Ceccarelli et al. (2014) published simulation results from a dynamic model of an integrated amine based post-combustion capture unit operating on an NGCC power plant. Their findings indicate that variations in flue gas flow rate from 100 to 40% at a ramp rate of 5%/min can be followed by steam and solvent flow variations with little latency, assuming sufficient size sumps in columns, or available

stores of solvent. The capture level was found to be controllable to within 3% points of the design capture rate. In a reboiler shut down, capture unit bypass condition, CO_2 rapidly drops off from compressor and the capture level increases to almost 100%. However, it was shown that bypass with circulating solvents leads to rapid cooling in the system and therefore higher lean loading on start-up. Shutting down the system totally would avoid this problem but wetting of the packaging would be required. In Ceccarelli et al. (2014), after the bypass operation, design capture levels were achieved in ten minutes, on the condition that there was sufficient solvent available. Ceccarelli concludes:

"*An amine-based CO_2 capture plant can demonstrate fast dynamics that allow for load following as well as fast shutdowns without additional CO_2 losses"*

He & Ricardez-Sandoval (2016) also more recently developed a dynamic model of an integrated amine-NGCC post-combustion capture plant. They found that in capture plant turn down conditions, while power outage changed instantly with reboiler duty, capture level took up to one hour settling time. However, coupled shifts in flue gas flow and reboiler duty saw capture levels following demand patterns over a day, moving smoothly between capture levels of 79% and 94%.

Further to the above described studies, an extensive review of the research on flexible operation and dynamic process modelling for optimising post-combustion CO_2 capture is presented in Bui et al. (2014).

3.4.4 Literature summary

Table 3-2 provides examples of some literature results of the baseline MEA capture simulations operating 90% capture with NGCC presented for comparison with this work.

Table 3-2 Simulation results reported in the literature for performance of 30 wt% MEA-based post-combustion capture on NGCC power plant.

Study	**Flue gas CO_2**	**Stripper pressure**	**Reboiler duty**	**Compressor work**	**Total EOP**	**Modelling software**
	Mol %	Bara	GJ_{th}/tCO_2	kWh_e/tCO_2	$kWhe/tCO_2$	
Amrollahi et al. 2011	3.8	1.72	3.86	83.3	377.778	GT PRO/UniSim Design software
Amrollahi et al. 2012	3.8	1.86	3.74	91.7	386	GT PRO/UniSim Design software
Biliyok et al. 2015	4.0	1.5	4.63	95.8	516	Aspen HYSYS validated with coal data
Biliyok et al. 2013	4.0	1.5	4	93.7	453	Aspen HYSYS validated coal data
Canepa et al. 2015	4.0	2.1	4.1	80.42	No value	GateCycle/Aspen Plus validated with coal data
Hu et al. 2017	4.0	2	4.04	70.8	359	UniSim Design software
Jordel et al. 2012	4.2	1.8	3.91	89.5	433.8	GT PRO/ProTreat
Karimi et al. 2012	4.0	No value	3.56	No value	322	UniSim Design software
Lindqvist et al. 2014	4.0	1.8	4	No value	377.6	CO2SIM developed at SINTEF/NTNU
Luo et al. 2015	4.5	2.1	4.54	100	418.6	GT PRO/Aspen plus
Sipocz & Tobiesen 2012	4.2	2	3.97	85.6	404.3	CO2SIM developed at SINTEF/NTNU
Rezazadeh et al. 2016	3.9	1.72	3.64	87.3	419.1	Aspen plus, validated with PACT

4 Methodology for optimising CO_2 capture levels

This chapter first introduces the concepts of design and operating CO_2 capture levels, and the specific Electricity Output Penalty of CO_2 capture. It goes on to diagrammatically describe the relationship between these two concepts. A methodology for maximising short run net cash flow of power plants operating CO_2 capture by varying the capture level is then described. The chapter goes on to define three low carbon electricity market case studies and develops parametric solutions describing the optimum capture level for each scenario.

4.1 The relationship between operating capture level, electricity output penalty and power plant electrical and CO_2 output

4.1.1 Design versus operating CO_2 capture levels

In this work, the capture level is defined as the proportion of total CO_2 produced through fuel combustion that is captured in the power plant, and therefore not released to the atmosphere. Lifecycle CO_2 emissions are outside the scope of this work.

Design capture level: Capture level is a design criterion of a carbon capture plant. There will be a specified capture level design point for a given capture plant, at a cost function minimum that accounts for both capital and operating costs. For a post-combustion capture plant, this optimisation dictates the size of columns, as well as the rich/lean loading requirements which in turn dictate solvent flow rate, condenser and pump sizing. Because energetic penalties are closely related to operating costs, it is likely that this design point will correspond somewhat with an energetic minimum for capture, but capital cost influence may offset this relationship.

Studies have been undertaken which have attempted to assess different energy penalties and costs associated with different design capture levels (Rao & Rubin 2006; Abu-Zahra et al. 2007a; Abu-Zahra et al. 2007b; Mac Dowell & Shah 2013). All these studies used a cost function to optimise the sizing and capture level of plants. The work by Rao and Rubin (2006) found economic optimum capture levels of between 80 and 90% for a post-combustion unit on a supercritical plant fired with bituminous coal, depending on the unit size, with smaller base plants encouraging higher capture levels. However, this work had certain limitations, such as using cost

per tonne of CO_2 avoided as a metric, which can provide non-comparable results when evaluating different fuel carbon intensities; it also limited simulations to an absorber height of 12m, although this has proven to be a conservative limit in the light of real construction projects. For example, the post-combustion Boundary Dam plant in Canada has an absorber height of 21m (Cansolv 2013).

Abu-Zara et al. (2007b) used a cost of carbon avoided and a levelised cost of electricity (LCOE) calculation without explicit absorber height restrictions for a 600 MW bituminous coal plant. They found that there was a shallow minimum at 90% capture for a cost per tonne of CO_2 avoided calculation, that increased only marginally down to 80% capture and up to 95% capture, before increasing significantly. The LCOE was found to increase gradually but non-linearly with capture level across the range of capture levels (25 – 99%). However, no CO_2 emission cost or other incentives for low carbon generation was included in this calculation.

Some work has suggested that capture levels above 90% should be considered for capture plant design, particularly when cost of electricity performance metrics are considered. MacDowell and Shah (2013) carried out an analysis of annualised costs of electricity with different capture levels under different carbon prices and found that capture levels higher than 90% can be optimal, in some market circumstances. However, compression is not explored in this work.

Bernier (2010) undertook a modelling study specifically on integrated NGCC with post-combustion capture and observed that the absorber was not chemically pinched so higher capture rates could be achieved, and indeed higher capture levels were optimal under their LCOE optimisation.

By contrast, Mores et al. (2014) used an equation based optimisation approach to consider the impact of design capture level from different CO_2 prices, specifically for a 788MW (standalone) NGCC. Their analysis concluded an optimal solution of 82.1% capture by means of a three capture-train arrangement, where 13.4% of the flue gas stream was bypassed and 94.8% of the CO2 was recovered at each unit. However, this work did not consider the possibility for varying operating capture levels. At nearly 95% capture efficiency in the columns, a solvent pinch was approached, and increasing flue gas flow rate in the absorber would have implications for approaching the flooding limit.

The range of design capture levels published in optimisation studies implies that the optimal capture level will be specific to a given plant, operating in given market conditions (for example, accounting for fuel prices, steel prices, carbon prices, water availability etc.). Therefore, in line with the current convention in large comparative power generation reports that assume a capture level of 90% (NETL 2015; DECC 2013), and for ease of comparison and correspondence with IEAGHG (2012b), a design capture level of 90% is used in this work.

Operating capture level: Deviations from the design capture point will be both possible and probable. Variation in absorber conditions could be intentional, using variations in flue gas inlet flow or solvent conditions to deliberately control the proportion of CO_2 absorbed, or unintentional, for example due to changes in ambient conditions or upstream power plant operation. Whether intentional and unintentional, variations in capture level will require control strategies to manage them. The analysis in this thesis assumes, therefore, that adequate control strategies would be in place to allow deliberate controlled variations to the operating capture level.

In this work, capture level refers to the operating capture level unless otherwise specified.

For a given plant, with a given design point capture level, there is a specific energy penalty associated with CO_2 capture which will vary with operating capture level (detailed in Section 4.1.2). Turning the capture level down or up will therefore impact net power plant efficiency and enable increased or decreased plant electrical output. Corresponding CO_2 emissions will rise and fall accordingly.

4.1.2 Electricity output penalty of CO_2 capture and compression

To quantify the energy loss associated with CO_2 capture and compression, the metric of specific Electricity Output Penalty (EOP) is described in the following paragraphs.

Specific EOP is defined as the total reduction in electricity exported due to the capture and compression of given mass of CO_2. EOP can be a useful metric for techno-economic analysis as it quantifies the energy penalty for a given mass of CO_2 captured as electricity which would otherwise be sold to the grid for income. By considering the EOP of a capture process at given conditions, opportunities for flexible power provision in the form of responsive changes to electricity export can be quantified from forced EOP variations through capture plant operating decisions,

independent of the main power plant. EOP is specific to the configuration and technology of each capture unit, and dependent upon the CO_2 concentration of the flue gas and the CO_2 capture level, but independent of the base power plant efficiency. That is, an inefficient power plant can have the same EOP as a more efficient one if the capture process and flue gas compositions are equivalent.

EOP is calculated from the net power output losses and the mass flow rate of CO_2 captured. The net power loss from a post-combustion capture process is described as the sum of four components as described below and in Equation 4.1:

1. Turbine power output losses resulting from the diversion of steam from the power cycle to the solvent reboiler

2. Electrical power to drive the CO_2 compression train

3. Electrical power to drive the booster fans situated before the post-combustion capture unit

4. Electrical power to drive solvent pumps and other small ancillary equipment

$$EOP\ \left(\frac{kWh_e}{tonne}\right) = \frac{loss\ of\ generator\ output + compression\ power + fan\ power + ancillary\ power\ (kW_e)}{mass\ flow\ rate\ of\ CO_2\ captured\ and\ compresed\ \left(\frac{tonne}{hr}\right)} \quad (4.1)$$

The four EOP components will be differently affected by changes to operating capture levels, and can together be used to analyse the energetic response of the whole CO_2 capture process.

The relationship between power plant output, plant efficiency and capture level is given in Equation 4.2. The net electrical power output ($Net\ electricity$) is equal to fuel input rate (MW_{th}) multiplied by the operating plant efficiency with capture (η_{cap}). The net plant efficiency with capture is in turn defined as the base plant efficiency without capture (η_{base}) minus the percentage point efficiency penalty of capture. The capture unit percentage-point efficiency penalty is the product of the EOP at a given capture level ($EOP(c)$), the mass of CO_2 generated per thermal unit of energy, or the fuel specific CO_2 intensity (ϵ), and the fraction of this CO_2 captured (c).

$$Net\ electricity = MW_{th}\ \eta_{cap} = MW_{th}\ (\eta_{base} - EOP(c)\ \epsilon\ c) \quad (4.2)$$

In turn, the net CO_2 emissions ($Net\ CO_2$) can be defined as equation 4.3.

$$Net\ CO_2 = MW_{th}\ \epsilon\ (1 - c) \quad (4.3)$$

This relationship between capture level, net plant efficiency, EOP, electrical power export and CO_2 emissions in a power plant operating CO_2 capture is illustrated schematically in Figure 4-1.

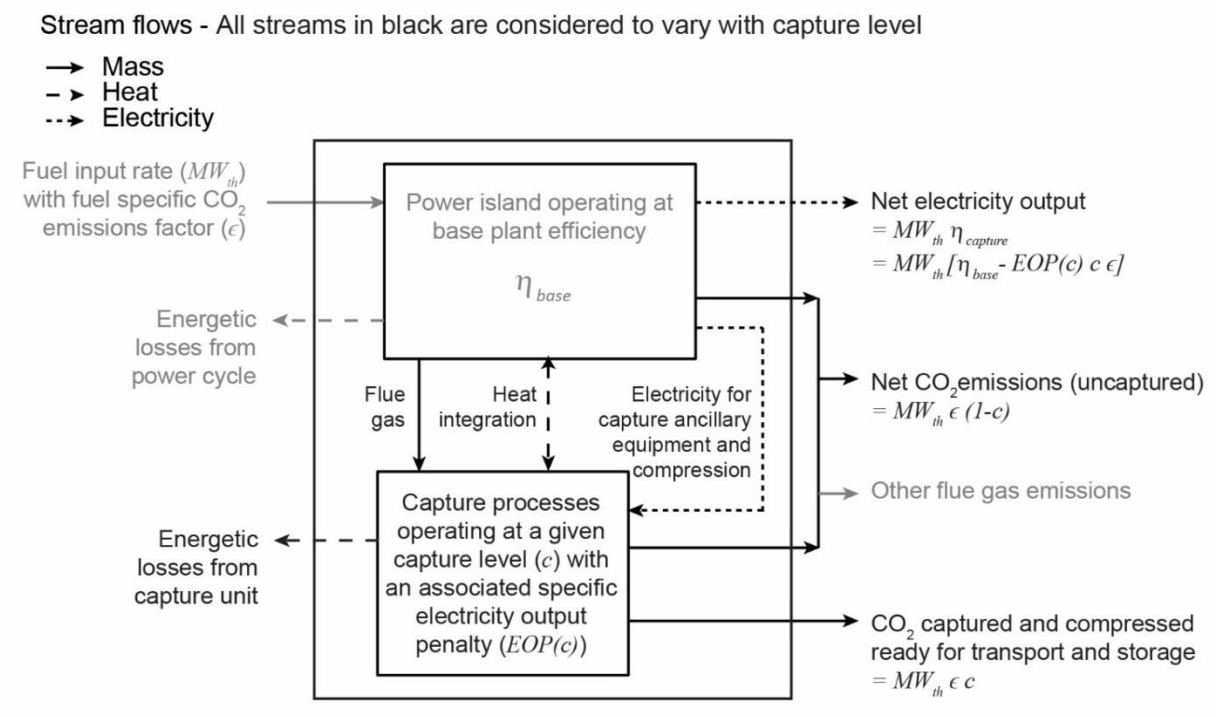

Figure 4-1 Schematic of the relationship between plant capture level and overall plant efficiency, net electricity output, EOP, CO_2 emissions, revenue streams and other costs for a CO_2 capture plant

The primary revenue stream for power plants is the sale of electricity. When operating with an electricity output penalty from CO_2 capture and compression, there is, therefore, a significant revenue penalty. It follows that a plant profitably operating CO_2 capture in a low carbon energy market must have an incentive to capture CO_2, either through fiscal penalties for emitting CO_2 (e.g. a carbon price), or through a premium payment for low carbon electricity. The net plant income, accounting for revenue generated by electricity exports and net economic gains from CO_2 capture, therefore depend on the market prices of wholesale electricity, as well as CO_2 and/or premium low carbon electricity payments. The balance of these market prices provides a direct relationship between plant net income and the level of CO_2 capture operated. The market value of CO_2 abatement is likely to fluctuate less than electricity price, but has

the potential to change over longer time periods as policies and markets develop and shift, and as carbon budgets are reduced in line with scientifically advised greenhouse gas reduction targets, e.g. IPCC (2014). In low carbon electricity markets there will therefore be times when the provision of electricity is more valuable than the abatement of CO_2, and vice versa, with the frequency and likelihood of this shift being dependent upon on several factors, including shifts in demand for additional generation above baseload, and the required reductions in CO_2 emissions at any given point.

4.1.3 Short Run Net Operating Cash Flow

While investment decisions are typically made on predicted values of LCOE, operating decisions for power plants operating in markets will be made based on short run net operating cash flow (SRNCF). The SRNCF of a power plant with CO_2 capture can be defined as the difference between the plant revenue and the short run marginal cost (SRMC) for a given time period of operation, often covering a single set of market conditions. SRMC is the operating cost of a plant, independent of whether a plant is operating or not (detailed in Chapter 2). When SRNCF is positive, operating the plant generates earnings, and continuing to run the plant when SRNCF is negative will result in the operator losing money. Therefore, zero or negative values of SRNCF will generally lead to the plant being turned off where feasible, although in some cases a plant could operate at low load to avoid shutdown penalties.

The general equation for SRNCF for a power plant with CO_2 capture is defined in Equation 4.4.

$$SRNCF = income\ from\ elecricity\ sales - fuel\ costs - CO_2\ emission\ costs - CO_2\ capture\ variable\ opex - \ base\ plant\ variable\ opex \quad (4.4)$$

Power plant income is primarily generated from electricity sales, and thus income is a function of electricity output and electricity market selling prices.

An operator will aim to maximise short run net cash flow within the markets in which the plant operates. In this way, power plants operating flexibly with CO_2 capture will be able to access the potential for increased cash flow in low carbon electricity systems by varying the amount of CO_2 captured and compressed in response to dynamic, shifting markets of electricity, carbon, and fuel prices. This is conceptually illustrated in Figure 4-2.

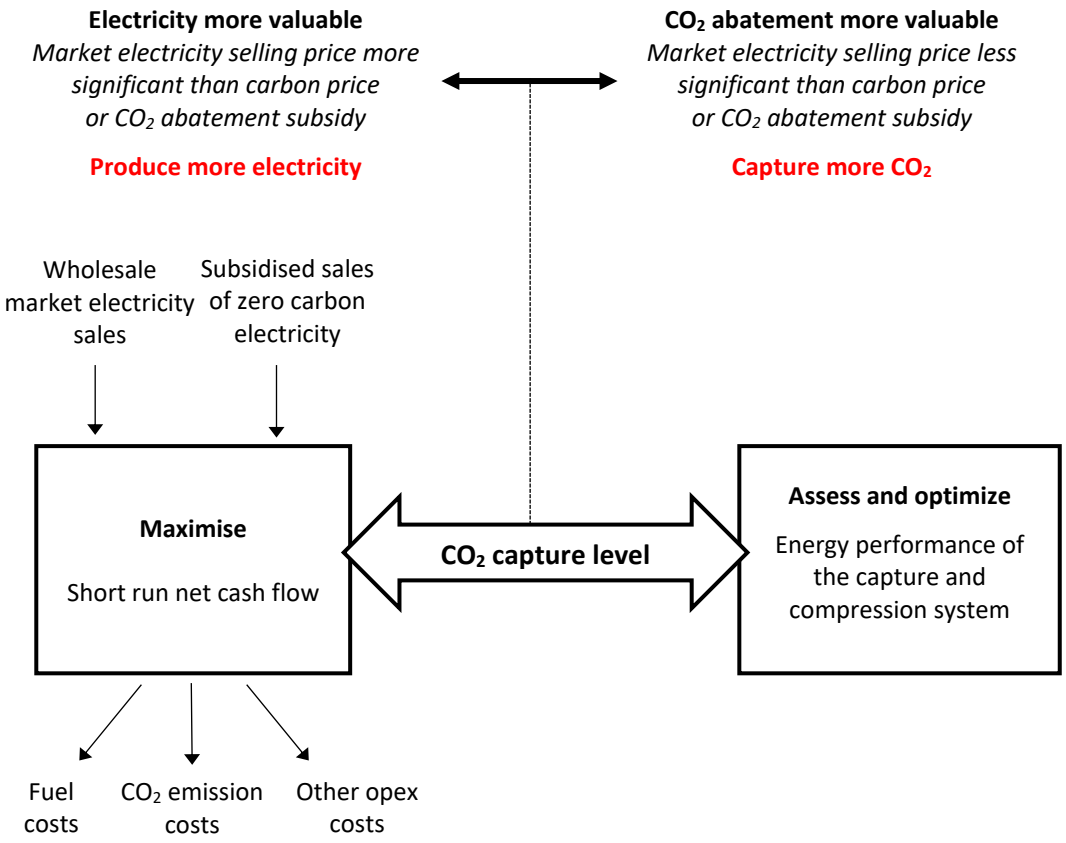

Figure 4-2 A schematic diagram illustrating the concept of maximising short run net cash flow for power plants with CCS through variation in plant capture level in response to market incentives, with respect to individual plant performance

4.1.4 Methodology for optimising operating capture level

The SRNCF of a power plant operating with CCS is dictated by real time values of electricity, fuel and CO_2 emissions abatement. The capture level of the plant changes the amount of electricity and CO_2 produced for a given fuel rate, and so it is possible to vary CO_2 capture operations with the real-time market value of each commodity to maximise cash flow, thereby optimising CO_2 capture level. By calculating the SRNCF as a function of capture level, it is possible to determine the optimal operational capture level, found at the maximum of the differential of SRNCF with respect to capture level, as shown in Equation 4.5, where c_{opt} is the optimised capture level.

$$c_{opt} = \frac{dSRNCF}{dc} = 0 \qquad (4.5)$$

4.2 Low carbon electricity market case studies

As detailed in Chapter 2, CO_2 emissions are commonly included in techno-economic studies using a carbon price. However, investment decisions based on unstable carbon markets are difficult, and instead alternative fiscal methods for incentivising low carbon electricity may be used for financing CCS (and other low carbon) projects, particularly in the short to medium term.

This work therefore considers additional market incentives for low carbon electricity systems beyond the introduction of a CO_2 price. Three policy mechanisms for the inclusion of absolute CO_2 emissions are assessed.

The first case, called a “Carbon Price” market scenario considers an open wholesale electricity market with a carbon price only. The second and third cases, respectively called “Proportional Subsidy” and “Counterfactual Subsidy”, consider scenarios where plants operate within wholesale electricity and carbon markets, and with additional premium electricity price payments made available for zero carbon electricity generation. The difference between these two cases is how ‘zero carbon electricity’ eligible for the premium price is defined.

In the “Proportional Subsidy” market scenario, zero carbon electricity output is assumed to be the net exported electricity output proportional to the CO_2 capture level. This definition implies that an equivalent plant without capture is used as a counterfactual. In the “ Counterfactual Subsidy” market scenario, CO_2 emitted by a plant is compared with an accepted, defined, standard grid counterfactual CO_2 emission intensity or Emission Limit Value (ELV). The total CO_2 emissions of the CCS power plant are compared to this counterfactual to determine the amount of non-zero carbon electricity that is generated at this standard grid CO_2 emission intensity. This amount of non-zero carbon electricity is valid for sale on a wholesale market. The remainder of the electricity exported by the plant is then defined, across all plant, as zero-carbon electricity valid for premium low carbon electricity payments. It follows that when the overall emissions intensity of the plant is equal to or greater than the ELV, export of zero carbon electricity would be zero, and the definition of SRNCF reverts to that of the carbon price market scenario.

It is also possible that plants that are unable to meet an ELV would not be allowed to operate, at the expense of using the flexibility of the CCS power plants. An ELV can either operate as a limit that may never be exceeded by any plant, in which case the

minimum allowable capture level would be the point at which the plant CO_2 emissions intensity met that of the ELV. Alternatively, CO_2 as a greenhouse gas rather than a pollutant based on local concentration measurements can be measured in annual emissions to meet this ELV. This allows for additional flexibility for the electricity grid network and additional available income for plant operators. This work assumes that the regulatory framework recognises the value of flexibility.

These case studies are summarised in Table 4-1.

Table 4-1 Summary of three low carbon electricity market case studies

<table>
<tr><td>CCS is incentivised by a price on CO_2
Specific costs incurred for the mass of CO_2 emitted to the atmosphere (non-captured CO_2).</td><td colspan="2">CCS is incentivised by a premium subsidy paid for ‘carbon zero’ electricity
Net electricity output ----► Premium electricity deemed ‘carbon zero’ at
----► ‘Carbon intensive’ electricity sold at market price</td></tr>
<tr><td>Carbon price

Total exported electricity is sold at electricity market price ($£_E$).

A carbon market price ($£_{CO2}$) is paid for the net CO_2 emissions.</td><td>Proportional subsidy

Carbon zero electricity is defined as the total exported electricity multiplied by the capture level. This electricity is sold at a premium price ($£_{PE}$).

The remainder of exported electricity is sold on the wholesale market ($£_E$).</td><td>Counterfactual subsidy

Carbon intensive electricity is given a set Emissions Limit Value (ELV) ($kgCO_2/MWh_e$), based upon carbon budgets. The amount of electricity generated at the carbon intensity of the ELV can then be calculated from the total mass of CO_2 emitted by a plant after CO_2 capture. This electricity is sold on the wholesale electricity market ($£_E$).

Carbon zero electricity is defined as any electricity exported in addition to electricity generated at the ELV. This electricity is sold at a premium price ($£_{PE}$). When the total emissions intensity of the plant is equal to or greater than the ELV, export of zero carbon electricity is zero, and the SRNCF reverts to that of the carbon price scenario.</td></tr>
<tr><td colspan="3">Income from electricity sales at market price $£_E$</td></tr>
<tr><td>$= £_E[Net\ electricity]$</td><td>$= £_E\,[Net\ electricity]\,(1-c)$</td><td>$= £_E\,[Net\ CO_2]\,ELV^{-1}$</td></tr>
<tr><td>Cost of CO_2 emissions</td><td colspan="2">Income from carbon zero electricity sales at premium price $£_{PE}$</td></tr>
<tr><td>$= £_{CO_2}[Net\ CO_2]$</td><td>$= £_{PE}\,[Net\ electricity]\,c$</td><td>$= £_{PE}([Net\ electricity]-[Net\ CO_2]\,ELV^{-1})$</td></tr>
</table>

The definitions of income and CO_2 costs given in Table 4-1 can then be combined with Equations 4.2, 4.3 and 4.4, and expanded to define short run net cash flow as a function of capture level for each market scenario. Fuel input is considered constant in this analysis and is therefore a function of capture level here. The variable costs of the base power plant are also assumed to be unaffected by capture level changes in this work.

$$SRNCF_1 = MW_{th}\left[£_E[\eta_{base} - EOP(c)c\,\epsilon] - £_f - £_{CO_2}(1-c)\epsilon - vc_{cap}\,c\,\epsilon - vc_{base}\eta_{base}\right] \quad (4.6)$$

$$SRNCF_2 = MW_{th}\left[£_E\,[\eta_{base} - EOP(c)c\,\epsilon](1-c) + £_{PE}\,[\eta_{base} - EOP(c)c\,\epsilon]c - £_f - £_{CO_2}\,(1-c)\epsilon - vc_{cap}\,c\,\epsilon - vc_{base}\,\eta_{base}\right] \quad (4.7)$$

$$SRNCF_3 = MW_{th}\left[£_E\,\epsilon\,(1-c)\,ELV^{-1} + £_{PE}([\eta_{base} - EOP(c)c\,\epsilon] - \epsilon\,(1-c)\,ELV^{-1}) - £_f - £_{CO_2}\,(1-c)\epsilon - vc_{cap}\,c\,\epsilon - vc_{base}\,\eta_{base}\right]$$

$$[Net\ CO_2]\,ELV^{-1} \geq [Net\ electricity] \Leftrightarrow SRNCF_3 = SRNCF_1 \quad (4.8)$$

Where:

$SRNCF$	Short run net operating cash flow	£/hr
MW_{th}	Rate of energetic input from fuel	MW_{th}
η_{base}	Efficiency of base power plant operating without CO_2 capture	MWh_e/MWh_{th}
η_{cap}	Efficiency of base power plant operating with CO_2 capture	MWh_e/MWh_{th}
c	Fraction of CO_2 captured from flue gas; operating capture level	–
$EOP(c)$	Electricity output penalty at a given capture level	kWh_e/tCO_2
ϵ	Fuel specific CO_2 emissions factor	tCO_2/MWh_{th}
$£_{CO_2}$	Cost of carbon emissions	£/tCO_2
ELV	Standard electricity grid counterfactual CO_2 intensity	$kgCO_2/MWh_e$
$£_E$	Wholesale market electricity selling price	£/MWh_e
$£_{fuel}$	Fuel costs per thermal input	£/MWh_{th}
$£_{PE}$	Premium electricity price for zero carbon electricity	£/MWh_e
vc_{base}	Specific variable costs of power plant per unit electricity gen.	£/MWh_e
vc_{cap}	Specific variable costs of capture plant per tonne CO_2 captured	£/tCO_2

Subscripts

1	”Carbon price” scenario
2	“Proportional subsidy” scenario
3	“Counterfactual subsidy” scenario
bp	Capture plant bypass

As described in Chapter 2, full bypass of the CO_2 capture process can offer an additional operating option and is optimal where bypass provides higher SRNCF than operating at any available capture level. Full capture plant bypass is defined as a diversion of the total quantity of flue gas entering the CO_2 capture or processing units, directly to the stack, fully bypassing the capture process and thereby enabling electricity previously utilised in CO_2 capture to be exported to the grid.

As there is no low carbon electricity generated during capture plant bypass the definition of SRNCF at bypass is the same for all three market cases, given in Equation 4.9.

$$SRNCF_{bp} = MW_{th}\left[£_E\left[\eta_{base} - anc\right] - £_{fuel} - £_{CO_2}\,\epsilon - vc_{base}\,\eta_{base}\right] \qquad (4.9)$$

Where *anc* is a fixed penalty for ancillary equipment operating during bypass in kWh_e/tCO_2.

It is likely that at least some capture plant ancillary equipment need be maintained in operation during a full bypass. For the quantitative analysis reported in this paper, the energy associated with this ancillary equipment is modelled, excluding the flue gas inlet fan and the CO_2 compressors, running with energy penalty equivalent to 90% capture.

When SRNCF at bypass exceeds SRNCF at optimum capture, a capture plant bypass operating regime is the optimal operating scenario, as in Equation 4.10.

$$SRNCF_{bp} \geq SRNCF_{(copt)} \Leftrightarrow Operate\ bypass \qquad (4.10)$$

4.3 Analytical solutions for calculating optimum capture levels

Operating at optimal operating capture level or bypass regime provides a CCS power plant with net maximum SRNCF for given market conditions. Analytical solutions to the optimum capture level (Equation 4.5) are given in Equations 4.11 to 4.13, finding maxima with respect to capture level for each of the three low carbon electricity market case studies SRNCF equations given in Equations 4.6 to 4.8.

The optimal operating capture level with a carbon price only:

$$c_{opt_1} = \left(\frac{£_{CO2} - v_{cap}}{£_E} - EOP(c_{opt})\right)\frac{dc_{opt}}{dEOP(c_{opt})} \qquad (4.11)$$

The optimal operating capture level with a proportional subsidy for zero CO_2 electricity:

$$c_{opt_2} = \frac{£_{CO2} - v_{cap} + (£_{EP} - £_E)\frac{\eta_{base}}{\epsilon} - £_E\, EOP(c_{opt})}{£_E \frac{dEOP(c_{opt})}{dc_{opt}} + (£_{EP} - £_E)\left(c_{opt}\frac{dEOP(c_{opt})}{dc_{opt}} + 2EOP(c_{opt})\right)} \quad (4.12)$$

The optimal operating capture level with a subsidy for zero CO_2 electricity compared against a counterfactual emission intensity:

$$c_{opt_3} = \left(\frac{£_{CO2} - v_{cap} + \frac{£_{EP} - £_E}{ELV}}{£_{EP}} - EOP(c_{opt})\right)\frac{dc_{opt}}{dEOP(c_{opt})} \quad (4.13)$$

An analysis of these results presented in Equations 4.11 to 4.13 indicates a general conceptual equation for optimal capture level, given in Equation 4.14 below.

$$c_{xopt} = \frac{\frac{Financial\ opportunity\ of\ capture}{Financial\ opportunity\ of\ electricity\ sales} - Electricity\ output\ penalty\ of\ capture}{Change\ in\ electricity\ output\ penalty\ with\ the\ capture\ level} \quad (4.14)$$

The optimum capture level will, therefore, depend on the ratio between carbon capture incentives (carbon price, premium electricity price difference) and electricity prices, with high carbon prices or subsidies incentivising high capture levels and high market electricity prices incentivising lower capture levels.

Optimum capture level is not a function of fuel price when the base plant operates at full load as fuel input is constant. Optimum capture level is also independent of base plant efficiency and fuel CO_2 intensity, except in the proportional subsidy scenario. Variable capture costs are assumed to be constant in this work since they are usually small compared with other costs.

For a given market price condition therefore, the optimum capture level contours are entirely specific to the shape of the relationship curves between EOP and capture level. The optimal capture analytical solutions illustrate that maximum SRNCF is achieved by balancing changes in EOP against financial benefits for decreasing the amount of CO_2 emitted. The impact of the ratio of capture incentives to wholesale electricity price is tempered by both the absolute and the change in EOP with capture level; the nature of the plant's energy loss response to changes in capture level.

Higher absolute values of EOP will lead to lower optimal capture levels. However, the significance of this difference when operating in markets will be dictated by the gradient of the EOP curve – a steeper curve will lead to a larger change in revenue for a smaller change in market dynamics. It is important to note that relationship between the EOP and the capture level is effectively embedded in the design of the CCS power plant, and could, in practice, be engineered by design at capture levels above 90% if there were a financial incentive to do so.

In the following chapters, these analytical solutions are used to find optimal capture levels for NGCC plant operating with post-combustion CO_2 in possible market scenarios for each low carbon market case study. First, the specific relationship between EOP and capture level must be ascertained. The following chapter provides a process modelling basis for this relationship.

5 Simulation of integrated NGCC plant with amine based post-combustion CO_2 capture

This chapter presents a process model of an 800MW (nominal) NGCC plant integrated with an amine based post-combustion CO_2 capture and compression unit. The integrated model can simulate off-design conditions, specifically in terms of the operating CO_2 capture level. Subsequently, the principal output from the simulation is a continuous relationship between the operating CO_2 capture level and net electricity output penalty per kg of CO_2 captured (the specific capture energy penalty in terms of electricity no longer available for sale). This relationship considers the complete integrated plant, accounting for off-design behavior in the steam cycle, capture plant and compression train, including turbomachinery, separation columns, heat exchangers and key pressure drops from variations in steam extraction.

This chapter begins with an introduction to the process simulated in this work (Section 5.1) and then presents the modelling methodology in detail (Section 5.2). The chapter concludes with some initial results (Section 5.3).

5.1 Modelling methodology

5.1.1 Simulation design basis

The design basis of the model presented in this thesis is based on a 2012 study by Parsons Brinkerhoff for IEAGHG, "CO_2 capture on Natural Gas Fired Power Plants" (IEAGHG, 2012). 'Scenario 3a' in this study provides simulation results for an integrated NGCC with post-combustion capture, using GTPRO and Thermoflex for the NGCC model, and Aspen Plus for the capture and compression models. The simulation undertaken for this thesis initially replicates the NGCC configuration and input conditions from IEAGHG (2012b) 'Scenario 3a'. The IEAGHG (2012b) configuration replicated in this work comprises a 2x1 NGCC, with two gas turbines, and two HRSGs feeding into a single triple pressure reheat steam turbine train. This choice is justified in the IEAGHG (2012b) report as the multi-shaft plants are preferable for post-combustion capture, due to the double flow low pressure steam turbines. Two post-combustion capture and compression trains used as a single unit

would require unfeasibly large absorber and stripper diameters. Figure 5-1 provides a block diagram of the simulation.

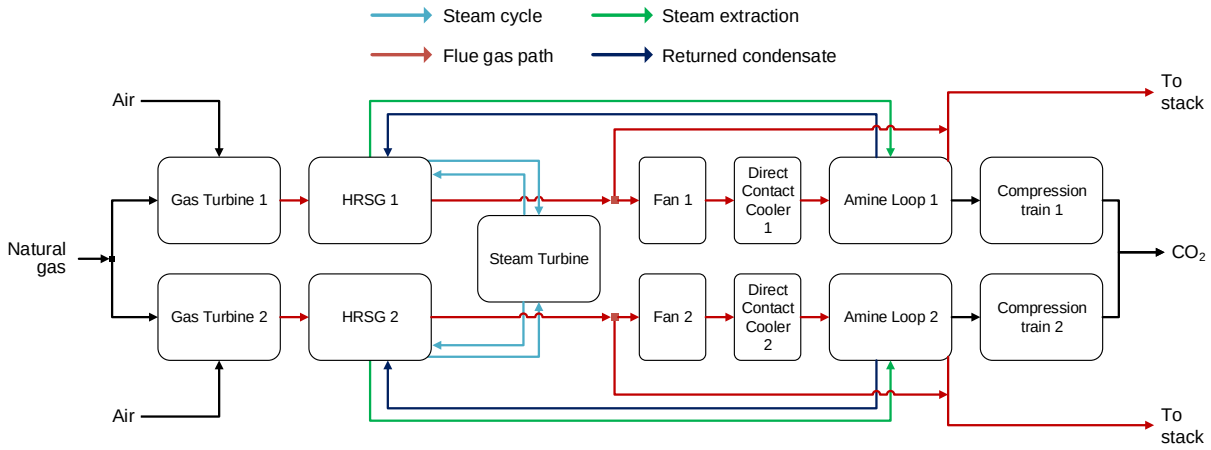

Figure 5-1 Block diagram illustrating the configuration of Aspen Plus simulation undertaken in this work, comprising integrated 2x1 NGCC with amine-based post combustion CO_2 capture and compression

In this thesis, modifications are made to the IEAGHG (2012b) study in the following sections:

- Modifications to the steam cycle are made to provide an 'oversized' unit to allow for flexible operation that can accommodate additional steam released from the post-combustion capture unit in the bypass condition.
- The post-combustion capture unit simulated in IEAGHG (2012b) is based on 35 wt% MEA, higher than the 30 wt% standard used in the literature. It is also not validated with natural gas flue gas. This work therefore develops a new capture plant model optimized for operation at 90% capture with 30 wt% and verified with pilot plant data from the CO_2 Technology Centre operating with natural gas flue gas.
- The compression train presented in this thesis is based upon a paper by Liebenthal and Kather (2011) that utilizes industrial experience of large scale integrally geared CO_2 compression as insufficient information was provided in the IEAGHG (2012b) report to simulate off design point compressor operation.

Simulation work for this thesis was carried out in Aspen Plus Version 8.0, process modelling software with an extensive database of pure component and phase equilibrium data and the ability to model various CO_2 separation technologies. This software does not fully include the ability to model off-design behaviour, therefore

this was simulated with FORTRAN coding in the Aspen model, using correlations found in the literature as detailed in the following sections.

The property packages used in this work are presented in Table 5-1.

Table 5-1 Property packages used in Aspen Plus simulations

Process/streams	**Property package**
Natural gas combustion and flue gas	Peng-Robinson with Boston-Mathias alpha function
Steam and free water	NBS/NRC steam table equation of state
Pure or nearly pure CO_2 streams	Soave-Redich-Kwong equation of state
Amine absorption loop	AspenPlus MEA property package

Figure 5-2 presents a process diagram for the integrated model developed for this thesis. The following sections provide detail on the modelling methodology for each element of the simulation.

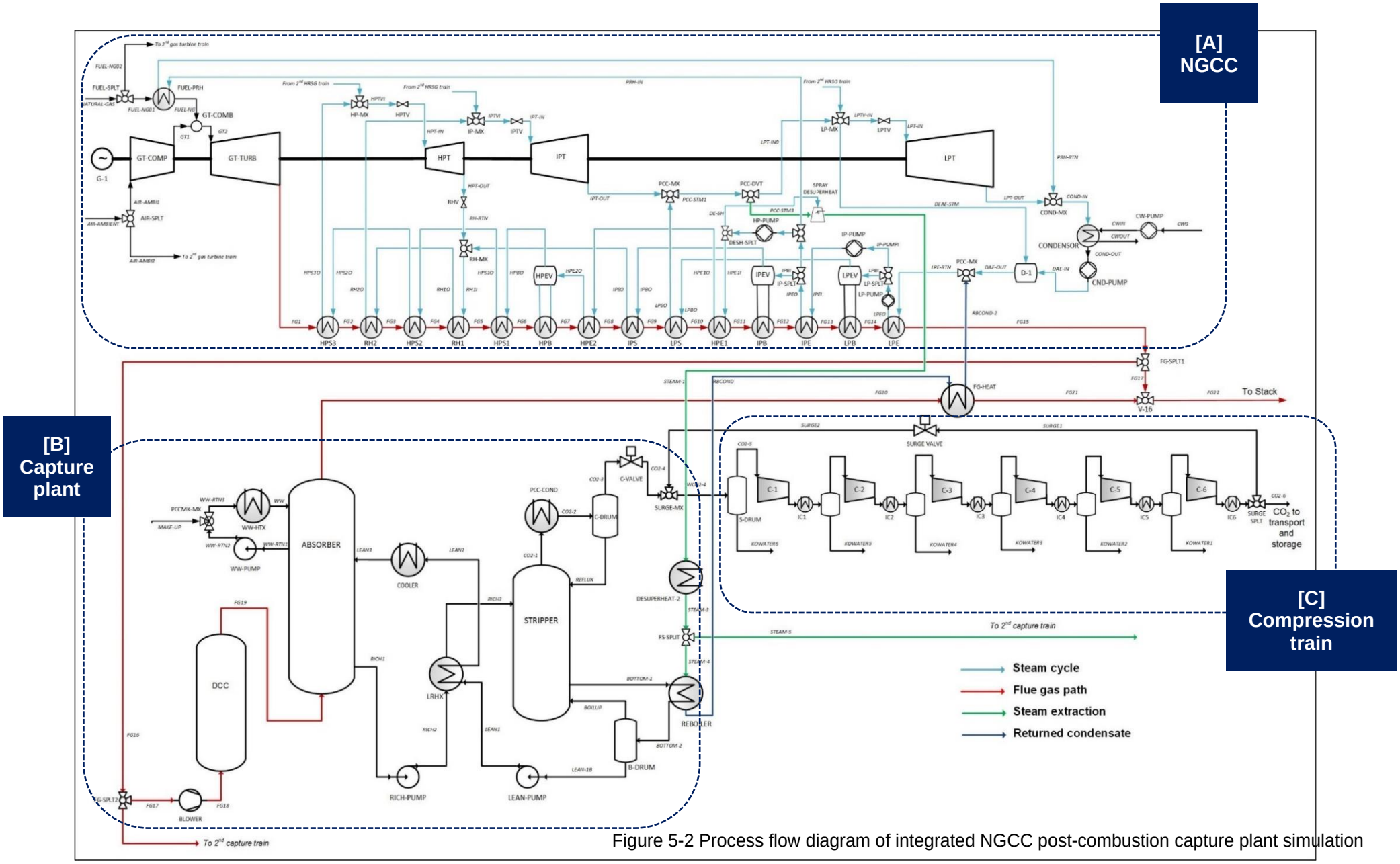

Figure 5-2 Process flow diagram of integrated NGCC post-combustion capture plant simulation

5.1.2 Natural gas combined cycle model

Input data for the initial simulation based on Scenario 3a of the IEAGHG (2012b) report is listed in Table 5-2. Data is taken from process stream and Thermoflex summary results in Appendix D and E of IEAGHG (2012b). Data not available in the IEAGHG (2012b) report was taken directly from GE the turbine manufacturer.

Table 5-2 Input data for NGCC simulation. Sources IEAGHG (2012b), GE Power (2015)

Parameter	Units	Value
Fuel inlet flow rate	t/hr	59.86
Fuel inlet pressure	Bar	30.43
Fuel inlet temperature	C	9 C
Air inlet flow rate	t/hr	2365
Air inlet pressure	Bar	1.013
Air inlet temperature	C	9
GT outlet temperature	C	640
GT compression ratio		18.4
GT compressor isentropic efficiency	%	85
GT turbine isentropic efficiency	%	89
GT gross output	MW	-295.16 (x 2 units)
Natural Gas fuel consumption (LHV)	MJ/s	1546.6
Fuel composition	Vol%	
Methane		89
Ethane		7
Propane		1
n-Butane		0.1
n-Pentane		0.01
Carbon Dioxide		2
Nitrogen		0.89
LHV@25C	kJ/kg	46506
HP/Reheat inlet temperature	C	600
HP/IP/LP pressure	bar	170/40/3.5
HP/IP/LP turbine efficiency	%	87.7/92.4/90.5
HRSG gas side pressure drop	bar	0.033
Pump isentropic efficiencies	%	60
Cooling water temperature	C	14.36

5.1.2.1 Gas turbine

The GE 9F.05 gas turbine (previously known as the GE 9FB (GE 2015)) is used as the reference turbine for this work, in accordance with IEAGHG (2012b). The IEAGHG (2012b) report selected this model as it was the only F-class turbine marketed in Europe at the time, and was also being actively considered for syngas firing (allowing for fuel flexibility). While more advanced gas turbine models (G, H and J-class) offering higher efficiency and greater operational flexibility have now taken over as the most common technology choice for heavy duty gas turbine sales[5], F-class turbines remain an industry standard. Publicly available performance data on the state-of-the-art advanced turbines is limited, and modelling the same turbine as IEAGHG (2012b) allows verification with their published simulation results. As this work examines the flexibility of the capture plant and the steam cycle, the gas turbine is considered to run at steady load throughout the analysis presented in this thesis, and so the performance of the gas turbine has limited significance beyond baseline efficiency. If this work were to be extended into flexible operation of the gas turbine, it could be advisable to upgrade the reference turbine simulation to a more advanced model where part load efficiency penalties and variations in flue gas compositions would be relevant.

Gas turbine modelling parameters are taken from the GE Power 9F.05 gas turbine data factsheet (GE Power 2015). Compressor and turbine efficiencies are inferred from the turbine air/fuel inlet temperatures and turbine flue gas exit temperature provided in the IEAGHG (2012b) simulation results (IEAGHG (2012b) Appendix E).

The compressor and turbine were modelled in Aspen Plus with ‘COMPR’ blocks input with isentropic efficiencies. The combustor was modelled as an equilibrium Gibbs reactor ‘RGIBBS’.

5.1.2.2 HRSG and Steam Cycle

A 2 GT/HRSG + 1 ST combined cycle arrangement is used in this simulation as a common configuration that provides greater efficiency and flexibility than a 1+1 arrangement (GE Power 2015). The triple-pressure reheat system employed is typical for combined cycle gas turbines of this class. The high pressure and reheat steam

[5] http://www.power-eng.com/articles/print/volume-119/issue-8/features/the-fall-of-the-f-class-turbine.html, https://www.asme.org/engineering-topics/articles/energy/a-new-era-for-natural-gas-turbines

conditions from the IEAGHG (2012b) report (detailed in Table 5-2) are in accordance with performance conditions provided in recent GE data sheets (GE 2015) and are considered typical conditions for plants built in the near future.

The steam cycle configuration used in this work, illustrated in Figure 5-2, is adapted from IEAGHG (2012b), Scenario 3a. The steam cycle comprises an HP, an IP and an LP turbine, a condenser and condensate pump. The feedwater is split into the two HRSG trains. Each HRSG train comprises:

- Three low pressure (LP) heating stages: LP economiser, LP boiler/evaporator and LP superheater
- Five intermediate pressure (IP) heating stages: IP economiser, IP boiler/evaporator, IP superheater, and two additional reheat stages including steam exiting the HP turbine
- Six high pressure (HP) heating stages: two HP economisers, HP boiler/evaporator, and three HP superheating stages.
- Three pumps: LP, IP and HP

After each pressure stage, steam from the two HRSGs is mixed prior to each steam corresponding turbine inlet.

Steam flow rates, pressures and heat exchanger temperature approaches in the HRSG were replicated from the IEAGHG (2012b) report, Scenario 3a.

5.1.2.3 Full load results and verification of NGCC

Results from the initial NGCC simulation directly replicating Scenario 3a of the IEAGHG (2012b) report in Aspen Plus are summarized in Table 5-3, providing a comparison of the output differences between the Aspen Model and the IEAGHG (2012b) simulation. This initial step provides a validation check for the Aspen Plus NGCC model developed for this thesis. The maximum errors are seen in the GT output and the final HRSG flue gas exit temperature. These differences may be due to differences in the property packages used for the natural gas combustion and flue gas (thermo-physical methods are not given in IEAGHG (2012b)).

Table 5-3 Comparison of combined cycle model with IEAGHG (2012b)

Parameter	IEAGHG (2012b)	Aspen Plus replication	delta
Net work GT (MW)	-295.16	-302.89	2.62%
Net work ST (MW)	-269.81	-269.85	0.02%
Gas turbine exit temperature (°C)	639.8	639.8	0.00%
Flue gas composition (mol %)			
H_2O	0.0882	0.0882	0.00%
N_2	0.7427	0.7427	0.00%
O_2	0.118	0.118	0.00%
CO_2	0.0426	0.0426	0.00%
Ar	0.0085	0.0085	0.00%
HRSG gas exit temperature (°C)	81.8	85.1	4.03%

5.1.2.4 Updates to IEAGHG (2012b) NGCC model

To enable flexible behavior in the steam cycle of the NGCC, the following adaptations were introduced, building on IEAGHG (2012b) ‘Scenario 3a’:

1. This initial simulation of an NGCC replicated from IEAGHG (2012b) Scenario 3a is designed for a capture plant operating 90% capture, where nearly half of the low-pressure steam is diverted to the PCC unit for solvent regeneration. The simulation developed for this thesis provides additional flexibility by oversizing aspects of the steam cycle, thereby providing capacity for additional steam to pass through the LP turbine during capture plant turn down or bypass. The LP turbine, the condenser and the condenser cooling water flow rate are re-proportioned corresponding to the maximum steam flow rate, which is determined by full bypass operation, where all low-pressure steam is passed through the LP turbine and condenser without a divert to the PCC unit. The new cooling water flow is dictated by a maximum increase in cooling water of 11°C (a limit set in IEAGHG (2012b)). Gas turbine conditions remain unchanged, as do IP and HP steam turbine conditions.
2. In IEAGHG (2012b), the condensate return from the PCC unit is returned to the condenser. In this work, the condensate from the PCC unit is directed back

to the low pressure economiser (LPE) to take advantage of any heat remaining in this stream. As such, the LPE must also be oversized.

3. Finally, there is no deaerator explicit in the simulation presented in IEAGHG (2012b), so a deaerator stage is added in this work after the condensate pump, heated by a small LP steam bleed.

Table 5-4 summarizes the design-point impact of these changes made to oversize the plant for added flexibility developed for this thesis, compared with the initial Aspen Plus replication of 'Scenario 3a' IEAGHG (2012b).

Table 5-4 Updated parameters for oversized combined cycle simulated for flexible operation

Parameter	**IEAGHG (2012b)**	**Replication (this work)**	**Revised replication for flexible simulation (this work)**
Net work GT (MW)	-295.16	-302.89	-302.89
Net work ST (MW)	-269.81	-269.85	-340.41
Steam to LP turbine (kg/s)	113.6	113.6	216.9
HRSG flue gas exit temperature (°C)	81.8	85.1	80.38
Condenser pressure (bara)	0.0387	0.0387	0.0381
Cooling water for condenser (kg/s)	5618	5618	10972

To simulate off-design conditions of the variable steam flows to the PCC unit, the following methods were used for each component:

5.1.2.4.1 Heat exchangers

Variations in steam extraction to the PCC unit will affect change in the condenser as only steam not diverted to the PCC plant is condensed in the steam cycle condenser (the diverted steam is condensed in the PCC reboiler and re-routed as condensate). The proportion of steam diverted will also impact the temperature of condensate passing into the low-pressure economizer. Any additional upstream impacts in other heat exchangers are assumed to be negligible for this HRSG configuration while the GT is operated at constant output.

Off-design behavior of the condenser and the LPE heat exchangers is simulated by considering the variation in overall heat transfer coefficients under different conditions. The overall heat transfer coefficient of a heat exchanger, excluding any

fouling effects, can be expressed as a general equation given in Equation 5.1 (Cengel & Ghajar 2015):

$$\frac{1}{UA} = \frac{1}{h_c A_c} + \frac{dx_w}{k_w A} + \frac{1}{h_h A_h} \quad (5.1)$$

Where U is the overall heat transfer coefficient (W/m^2 K), A is the contact area of each fluid side (m^2), h is the convective heat transfer coefficient for each fluid (W/m^2 K), dx_w is the thickness of the exchanger wall (m), and k_w is the thermal conductivity of the wall material (W/mK). Subscripts *c* and *h* refer to the hot and cold sides of the heat exchanger.

Using the Nusselt number, convective heat transfer coefficients can be considered in the empirical correlations in Equation 5.2 (Cengel & Ghajar 2015):

$$Nu \equiv \frac{hD}{k} = CRe^n Pr^m \quad (5.2)$$

Where Nu is the Nusselt number, Re the Reynolds number and Pr the Prandlt number. D is the diameter, and k the thermal conductivity of the fluid. C, n and m are constants dependent on the geometry of the heat exchanger and internal flow regimes.

For the steel heat exchangers considered in this thesis, the wall conduction term in Equation 5.1 is assumed to be both negligible and largely constant, so can be omitted from the off-design analysis. The contact areas A and diameter D are also constant. In this work, the off-design fluid conditions maintain the same phase as the design condition and have limited variation in temperature and pressure. Therefore, the thermal conductivity of the fluids k and the Prandlt number are also considered to be constant. Under these assumptions, Equation 5.1 can be combined with Equation 5.2 to describe the off-design operating overall heat transfer coefficients as given in Equation 5.3:

$$\frac{UA}{U^0 A} = \frac{Re_c^n}{Re_c^{n0}} + \frac{Re_h^n}{Re_h^{n0}} \quad (5.3)$$

Considering $Re = \frac{\dot{m}D}{\mu A}$ and assuming μ is also constant under the range of operating conditions, Equation 5.3 reduces to Equation 5.4:

$$\frac{UA}{U^0 A} = \left(\frac{\dot{m}_c}{\dot{m}_c{}^0}\right)^{n_c} + \left(\frac{\dot{m}_h}{\dot{m}_h{}^0}\right)^{n_h} \quad (5.4)$$

As stated, exponents n are related to the nature of the fluid flow through the heat exchanger. It is assumed that turbulent flow will be experienced under both design and off-design conditions in all heat exchangers, a reasonable assumption for a well-designed heat exchanger, particularly where flow is forced (pumped streams). Under these assumptions shell side flow normal to the long axes of an array of tubes can be given an exponent of 0.6, and an exponent of 0.8 used for tube side flows (Stultz & Kitto 2005, chap.4). Approximate initial values of U for each heat exchanger design point are taken from Perry's Chemical Engineering Handbook chap. 11.

In the steam cycle condenser and the LPE, with a gaseous hot side and liquid cold side, $h_c \gg h_h$ and Equation 5.4 is further simplified with the term for the cold side fluid omitted. Values of A are calculated by Aspen Plus at the design point, which in this work refers to full capture plant bypass when the maximum steam flow must be condensed, and then set to constant.

This method can be considered +-25% accurate (Serth & Lestina 2014). A sensitivity of turbine operation given this uncertainty is provided alongside the interim results presented in the following section.

5.1.2.4.2 Turbines

In this simulation, a throttled LP turbine configuration is used (see Section 3.4.2) whereby steam is throttled into a valve before entering the LP turbine inlet, following the IP/LP cross over. This configuration leads to smaller variations in steam pressures as upstream high and intermediate steam cycles are not perturbed by variations in steam extraction to the reboiler, and therefore facilitates easier control for capture level set points. The gas turbine, HP and IP steam turbines are subsequently assumed to operate at constant load as the fuel input. However, the steam flow through the low-pressure turbine changes significantly in response to variable capture. The off-design behavior of the low pressure steam turbine is modelled using the Law of Cones or Stodola's Ellipse Law, which is widely used in the literature for off-design simulation of steam cycle behavior in CO_2 capture processes(Lucquiaud & Gibbins 2011; Oexmann 2011; Roeder & Kather 2014; Hanak et al. 2015; Rezazadeh et al. 2016; Sanchez Fernandez et al. 2016). Stodola's Law provides a relationship

between steam flow and pressure drop in the turbine, on the condition that the turbine is not choked. Hanak et al. (2015) carried out a comparison between Stoloda's correlation and operating data in the literature and found a maximum deviation of +/- 2.17% for turbine response down to a 40% load. This uncertainty is also considered in the interim simulation results presented in this section.

Stodola's law is presented in Equation 5.5

$$\frac{\dot{m}_{in}}{\dot{m}_{in}^{0}} = \frac{\bar{V}}{\bar{V}^{0}} \times \frac{p_{in}}{p_{in}^{0}} \times \sqrt{\frac{p_{in}^{0}\, v_{in}^{0}}{p_{in}\, v_{in}}} \times \sqrt{\frac{1-\left(\frac{p_{out}}{p_{in}}\right)^{\frac{n+1}{n}}}{1-\left(\frac{p_{out}^{0}}{p_{in}^{0}}\right)^{\frac{n+1}{n}}}} \qquad (5.5)$$

Where $\dot{m}$ is the steam mass flow, $\bar{V}$ is the average swallowing capacity of the turbine, p is the pressure, v the specific volume and n the polytropic exponent. Suffix 0 represents the design point, and suffixes in and out, the inlet and outlet of the turbine respectively.

For a condensing LP turbine, with a low pressure ratio and swallowing capacity approaching 1 the equation can be simplified (Rezazadeh et al., 2015) and the equation rearranged as described in Equation 5.6 (Knopf 2012). This version of the equation allows calculation of mass flow and pressure relationships for each set of off-design conditions through the inclusion of a constant K, calculated at design point conditions. A Fortran subroutine integrating Equation 5.6 into the Aspen Plus simulation was created.

$$\dot{m} = K\sqrt{\frac{(p_{in})^2-(p_{out})^2}{p_{in}\, v_{in}}} \qquad (5.6)$$

Maintaining Stodola's constant K in equation 3.6 implies that the LP turbine has a roughly constant inlet volumetric flow. The velocity vectors in the LP turbine will, therefore, be largely unchanged and so the efficiency will also remain roughly constant. The sensitivity of this assumption can be demonstrated using an approximation for turbine efficiency proposed by Sailsbury in 1950 and used by Knopf (2012) and Hanak (2015) – provided in Equation 5.7.

$$\frac{\eta}{\eta^0} \cong 2\ \frac{a}{\frac{V_{in}^0}{V_{in}}} \times \left[\left(a - \frac{a}{\frac{V_{in}^0}{V_{in}}} \right) + \sqrt{\left(a - \frac{a}{\frac{V_{in}^0}{V_{in}}} \right)^2 + 1 - a^2} \right] \quad (5.7)$$

Where η is turbine efficiency, V is steam velocity and a is equal to $\sqrt{1-x}$ when x is the fraction of stage energy released in the bucket (blade) system. Assuming the turbine is optimized for 50% reaction blading, then $x = 0.5$ and $a = 0.707$ (Knopf, 2012). As the dimensions of the turbine inlet are unchanged at off-design conditions, the ratio of steam velocities is equal to the ratio of volumetric flow. Taking the ratio of volumetric flows at design point and off-design point to be unity, the right-hand side of Equation 5.7 is unity, implying constant efficiency of the LP turbine can be assumed under non-condensing conditions.

The LP turbine outlet pressure (p_{out}) in Equation 5.6 is calculated by the available cold sink in the condenser.

At design point, which in this work refers to full capture plant bypass (when the maximum steam flow is condensed), the condenser is sized according to the available cooling water temperature and maximum allowable temperature increase (14.36°C and 11°C respectively (IEAGHG (2012b)). The temperature of the cooling water source is considered constant in this analysis.

It is also assumed in this work that the cooling water flow rate remains constant, as is typical in sliding pressure mode operated in modern NGCC off-design operations. Under reduced steam flow, the fixed area condenser will therefore experience a decreased internal temperature difference between steam and cooling water, condensing steam at a lower temperature, corresponding to a lower saturation pressure. This saturation condition determines the off-design LP turbine outlet pressure. The new inlet pressure for the LP turbine is subsequently determined through Stodola's law based on maintaining a constant volumetric flowrate.

Figure 5-3 presents the off-design condenser operating conditions, illustrating the decreasing condenser pressure responding to decreased internal temperature approach between steam and cooling water at lower steam flow rates passing through a fixed size condenser. This relationship between turn-down and condenser pressure

relies on the values of *U* calculated with Equation 5.4, indicated as +- 25% accurate. This uncertainty is depicted as error bars in Figure 5-3.

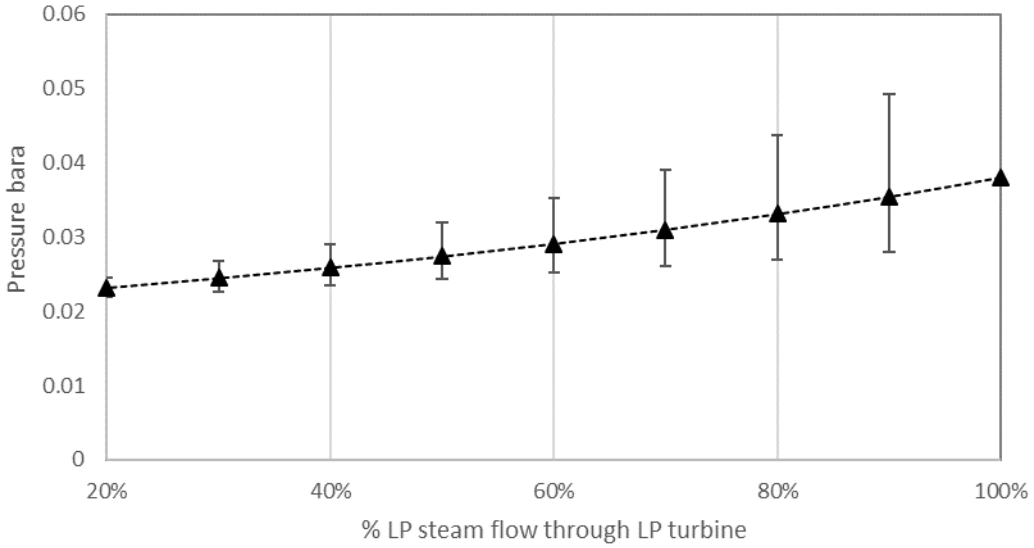

Figure 5-3 Sliding pressure condenser conditions resulting from variations in steam flow to the LP turbine. Off-design conditions calculated with Equation 5.4, error bars indicate +-25% accuracy of this method.

If the off-design overall heat transfer coefficient is 25% higher or lower, the pressure in the reboiler increases or decreases correspondingly, with the effects greater at higher steam flow rates. This variation can be explained by considering the relationship between the heat transfer coefficient U (W/m^2 K), the heat exchanged Q (W), the area of heat exchange A (m^2), and the temperature difference between the hot and cold streams along the heat exchanger (K). In the steam cycle condenser, the cooling water inlet temperature and flow rate are assumed to be constant. The cooling available in the condenser is, therefore, dictated by the temperature approach limit in the heat exchanger, which dictates the saturation temperature, and thus pressure, of the condensing steam. The hot stream inlet and outlet temperature will both be saturated. The corresponding enthalpy of condensation for those saturation conditions and the corresponding steam flow rate will subsequently dictate the heat exchanged (*Q).* The constant flow rate of the cooling water dictates the outlet temperature of the cooling water. A 25% increase or decrease in calculated values of *U* will therefore lead to larger differences in condenser pressure at higher steam flow rates, as illustrated in Figure 5-3. The uncertainties in condenser pressure are asymmetrical (lower when *U* is decreased) as the enthalpy of condensation increases as lower pressures, leading to a lower relative sensitivity to the value of *U*.

Figure 5-4 presents the relationship between the pressure ratio of the LP turbine and the turn down of steam flow rates. The minimum flow through the LP turbine is assumed to be 20% of full load to maintain cooling in the turbine. The results in Figure 5-4 illustrate that the inlet pressure to the LP turbine decreases from 3.75 bara to 0.75 bara at 20% steam flow, as the volume at the turbine inlet remains largely unchanged. The relatively small variations in LP turbine outlet, related to the condenser pressure, do not significantly impact the variation in turbine inlet pressure as the above described variation in mass flow dominates. Error bars are included for both LP turbine outlet, which corresponds to Figure 5-3, and LP turbine inlet, which corresponds to Equation 5.6 with +/- 2.17% accuracy. It is evident that the error bars shown in Figure 5-4 are too small to be significant in this scale.

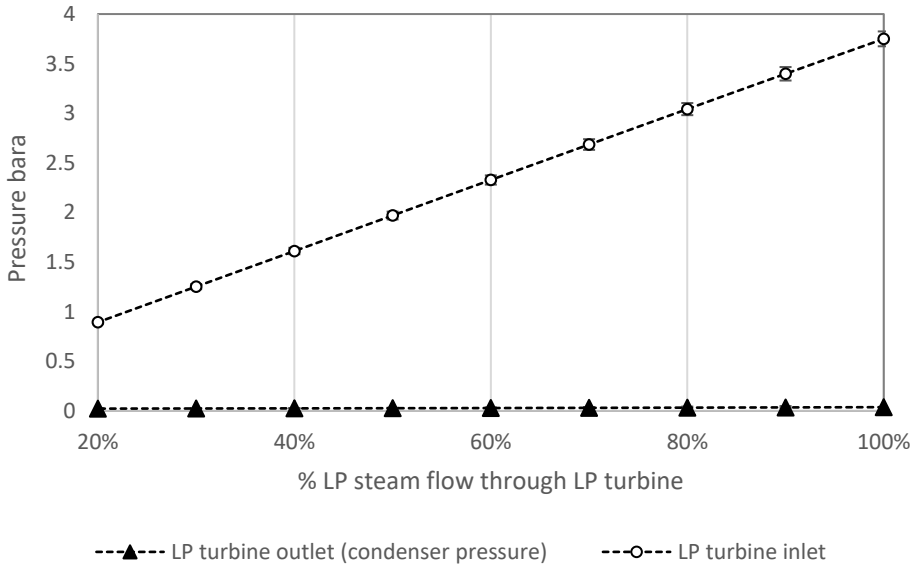

Figure 5-4 Low pressure turbine inlet and outlet pressures, with error bars showing the insignificance of the off-design modelling uncertainties on turbine pressure ratios

However, the LP turbine is a condensing turbine, and so efficiency penalties will vary with differences in the quality of steam exiting the turbine as droplets can impact on efficiency significantly.

In this work, the dryness fraction of the LP turbine exit at design point is 0.905, roughly typical of industrial turbines and in line with the IEAGHG 2012 study. Simulation results presented here see LP turbine exit steam quality increase at lower steam flow rates (Figure 5-5), implying an increase in turbine efficiency at lower steam loads. The increase in steam quality can be explained by the reduction in LP exit pressure, and

the pinch in the condenser. The Baumann correlation can be used to estimate the correlation between dryness and turbine efficiency (Roeder & Kather 2014; Oexmann 2011; Moon & Zarrouk 2014) where 1% moisture approximately represents a 1% efficiency penalty. The Baumann correlation as a simple equation is given in Equation 5.8.

$$\frac{\eta}{\eta_{dry}} = B\ \frac{x_{in}-x_{out}}{2} \qquad (5.8)$$

Where η is the operating efficiency of the turbine, η_{dry} is the turbine efficiency under non-condensing conditions, B is the Baumann factor (an empirical value shown to vary between 0.4 and 2, assumed here to be equal to 1 as is typical according to Moon and Zarrouk (2014)), x_{in} is the steam quality entering the turbine (equal to 1) and x_{out} the steam quality at the exit. Applying this correlation to the variation in the quality of the range of steam flow rates through the LP turbine results in the variations in efficiency shown in Figure 5-5. This variation is incorporated into the Aspen Plus NGCC simulation using a Fortran subroutine. As the approach in the condenser does not significantly change with uncertainties in condenser pressure at off-design point operation, the additional uncertainty in turbine dryness fraction was not significant, and so no further error bars are included here.

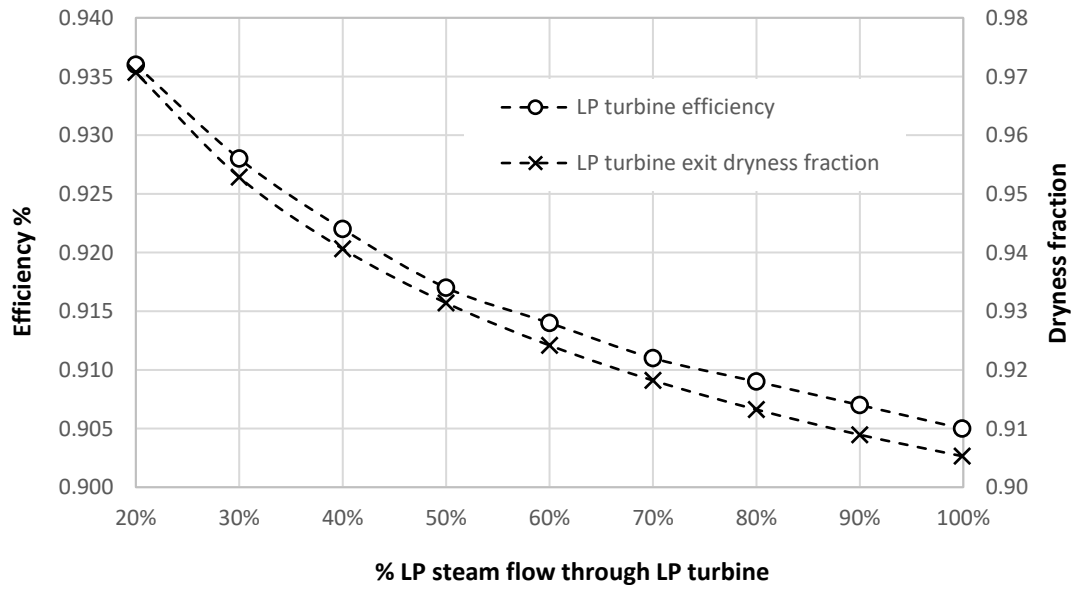

Figure 5-5 Variation in LP turbine exit dryness fraction, and implied efficiency based on the Baumann correlation (Equation 5.8) as a function of steam flowrate

Together, the above simulations can provide a quantitative assessment of the electricity output penalty of steam diversion to the capture plant (the inverse of the LP steam flow through the LP turbine). This is illustrated in Figure 5-6, where the non-specific EOP (i.e. the dynamic energy penalty, not specific to CO_2 flow rate) is given as a function of steam diversion for the simulated NGCC unit. Error bars from the uncertainty in the off-design point modelling assumptions of the heat transfer coefficient of the condenser, and Stodola's equation are too small to be detectable at this scale.

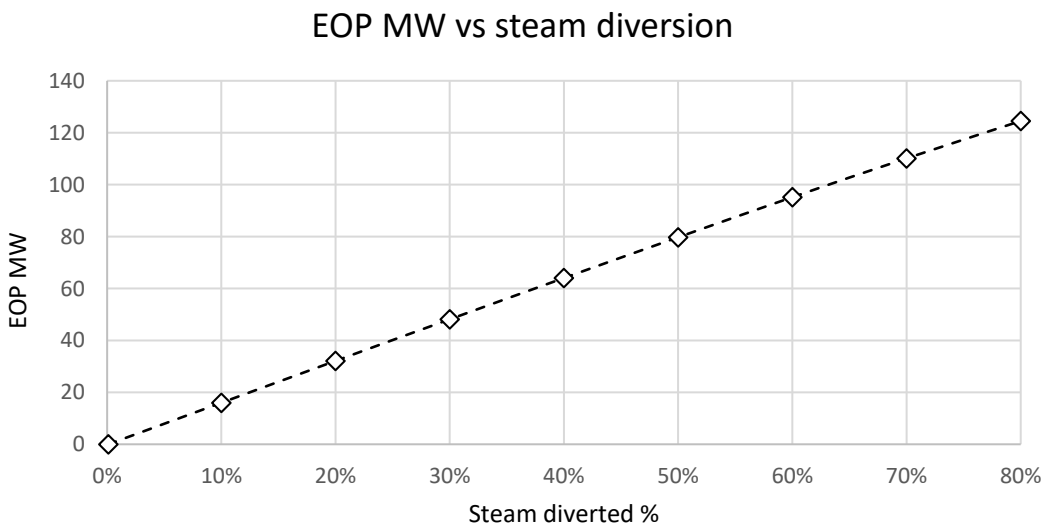

Figure 5-6 Low pressure turbine Electricity Output Penalty (not specific to CO_2 mass flow) as a function of steam diverted to the post-combustion capture unit

5.1.2.4.3 Steam extraction for PCC

As stated previously, a steam extraction line is taken at the IP/LP turbine crossover for steam diversion to the post-combustion capture unit. The steam extraction pressure is based upon the post-combustion capture unit reboiler operation: for a design point 90% capture level, the reboiler operates with an internal solvent temperature of 120°C and 10°C pinch to the steam side, a 1.05 bar pressure drop is assumed between the IP/LP steam extraction point and the PCC unit reboiler. This equates to a reboiler hot-side saturated steam extraction temperature of 130°C, with a pressure of 2.7 bar, requiring an upstream IP/LP cross-over pressure of 3.75 bar. These conditions are selected in line with the IEAGHG (2012b) report. The temperature of 120°C is considered the highest reasonable temperature to operate the MEA reboiler before thermal degradation becomes a significant issue. The

reboiler pinch of 10°C is conservative compared with some other literature studies, which use 5°C or less (Amann & Bouallou 2009; Sipöcz & Assadi 2010; Lindqvist et al. 2014; Rezazadeh et al. 2016), as is the provision of the 1.05 bar pressure drop.

Under part load conditions, as steam flow rates vary, so does the pressure drop between the steam cycle extraction point and the reboiler. In this work, a dimensionless version of the Darcy–Weisbach equation using a single pressure drop correlation parameter, k, to account for pipe roughness and pipe dimensions is integrated into Aspen Plus, as given in Equation 5.9.

$$\Delta P = kM^2 \frac{{}^1/_{\rho_{in}} + {}^1/_{\rho_{out}}}{2} \quad (5.9)$$

Where k = pressure drop correlation parameter, M = mass flow rate, ρ_{in} = density at inlet and ρ_{out} = density at outlet. The value of k was set to 0.9 to achieve the 1.05 bar pressure drop under the steam flow rate for 90% capture (IEAGHG 2012b). Under this pressure drop parameter, significant variation in pressure drop is experienced as steam flow rate increases or decreases in response to changes in capture level. This leads to changes in hot side reboiler temperature (steam saturation temperature) as illustrated in Figure 5-7.

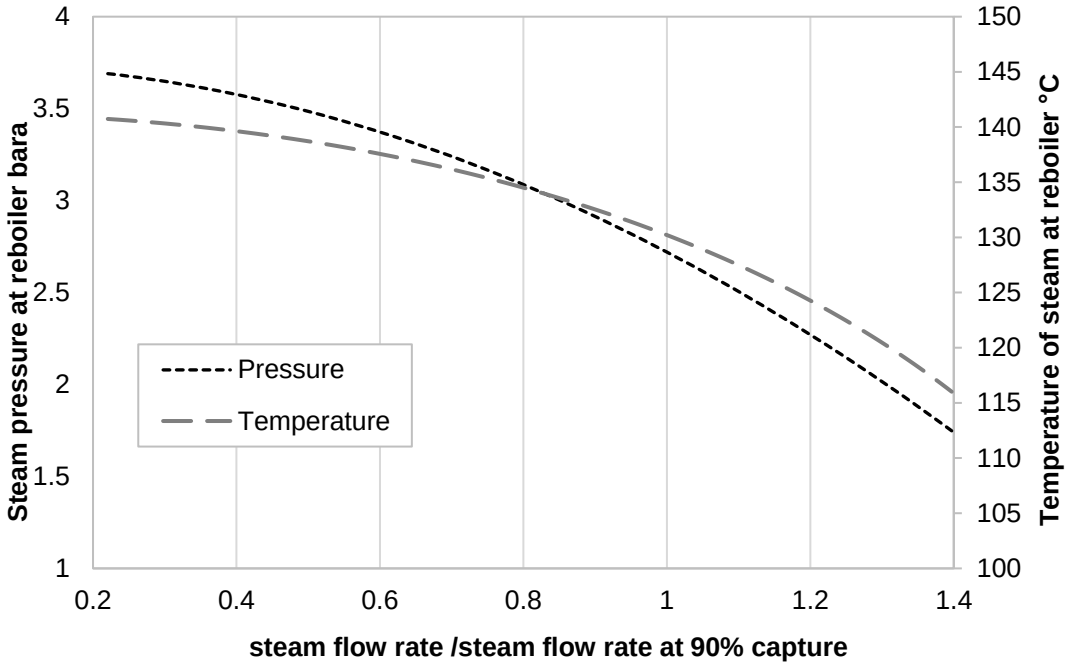

Figure 5-7 Off-design reboiler conditions as a function of steam flow rate

At lower capture levels, the lower steam flows lead to hotter conditions in the reboiler. This could lead to excessive thermal degradation if operated for longer periods of time. A throttle valve may be necessary in these circumstances, although that is not considered in this work. At higher capture levels the pressure drop will be greater and so lower temperature reboiler conditions will be experienced. From a control perspective this is important as other studies that do not include this consideration can omit to include the additional energy penalty involved in achieving very high capture levels at reduced reboiler temperatures

As detailed in the literature review, the net efficiency of the integrated plant is sensitive to these parameters, and so it is important to stress that the specific electricity output penalties of CO_2 capture described in this modelling are subject to these assumptions of pressure drop and cross-over pressure extraction.

This work considers the IP/LP cross over conditions to be fixed, and there to be limited control for achieving the reboiler temperature further than this (although a control valve could be used).

5.1.3 MEA capture plant

5.1.3.1 Description of modelling methods underpinning MEA capture plant

The Aspen Plus rate-based model with aqueous MEA was used as the basis for the absorption loop simulation. This is a rigorous rate-based MEA model using the unsymmetrical electrolyte NRTL activity coefficient model for liquid and the PC-SAFT equation of state for vapor, electrolyte transport property models, and activity-based reaction kinetics (Aspen Tech, 2012). The physical and transport property details of the model are detailed in “Rate-Based Model of the CO_2 Capture Process by MEA using Aspen Plus” (Aspen Tech, 2012). A summary is provided in Appendix A.

The Aspen Plus package uses pilot plant data from the University of Kaiserslautern (Notz et al. 2012) running a natural gas burner with 5.4 v/v CO_2 concentration in the flue gas. To validate the model at lower concentrations and with larger absorbers, data from the CO_2 Technology Centre Mongstad is used in this work.

The topography of the simulation for the post-combustion capture unit in this work is a basic amine loop, without added configurations for efficiency savings. This was selected for ease of comparison with other baseline studies for the indicative purposes

required for this techno-economic study on flexibility. The impact on flexibility of more complex configurations is a topic of interest, but outside the scope of this work.

5.1.3.2 Chemistry of MEA-H_2O-CO_2 absorption

The chemistry of CO_2 absorption in MEA is represented by the reactions given in Equations 5.10 to 5.16 below. MEA is a primary ethanolamine. It reacts with CO_2 to form a carbamate ion $MEACOO^-$ (Equations 5.10 and 5.11). CO_2 can also react with the aqueous solution to form bicarbonate ions (Equations 5.12 and 5.13). The kinetics of these reactions are important in simulating the absorption process, particularly for off-design simulations, as the reaction kinetics under any specific operating conditions will dictate the level of CO_2 absorption/desorption for a given column design. MEA hydrolysis and water and bicarbonate dissociation also occur, but these reactions are typically assumed to be in equilibrium (Equations 5.14 to 5.16).

$$MEA + CO_2 + H_2O \rightarrow MEACOO^- + H_3O^+ \quad (5.10)$$

$$MEACOO^- + H_3O^+ \rightarrow MEA + CO_2 + H_2O \quad (5.11)$$

$$CO_2 + OH^- \rightarrow HCO_3^- \quad (5.12)$$

$$HCO_3^- \rightarrow CO_2 + OH^- \quad (5.13)$$

$$2H_2O \leftrightarrow H_3O^+ + OH^- \quad (5.14)$$

$$HCO_3^- + H_2O \leftrightarrow H_3O^+ + CO_3^{2-} \quad (5.15)$$

$$MEA + H_3O^+ \leftrightarrow MEAH^+ + H_2O \quad (5.16)$$

The Aspen Plus amine package calculates equilibrium constants from standard Gibbs free energy change. The kinetics for the rate-controlled reactions (Equations 5.10 to 5.13) are calculated with the general power law expression using kinetic parameters pre-programmed into the Aspen Plus package (see Aspen Plus (2012)). Appendix A describes the Aspen amine model in more detail, including correlations for each mechanism.

5.1.3.3 Model validation with pilot plant data (CO_2 Technology Centre Mongstad)

The IEAGHG (2012b) report, Scenario 3a, uses 35 wt% MEA with limited detail on absorber performance and stream composition. Therefore, this work initially replicates absorber and stripper design conditions from Mongstad pilot plant data (Hamborg et al. 2014). Key input parameters are given below in Table 5-5.

Table 5-5 Input parameters for pilot plant at CO_2 technology Centre Mongstad

Parameter	Value
Flue gas flow rate Sm^3/hr (15 °C, 1atm)	46,970
Flue gas CO_2 concentration vol%	3.7
30 wt% MEA flow rate kg/hr	54,900
Reboiler temperature °C	122.3
Stripper overhead pressure barg	0.9
Regeneration steam inlet °C	169
Regeneration steam barg	4.42
Absorber dimensions (W x L) m	3.55 x 2
Absorber packing height (total) m	24
Stripper dimensions (diameter) m	1.3
Stripper packing height (total) m	8
Packing: Flexipac 2X structured stainless-steel packing	

20 stages were used for the absorber in line with the temperature profile data from the Hamborg et al. (2014) study. The stripper has 8 stages, which provided the best fit to Mongstad data reboiler duty. An interfacial area factor of 0.8 was found to achieve the best absorber temperature profile. Heat losses in the cool, large scale absorber column were assumed to be negligible and so were not included in the simulation. Results are given in Table 5-6, comparing key streams, and Figure 5-8, which provides a comparative absorber temperature profile between this work and that of Hamborg et al. (2014).

Table 5-6 Simulation results compared with data from CO_2 technology Centre Mongstad (Hamborg et al. 2014)

Parameter	Data	Simulation
MEA lean loading molCO_2/molMEA	0.23	0.238
MEA rich loading molCO_2/molMEA	0.48	0.477
Reboiler duty MJ/hr	10,978	11,001
CO_2 capture level	90.8-95.0	90.1
Specific thermal use GJ/tCO_2	4.06	3.77

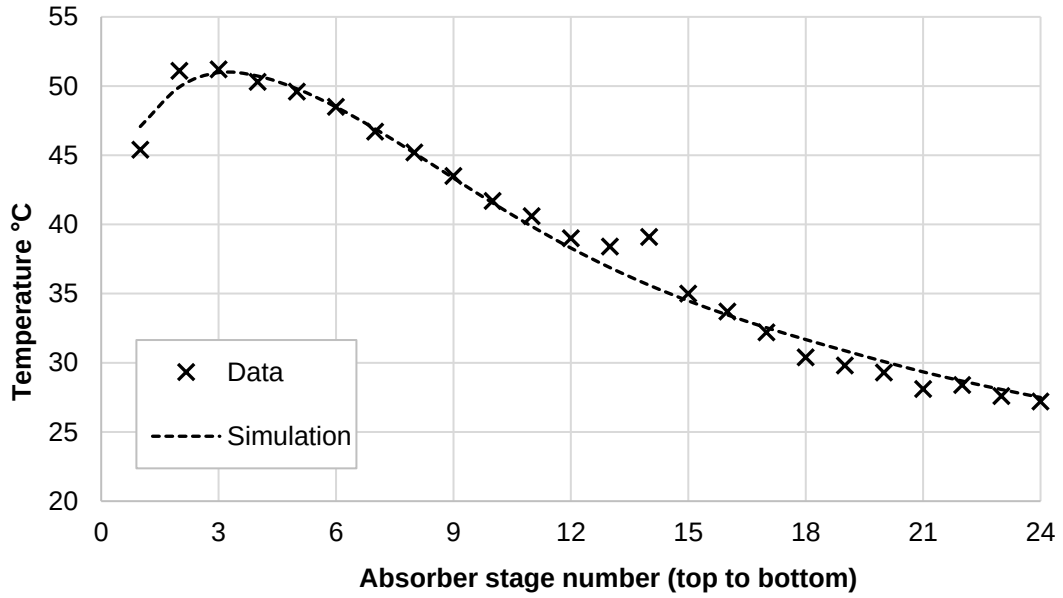

Figure 5-8 Simulated absorber temperature profile compared with pilot plant data from CO_2 Technology Centre Mongstad (Hamborg et al. 2014)

The level of agreement between the simulation results and the pilot data was considered a reasonable match. Simulation results for the absorber temperature profile matches well with the profile from the Hamborg data (Figure 3-8), as did the simulated lean/rich loading profiles and the absolute reboiler duty. However, there was a significant 10% discrepancy between the specific reboiler duty in the model and the published pilot plant operation. As the temperature profile in the absorber, and the absolute reboiler duty matches well with the Aspen Plus simulation, it is likely that the heat of absorption is well represented by the modelling package. Therefore, this difference is most likely explainable by discrepancies in the pilot plant CO_2 mass balance. The Hamborg et al. (2014) paper specifically notes the uncertainty around mass balance in their experiments, noting that the CO_2 mass balance of the plant is not fully accounted for in pilot plant instrumentation:

"The uncertainty in CO_2 capture is almost all due to uncertainty in CO_2 content of the CHP flue gas supply for the assigned total flow uncertainties… The fact that CO_2 recovery [mass balance] is less than 100% suggests that one or more of the flows has a significant bias error than calculated from instrument specifications."

5.1.3.4 Design operating conditions and model specifications

The model for the absorption loop integrated with the above described NGCC plant, depicted in Figure 5-2 section [A], was resized from the initial replication of Hamborg

et al. (ibid.) to account for the flue gas volumes specific to the 800MW NGCC plant used in this work. The absorber and the stripper were thus sized according to the original IEAGHG (2012b) report on which the NGCC plant was based. Although IEAGHG (2012b) column sizing relates to 35 wt% MEA, the 20m packing height in absorber and stripper were considered reasonable for the 30 wt% MEA simulation carried out in this work. González Díaz et al.(2013) presented a sensitivity analysis for column height versus reboiler duty for an NGCC plant of similar size and configuration to the simulation in this work, with the same concentration of CO_2 in flue gas. This analysis illustrates that the relationship between increasing absorber height and increasing rich loading (and therefore reduced reboiler duty) shallows and flattens at absorber heights of around 20m, relating to a rich loading of approximately 4.65 mol/mol. Further increases in height would increase capital costs without significant energy savings. On these grounds, the 20m packing height used in IEAGHG (2012b) is maintained in this work.

Column diameters are designed for a column fractional flooding capacity of 0.6. This is lower than other studies which use flooding capacities of 0.7-0.8 for the absorber (Jordal et al. 2012; Alhajaj et al. 2016). However, an absorber designed for a lower flooding capacity will be able to cope better with variations in the flow posed in this work on flexible operation without moving into the flooding regime. A capacity of 0.6 is also in line with the IEAGHG (2012b) report. A lower flooding capacity however implies larger column diameters. For the 800MW NGCC with two HRSG and two absorber trains (as illustrated in Figure 5-2) a flooding capacity of 0.6 requires absorbers with 19m diameters, exceeding the 18.2m (60ft) maximum diameter of cylindrical absorbers, as reported by Reddy et al. (2003) and repeated in IEAGHG (2012). However, in line with IEAGHG (2012b), and other large scale CO_2 capture projects (e.g. Boundary Dam as discussed in Ball (2008)) it is assumed that rectangular absorbers of equivalent dimensions can be used, without the expense of additional absorber trains. Aspen Plus requires cylindrical dimensions for simulation purposes, so 19m is the input value in this work's model. The remaining units of the post-combustion capture unit were sized from the IEAGHG (2012b) report where available, or from otherwise considered reasonable values as described in the following sections.

Fixed input parameters for the post-combustion capture unit are summarised in Table 5-7. A schematic of the post-combustion capture unit is shown in Figure 5-2 section [B]. The input model for the simulation can be found in Appendix B.

Table 5-7 Capture plant simulation fixed design parameters. These values refer to each absorber train.

Parameter	Units	Value
Pumps isentropic efficiency	%	85
Fan isentropic efficiency	%	85
Absorber packing height	m	20
Absorber internal diameter	m	19
Stripper packing height	m	20
Stripper internal diameter	m	8

5.1.3.5 Off-design point modelling in amine loop

To simulate off-design point behaviour in the PCC unit, heat exchangers were simulated as described in Section 3.4.2.4.1. The cross-heat exchanger (LHXR in Figure 5-2) and the reboiler heater were sensitive to temperature changes from the changes on both hot and cold sides. It is assumed that the lean solvent cooler maintains constant hot side outlet temperatures by varying the flowrate of cooling water.

Pumps and fans are assumed to be variable speed, and therefore capable of varying flow rates of 20-120% with a relatively small variation in efficiency based on the small contribution of their ancillary power to the overall electricity output penalty. Isentropic efficiencies of these equipment are, therefore, considered to be constant.

Hydrodynamic issues associated with variable flow rates in the columns are those associated with changes in pressure drop, including flooding or channelling, and those associated with distribution issues of the liquid on the packing, including minimum wetting. The fixed size absorber and stripper columns in Aspen Plus utilise flooding and pressure drop correlation calculations to predict hydrodynamic operational limits in the columns (see Appendix A). Fractional flooding capacity at each operating regime is calculated to ensure flooding is avoided. Operating under the minimum wetting is avoided according to the packing manufacturer specifications: Sulzter recommend a minimum liquid load of 0.2 m^3/m^2 h, and a maximum liquid load

of 200 m^3/m^2 h[6] for the packing (Mellapak 250 X/Y) as used in this simulation. At design point the liquid load is 10.3 m^3/m^2 h in the absorber, and 59.9 m^3/m^2 h in the stripper.

This work assumes a quasi-steady state simulation carried out in step changes. Therefore, while these operating states may avoid flooding regimes or other maldistributions in the columns, this does not provide information on transitional states. However, work done in a pilot scale post-combustion capture plant at the CCPilot 100+ post-combustion capture pilot plant at Ferrybridge power station indicates that transient states are manageable. Test programmes carried out ramping of both liquid and gas to 50% of the design level (90% capture) flow rates, and ramped solvent flow rates above the design point for higher capture levels without experiencing distribution issues (Fitzgerald et al. 2014). Additionally, dynamic modelling work (Ceccarelli et al. 2015) has indicated that reductions down to 50% flow of both gas and liquid appear to be stable.

5.1.4 Compressor model

Compression is a significant factor in post-combustion capture electricity output penalty performance, yet it is frequently simplified or even omitted from modelling studies, particularly in part load studies, possibly due to limited published information on compressor operation. To counter this trend, this work uses a compressor model based on Liebenthal and Kather (2011), a paper that presents a compressor model with a performance map from LÜDTKE based on manufacturing experience in agreement with ManTurbo and Siemens.

Compressors can typically operate in the range of 70-105% volumetric flow. Liebenthal and Kather (2011) provide a brief analysis of different strategies to increase the working range of CO_2 compressors, covering variable speed, suction throttling, adjustable inlet guide vanes and bypass/recycle operation. Variable speed, where the shaft speed is varied according to inlet volume flow, is the most energetically efficient method of controlling the required head, but requires additional equipment. Liebenthal and Kather (2011) posit that this will be problematic in the large

[6] https://www.sulzer.com/en/-/media/Documents/ProductsAndServices/Separation_Technology/Distillation_Absorption/Brochures/Structured_Packings.pdf

sized compression trains in CO_2 capture plant. Suction throttling, where a throttle is installed to regulate the minimum inlet volume flow, is straightforward to implement, but leads to a lower inlet pressure without controlling the pressure ratio of the compressor. Therefore, lower outlet pressures are created which may be problematic if specifications for CO_2 transport and storage are breached. Inlet guide vanes, adjustable vanes upstream of the impeller that can adapt the relative angle between the flow and the blades of the first stage, show good part-load efficiencies and can operate in large compressors. On these grounds, adjustable guide vanes are used in the compressor map taken forward by Liebenthal and Kather (2011). Operation is limited by surge, as well as maximal and minimal vane angles. This compressor map is used as the basis for the off-design compressor performance in this thesis.

As surge limits are approached in part load conditions, further reductions in mass flow necessitate exiting compressed CO_2 to be throttled and recycled to the suction inlet. Due to the Joule-Thomson Effect, the recycle should be located upstream of the compressor aftercooler to avoid freezing conditions. Regardless, the recycle will likely reduce temperature and, therefore, volumetric flow. As the intention is to increase volumetric flow with increased mass flow, the recycled mass flow can be disproportionately large, and therefore this method is increasingly inefficient. An additional option for increasing compressor operation range is to compress the CO_2 to supercritical condition, for example 80 bar, and then utilise an additional pump with a variable speed drive. This configuration leads to a much large working area in terms of pressure ratio and mass flow variation. However, for ease of simulation comparison, this option is not taken forward in this thesis and a single 6 stage compressor is used, with recycles operated where necessary.

5.1.4.1 Compressor model specifications

Figure 5-2 section [C] provides an illustration of the compressor configuration in this work, after Liebenthal and Kather (2011). The model represents an integrally geared (radial) six stage compressor with inlet guide vanes. Efficiencies and pressure losses are taken directly from Liebenthal and Kather (2011). At design point, the compressor has an initial pressure ratio of 2.2, with the pressure ratio of each stage decreasing by 2% per stage due to rotor dynamics. Each stage is proceeded by an intercooler taking the CO_2 to 40 °C. While waste heat from compressor intercooling can potentially be utilised in the plant for efficiency purposes (Gibbins & Crane 2004;

Romeo et al. 2008) this work again considers the simplest layout for ease of comparison and operability for the flexible comparison, rather than the most efficient, heat integrated option. Without heat integration, intercooling at every stage is the most energetically efficient and low-cost option (Liebenthal and Kather (2011)).

In this thesis simulation there are two compressor trains, one following each HRSG/absorber loop. Table 5-8 provides the specifications for the compressor, and Figure 5-9 replicates the compressor map from Liebenthal and Kather (2011) utilised for each stage. An output pressure of 120 bar maintained.

Table 5-8 Design operating parameters for compression train stages

	Stage 1	***Stage 2***	***Stage 3***	***Stage 4***	***Stage 5***	***Stage 6***
Polytropic efficiency	0.85	0.84	0.83	0.82	0.81	0.8
Mechanical efficiency	0.99	0.99	0.99	0.99	0.99	0.99
Pressure loss (mbar)	20	40	60	80	100	120
Pressure ratio	2.20	2.16	2.11	2.07	2.03	1.99

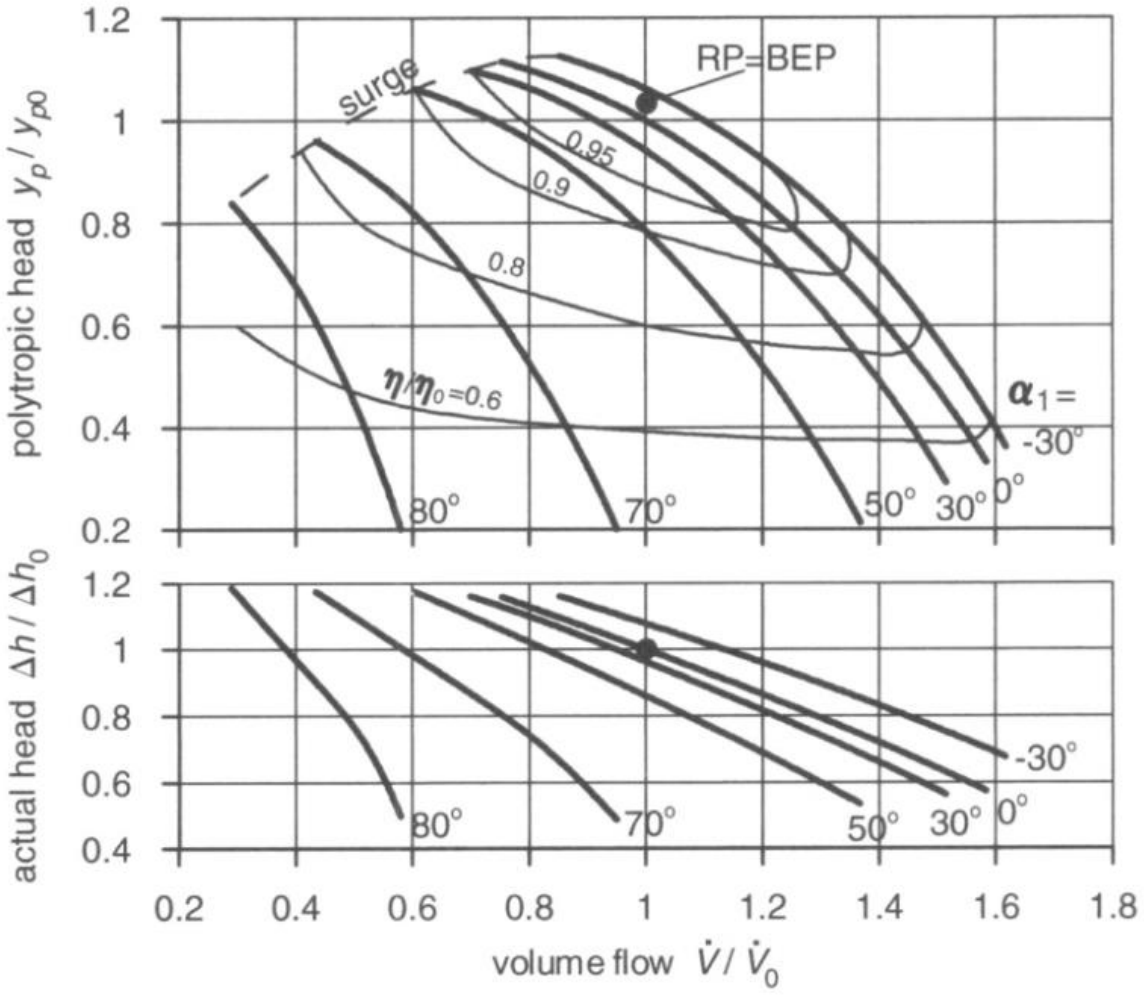

Figure 5-9 Typical performance map for compressor stage with adjustable inlet guide vane control, from Liebenthal and Kather (2011)

5.2 Capture level variation simulation and results

The aim of the modelling activity described in this chapter is to generate a relationship for the electricity output penalty of CO_2 capture and compression at a given CO_2 capture level.

5.2.1 Electricity Output Penalty at 90% capture design point

An initial EOP was ascertained at the design capture level of 90%, given the dimensions and configuration of the plant described in Section 5.1.3.4. The column heights and conditions and the inlet flue gas CO_2 flow rate are set variables; the absorber inlet MEA molar flow rate (i.e. the available MEA for reaction with the incoming CO_2) is therefore the single degree of freedom remaining for a specified

capture level. The absorber inlet MEA molar flow rate is dictated by the solvent loading and the solvent flow rate, i.e. for a given loading there must be a necessary solvent flow rate to capture the equivalent moles of CO_2 for a given capture level. The conditions in the stripper dictate the lean loading, and therefore the necessary solvent flow into the absorber. Higher temperatures in the reboiler favour the reverse chemical reactions for carbonate and bicarbonate disassociation (given in Equations 5.11 and 5.13) leading to regenerated lean solvent. Higher reboiler temperatures are also associated with higher vapour pressures, and therefore stripper pressure, which subsequently reduces CO_2 compression duty via thermal compression. Conversely, lower partial pressures of CO_2 in the stripper also favour carbonate and bicarbonate disassociation, and so operating with a lower overhead stripper pressure can reduce the loading of the solvent further. However, lower operating pressures increase the reflux ratio and therefore the energy penalty of solvent regeneration. A lower stripper pressure will also increase compression duty. On the other hand, higher solvent flow rates that enable equivalent capture levels for higher lean loadings have higher sensible heat requirements to heat the larger volumes of liquid solvent. Accordingly, there is a minimum energy bound at the confluence of these two effects, which provides a design value for lean loading at 90%.

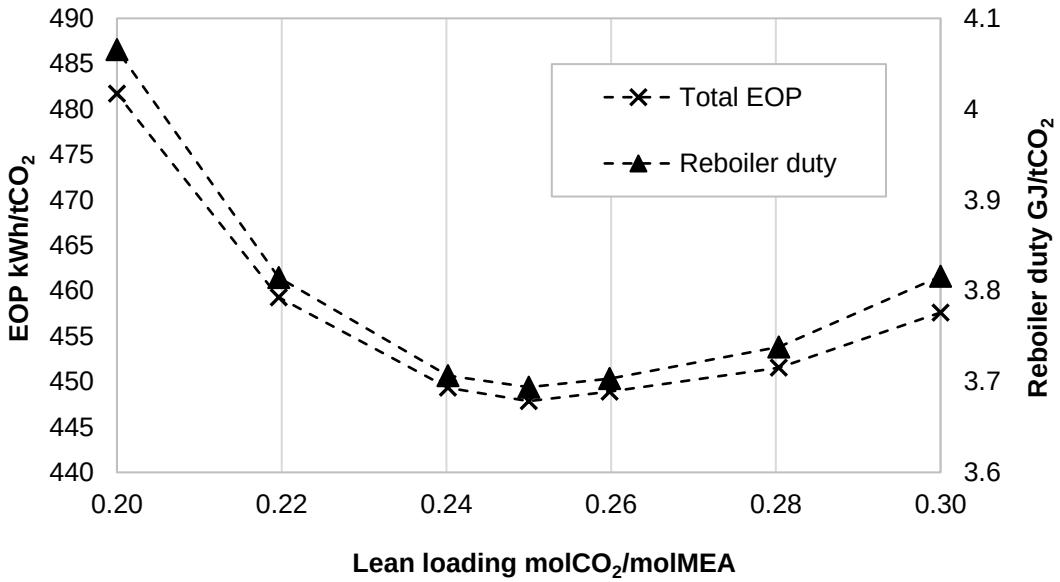

Figure 5-10 Total Electricity Output Penalty and associated reboiler duty for 90% capture for different lean loading values

The reboiler temperature at 90% capture is set to 120°C in this work. To vary the lean loading the solvent flow rate and the stripper overhead pressure are adjusted. Figure

5-10 shows the total EOP at different lean loading values. A minimum can be seen at 0.25 molCO_2/molMEA for both total EOP and reboiler duty, which can be seen to follow the same trend. Figure 5-11 illustrates the influence of the component EOP contributions (turbine losses, compressor duty and fan and pump duty) on total EOP. There are minor reductions in compressor duty at high lean loads resulting from the higher stripper pressure. In parallel, there are minor increases in pump duty at higher lean loadings due to the lower cycling capacity of richer solvents and therefore the higher solvent flow rates. However, these are minor compared with the steam turbine losses which dominate the reboiler duty variations.

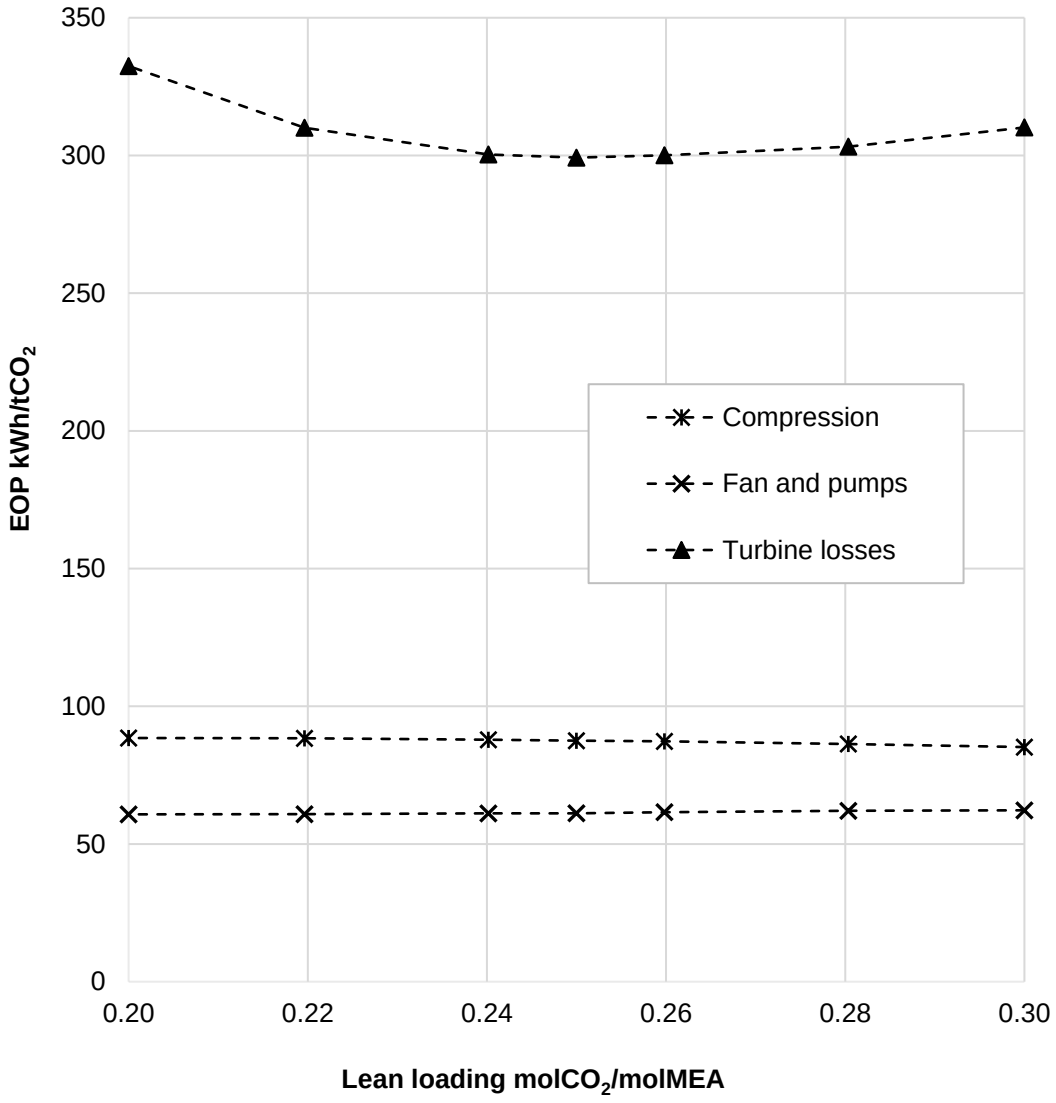

Figure 5-11 Contributions to Electricity Output Penalty for 90% capture for different lean loading values

The simulation results for the capture plant at the 90% capture design point are given in Table 5-9.

Table 5-9 Simulation input conditions and results for 90% capture level operating point

Parameter	Unit	Value
Flue gas flowrate prior to direct contact cooler	kg/s	675
CO_2 inlet concentration	mol%	4.26
Fan pressure increase	mbar	158
Flue gas absorber inlet temperature	C	33
Solvent flowrate	kg/s	861.14
Lean solvent inlet temperature	C	40
Lean loading	mol/mol	0.25
Rich loading	mol/mol	0.46
Cross heat exchanger pinch	C	10
Reboiler pinch	C	10
Reboiler temperature	C	120
Stripper overhead pressure	bar	1.85
Steam flowrate (to reboiler)	kg/s	68.5
Steam extraction line and desuperheater pressure drop	bar	1.05
Condenser pressure	bar	0.038
Condenser terminal difference	C	13.13

5.2.2 Electricity Output Penalty at variable capture levels

From this design point, CO_2 capture levels were varied in two different operating approaches:

1. By maintaining a constant stripper pressure, allowing the lean loading values to vary.
2. By maintaining a constant lean loading, varying the overhead stripper pressure through the control valve at the exit of the stripper column.

For capture levels below 90%, partial flue gas bypass was simulated. Here, a CO_2 removal rate of 90% was maintained in the absorber while treating only a proportion of the flue gas corresponding to the desired capture level. The remaining flue gas was sent directly to the stack. This approach reduces the fan duty, and has been found to be energetically efficient compared with treating all the flue gas as suggested in previous studies (Sanpasertparnich et al. 2010; Mac Dowell & Shah 2013). Additionally, full flue gas flow through the absorber where solvent flow rates are reduced to achieve lower capture levels will tend toward flooding regimes, as increasingly low liquid to gas ratios will be experienced. For capture levels above 90%, where the total flue gas flow already passes through the absorber, the CO_2 removal rate of the absorber is increased.

A minimum capture level of 40% was assumed, as below this point the flow rates of liquid and gas in the columns could approach distribution problems, and current pilot plant test programmes have not reported values below this point (see Section 5.1.3.5). 94% capture was found to be the highest capture level possible before the limits of compressor operation were reached; further increases in flow led to stonewall. Therefore, the following results show variations of capture level between 40% and 94% capture.

Where stripper pressure is constant as capture levels vary, the partial pressure of CO_2 in the top of the stripper must vary accordingly to achieve the specified capture level. As the stripper is assumed to operate at equilibrium, variable partial pressure of CO_2 in the stripper implies a variation in lean solvent loading. This is achieved by changing the flow rate of solvent in the absorption loop; the lower the solvent flow rate the lower the lean loading and vice versa. As such, specific solvent flow rate, and the

corresponding L/G radio are reduced below the design point at lower capture levels and increase at higher capture levels. This trend aligns with a previous study by Sanpasertparnich et al. (2010) that simulates variable capture level relationships for coal plant assuming a fixed stripper pressure. However, in this work, a small upturn in the lean loading at 40% capture level, with a corresponding rise in solvent flow rate. This is explained by the reduced pressure drop in the stripper and lower solvent flow rates, effectively enabling a higher partial pressure in the stripper for the equivalent lean loading. Sanpasertparnich et al. (2010) does not show this trend, where it can be assumed that the treatment of pressure drop in the stripper is either different or neglected.

Conversely, a variable stripper pressure directly varies the partial pressure of CO_2 exiting the stripper, and therefore maintains a constant lean loading and specific solvent flow rate except above 90% capture when additional solvent is required to push capture levels beyond the design point.

These operating conditions are shown in Figure 5-12 and Figure 5-13. Figure 5-12 illustrates the solvent flow rate and the corresponding liquid to gas ratio in the absorber at different capture levels with Figure 5-13 showing the related lean solvent loadings.

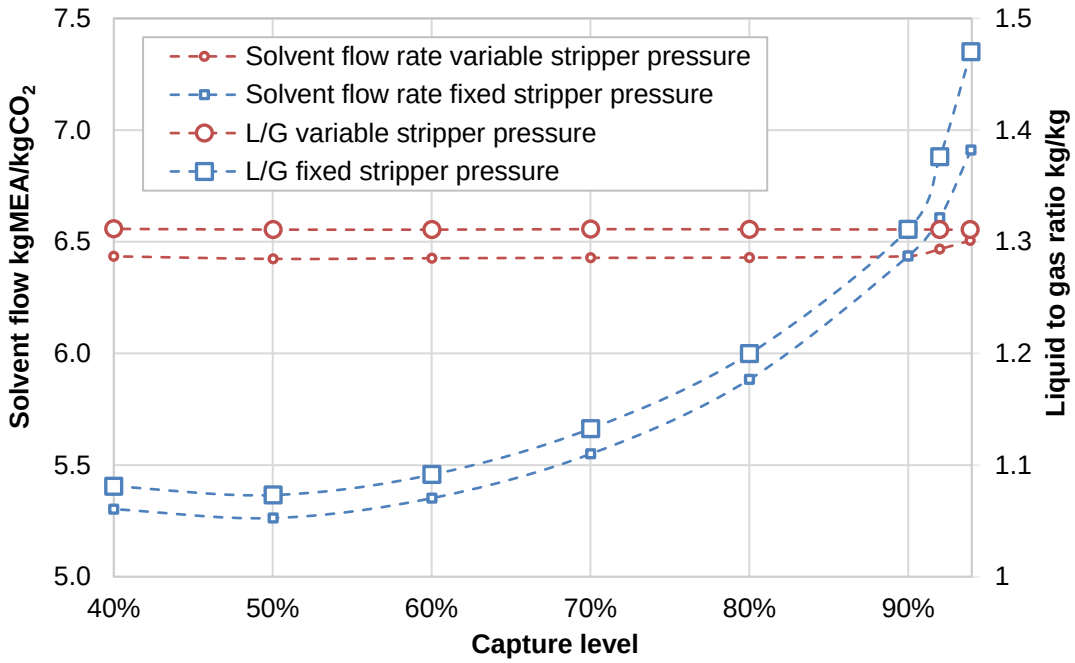

Figure 5-12 Variations in specific solvent flow rate per kg CO_2 captured (left axis) and liquid to gas ratios in the absorber (right axis) at different capture levels under variable and fixed stripper pressure operation

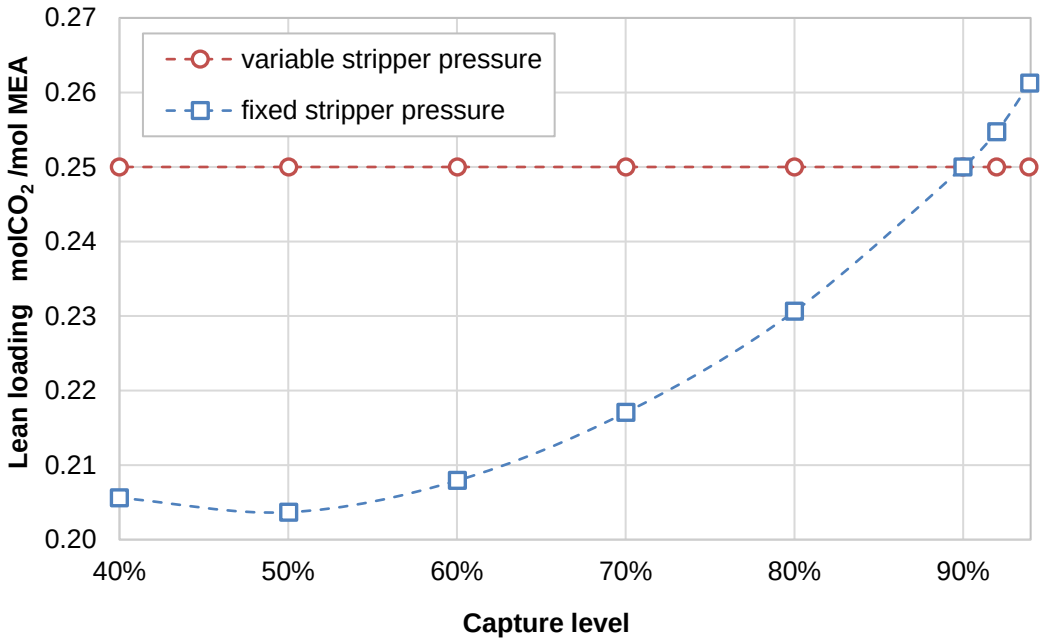

Figure 5-13 Variations in MEA lean loading at different capture levels under variable and fixed stripper pressure operation

Figure 5-14 and Figure 5-15 show the conditions in the stripper and the reboiler for the two operating approaches. The increase in steam pressure, and therefore temperature, at lower capture levels in the hot side of the reboiler is due to the smaller pressure losses in the steam extraction line from reduced mass flow, as shown in Figure 5-7. Steam pressures and temperatures are lower at higher capture levels for the same reason. The temperature difference in the reboiler can be seen to increase more significantly with fixed stripper pressure operation compared with variable stripper pressure operation. This is due to the absolute solvent flow rates decoupling from the capture level, and therefore the steam flow rate with fixed stripper pressures; at lower capture levels solvent flow rate decreases at a faster rate than steam flow rates. Conversely, fixed lean loadings under variable stripper operation lead to solvent flow rates that vary proportionally with capture level and therefore steam flowrate.

Solvent side reboiler temperatures can be seen to increase to over 125°C when variable stripper pressures are in operation. This is higher than the recommended 120°C design point for limiting solvent degradation. However, while Davis & Rochelle (2009) indicate that thermal degradation accelerates above 130°C, they also indicate that the relationship between temperature and degradation is complex and dependent on other factors such as MEA loading, concentration and oxygen content (Léonard et al. 2014), and the exposure time to higher temperatures. It is not clear whether an occasional 5°C increase to 125°C in temperature will cause significant increase to solvent degradation. Therefore, this work assumes this increase is acceptable. Should increased degradation be found, the steam extraction line could be throttled to reduce the hot side reboiler temperature at lower capture levels.

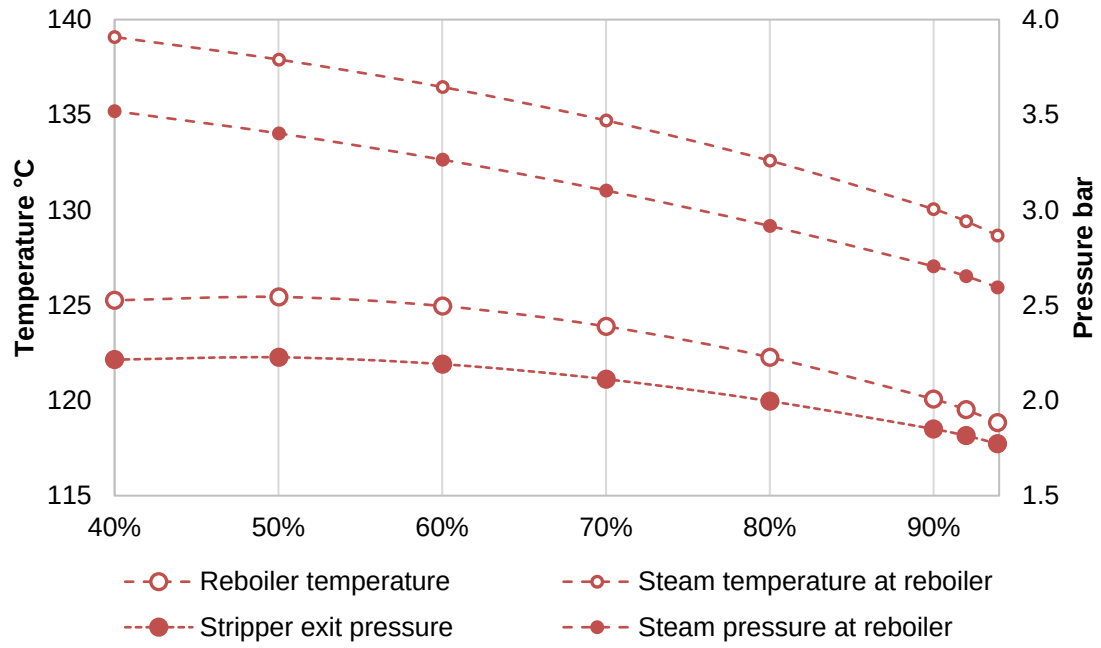

Figure 5-14 Temperature and pressure conditions in the stripper and reboiler at different capture levels under variable stripper pressure operation

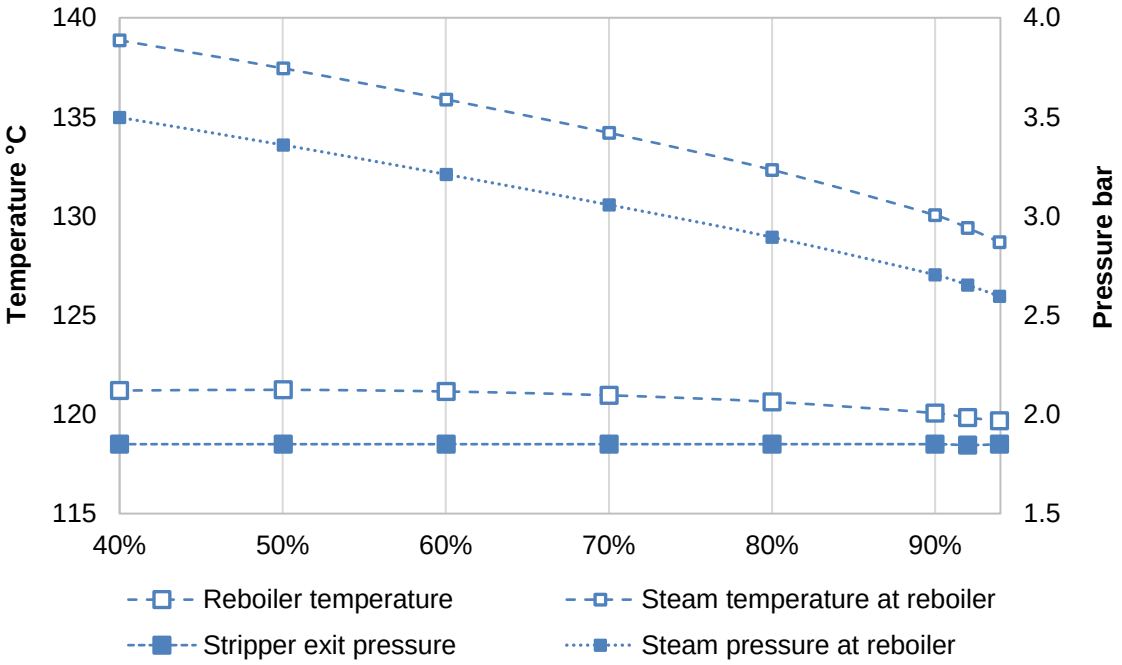

Figure 5-15 Temperature and pressure conditions in the stripper and reboiler at different capture levels under fixed stripper pressure operation

5.2.2.1 Reboiler duty as a function of operating capture level

The resulting reboiler duties and corresponding turbine losses from operating partial capture are shown in Figure 5-16. The shape of these relationships is discussed in the following paragraphs for each stripper pressure operating condition.

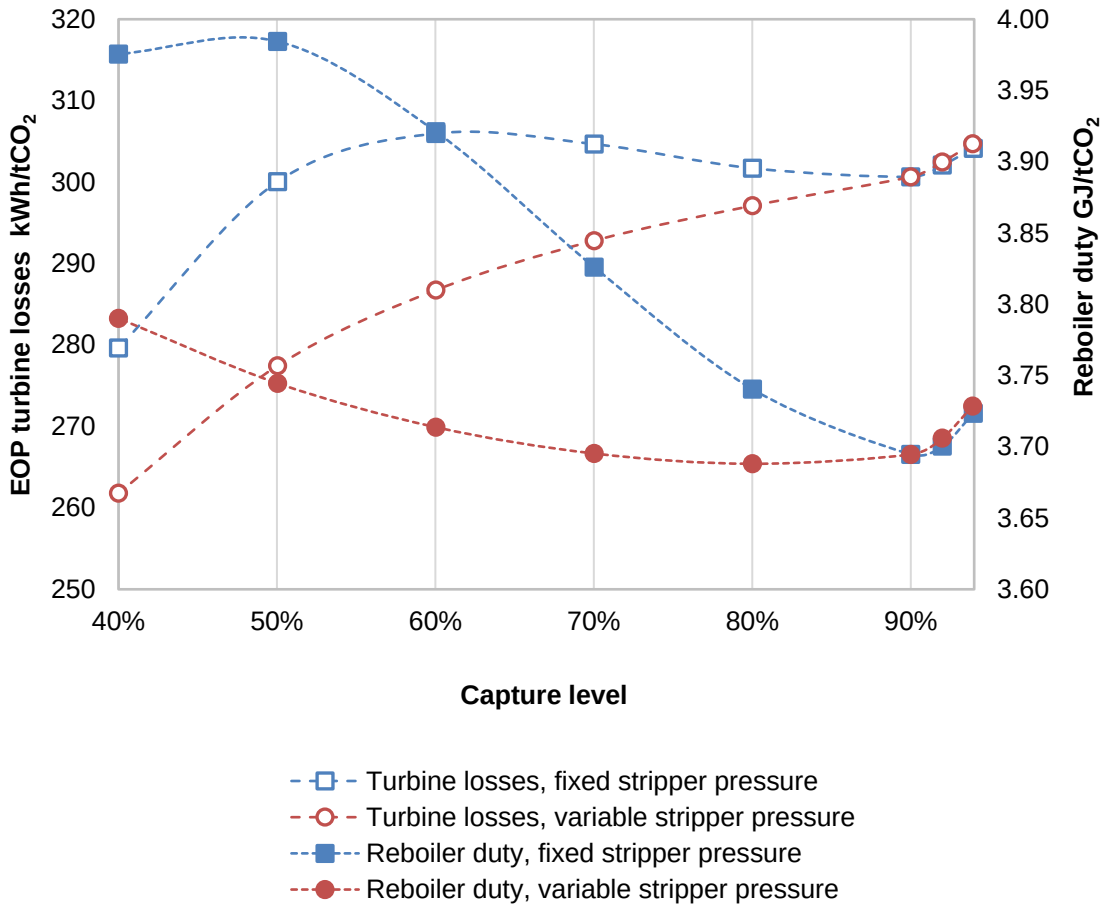

Figure 5-16 Specific reboiler duty (right axis) and corresponding turbine output penalty (left axis) at different capture levels under variable and fixed stripper pressure operation

5.2.2.1.1 Fixed pressure stripper specific reboiler duty

The specific reboiler duty can be seen to increase at both higher and lower capture levels compared with the 90% capture design point under fixed stripper pressure operation. The increase in specific reboiler duty at lower capture levels is predominantly due to the higher reflux ratio associated with the higher partial pressure of steam required to maintain an equivalent stripper pressure with a lower mass flow of CO_2. This is enhanced as the mass of CO_2 captured reduces. Although the solvent flow rate is reduced at partial capture (Figure 5-12), the latent heat requirement for the additional steam is larger than the saving in sensible heat savings achieved

through lower solvent flow rates. However, at capture levels above 90% the reboiler duty increases due to the steep rise in the required solvent flow rate (see Figure 5-12).

The reduction in reboiler duty at 40% capture is due to the reduced pressure drop at lower solvent flow rates in the stripper, effectively increasing the stripper pressure and therefore reducing the reflux ratio.

5.2.2.1.2 Variable pressure stripper reboiler duty

The specific reboiler duty can be seen also to increase at both higher and lower capture levels compared with the 90% capture design point under fixed stripper pressure operation, but to a lesser extent than under variable pressure operation. The increases in specific reboiler duty at lower capture levels are due to the increased pressure required in the stripper to maintain the capture level with lower mass flow rates of CO_2. Like fixed pressure operation, there is an associated increase in the latent heat duty, but the reflux ratio is lower, and therefore the reboiler duty is lower. The increase in specific duty is again enhanced by the reduction in the mass of CO_2 captured, increasing the specific reboiler duty for an equivalent MW reboiler load.

The increase in specific duty at higher capture levels, even though stripper pressures are reduced, is due to the increased solvent flow rate (Figure 5-12). The reduced stripper pressures at high capture levels imply a lower lean loading than for fixed pressure operation at the equivalent capture level, with a higher associated reflux ratio. Therefore, the reboiler duty becomes marginally higher than for fixed pressure operation above the design point.

5.2.2.2 The relationship between reboiler duty and turbine EOP

The non-linear relationship between specific reboiler duty and turbine losses are a consequence of the impact of steam flow rate on pressure drop in the steam extraction line, the impact of steam extraction on the flow rate through the LP turbine, and the subsequent turbine inlet pressure and to a lesser extent the variation in efficiency of the LP turbine.

The higher the steam flow rate, the lower the LP turbine EOP, as shown in Figure 5-6. However, the steam flow rate is dictated by the enthalpy of condensation at the steam saturation pressure, equivalent to the fixed pressure steam diversion point prior to the LP turbine value (3.75 bar) minus the pressure drop in the extraction line, which is a function of steam flow rate, as shown in Figure 5-7. Enthalpies of condensation are higher at lower pressures, therefore steam flow rates can be reduced for a given reboiler duty operating at a lower saturation pressure. This is enabled by the increase in heat exchanger temperature difference also experienced at lower flow rates, as shown in Figures 5-14 and 5-15, as the reboiler doesn't approach pinch conditions. Therefore, although higher specific reboiler duties are experienced at lower capture levels, the absolute reduction in steam flow rates leads to a positive feedback effect where lower saturation pressures require lower flow rates of steam for a given reboiler duty, and specific turbine losses reduce at lower capture levels accordingly. At higher capture levels this effect is reversed, and as such a rise in turbine EOP losses can be seen.

5.2.2.1 Sensitivity of reboiler duty to off-design modelling uncertainties

As discussed in Section 5.1.2.4.1, the basis of off-design heat exchange analysis considers a simplified correlation for off-design point values of the overall heat transfer coefficient *U* (Equation 5.3), which is +-25% accurate. However, a sensitivity analysis indicates that the impact of this accuracy range in the capture plant heat exchangers (the reboiler and the cross-heat exchanger) will have a small on the overall reboiler duty. The reboiler duty is determined by 1) the heat of absorption of CO_2, which is dictated directly by the capture level, 2) the latent heat requirement, which is dictated by the stripper pressure, and 3) the sensible heat of the solvent, influenced by the inlet solvent temperature. It is only this final aspect, therefore, that is impacted by the potential variation in *U*. The temperature difference in the reboiler is dominated by impacts from the pressure drop in the steam extraction line, which dictate the temperature of the reboiler hot side (see Figure 5-7) and the stripper pressure, which dictates the lean loading requirement and thus the heat of absorption (see Figures 5-14 and 5-15). Therefore, the impact of *U* acts only to vary the solvent side outlet only in the reboiler. In the cross-heat exchanger, a +-25% variation in *U* works to vary the temperature of solvent entering the stripper, and the temperature of cooled solvent entering the solvent cooler. However, as the cooling rate of the cooler is assumed to be variable, this does not impact on the absorber. The sensitivity analysis of +-25% variation in *U* saw maximum variations of 1.5K in the stripper hot solvent inlets,

relating to the reboiler exit temperatures and the cross-heat exchanger (rich-in and boil-up in Figure 5-2). This difference in the sensible heat duty resulted in insignificant error in total reboiler duty.

5.2.2.2 Total EOP as a function of capture level

Figure 5-17 shows the EOP contribution of the compression train and the flue gas booster fan at different capture levels.

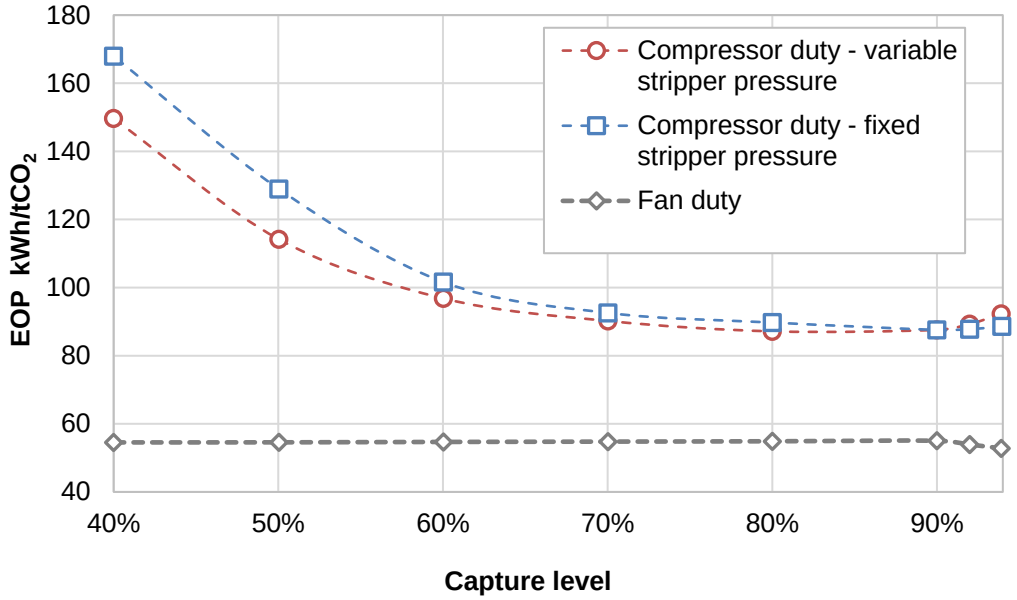

Figure 5-17 The specific electricity output penalty contribution of flue gas booster fan and CO_2 compression at different capture levels under variable and fixed stripper pressure operation

Pump penalties are not shown in this figure as the duty was negligible compared with compression and fan power, but pump penalties are included in overall EOP calculations, providing a contribution of 6 kWh/tCO_2 at 90% capture, increasing slightly at higher capture levels and reducing at lower capture levels.

The specific fan penalty is the same for both fixed and variable stripper approaches as flue gas flows are the same in each. The specific fan EOP is constant with reductions in capture level, due to the approach of partial flue gas bypass relating to a 1:1 turn down in flue gas flow with CO_2 capture. Higher capture levels show a slight reduction in specific EOP of the fan as all flue gas is treated at 90% capture and above, so additional CO_2 is captured for the same absolute fan duty as at 90% capture.

Under fixed pressure operation, the specific compressor duty increases at lower capture levels as the smaller mass of CO_2 being compressed doesn't correspond to reductions in duty as the pressure ratio remains constant. The efficiency is also reduced with deviations from the volumetric flow design point. Furthermore, at 60% capture and lower, the surge point is approached for fixed pressure stripper operation and recycles are required in the compressor, further increasing the EOP. At higher capture levels, the compression EOP increases slightly due to reductions in efficiency associated with the volumetric flow rates that are above the design point.

Under variable stripper operation, stripper exit pressures increase at lower capture levels. Therefore, the pressure ratios required to achieve the outlet pressure of 120 bar are reduced, and so the absolute compressor duty also reduces with capture level, and surge is not approached thus recycling is not required. Subsequently, although specific compressor EOP under also increases at lower capture levels under variable stripper pressure operation, due to the smaller quantities of CO_2 produced for the relative compressor duty, the increase is less than for fixed stripper pressure operation. However, at higher capture levels, stripper exit pressures decrease under variable stripper operation leading to an increase in compressor pressure ratios, and therefore a larger increase in specific compressor EOP.

The compression dynamics described above are illustrated in Figure 5-18, which shows a performance map of the complete compressor with operating points at different capture levels for both fixed and variable stripper pressure operation.

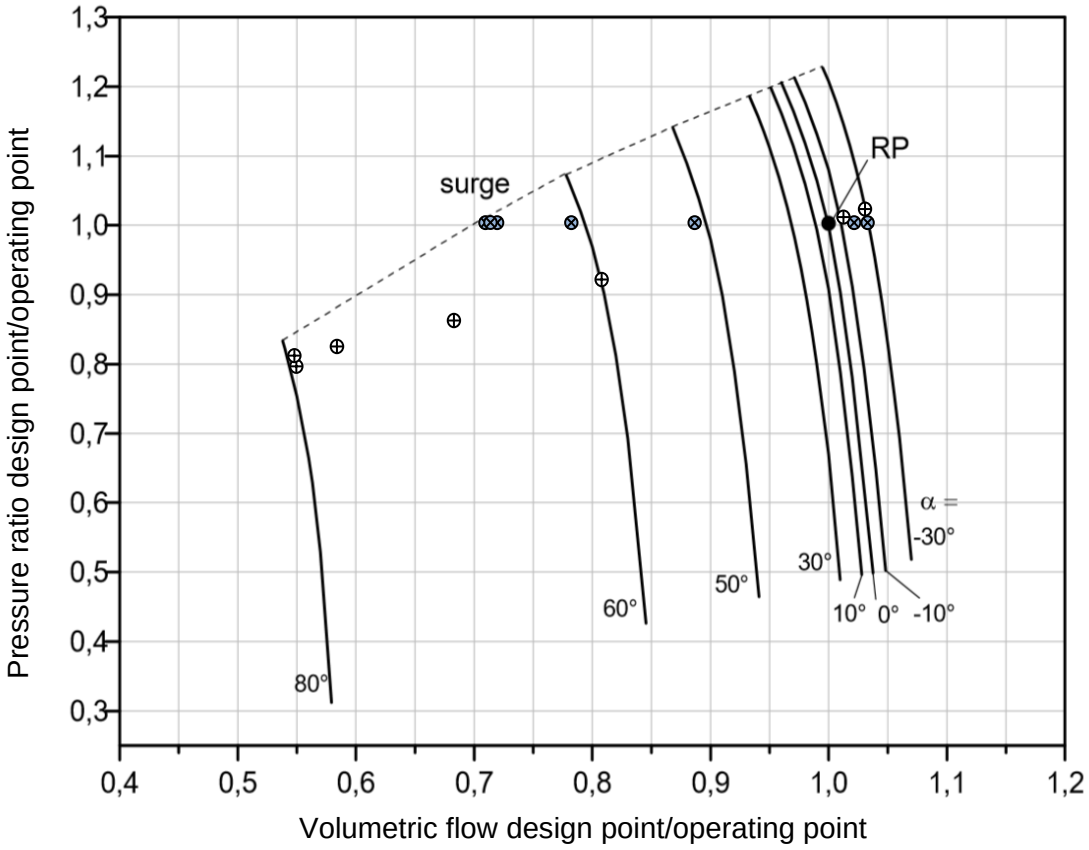

Figure 5-18 Overall compressor map showing surge line and inlet guide vane angles with operating points at different capture levels under both fixed stripper pressure operation (blue X circles) and variable stripper pressure operation (white crossed circles)

Finally, Figure 5-18 shows the total specific electricity output penalty of capture and compression for both operating approaches. These curves are the cumulative result of the variation with capture in reboiler duty and subsequent turbine losses, and the compression, fan and pump duties, as discussed above.

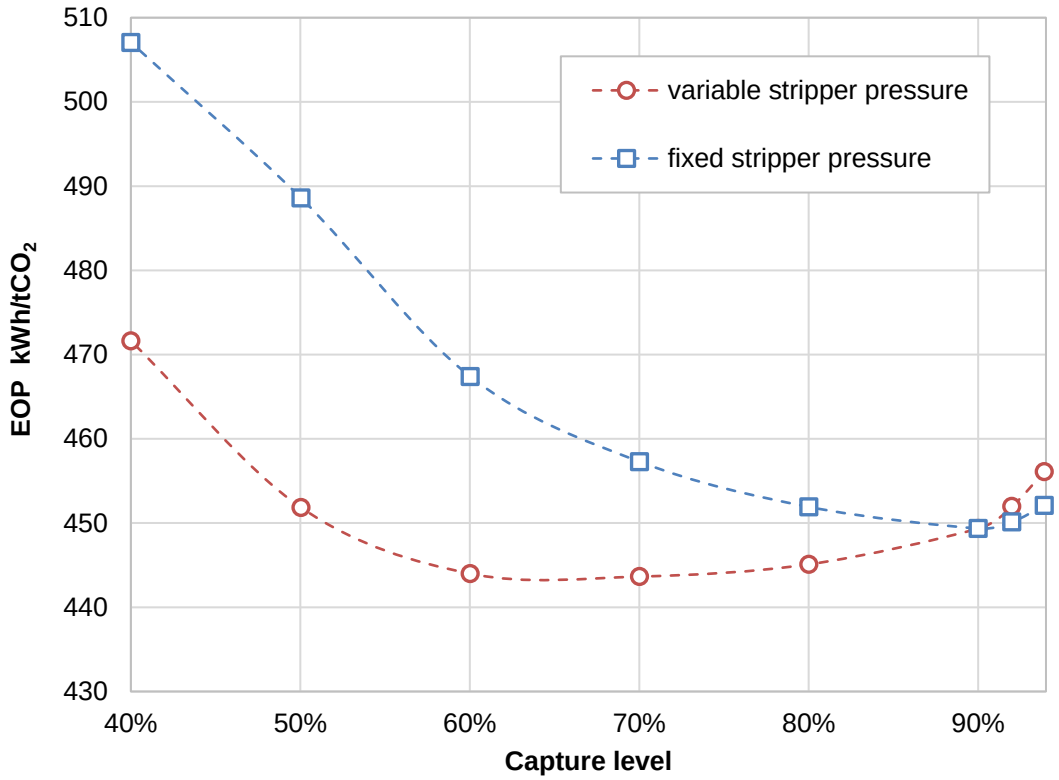

Figure 5-19 Total Electricity Output Penalty of CO_2 capture and compression at different capture levels under variable and fixed stripper pressure operation

At capture levels below the 90% design point, the resulting total EOP for variable stripper pressure operation is lower than for fixed stripper pressure operation. In contrast, at capture levels above the 90% design point, the resulting total EOP for fixed stripper pressure operation is lower than for variable stripper pressure operation.

To summarise the above process discussion, EOP reductions are the cumulative result of:

- lower specific turbine losses associated with:
    - higher lean loadings, leading to
    - lower reflux ratio in the stripper, leading to
    - lower reboiler duty, leading to
    - less steam diverted to the capture plant, leading to
    - lower pressure drops in the steam extraction line, leading to
    - further reductions in steam flow rates for an equivalent reboiler duty
- lower specific compression penalties associated with:
    - higher stripper exit pressures, leading to

- reduction in pressure ratios

At capture levels below the design point, variable stripper pressure operation leads to higher lean loadings and higher stripper pressures, therefore lower specific EOP compared with fixed stripper pressure operation. At capture levels above the design point, the opposite is true. Consequently, the EOP operating curve taken forward for economic analysis in this work assumes a binary operating regime: variable stripper pressures are operated to control partial capture (below 90%), beyond which the stripper pressure is fixed to achieve higher capture levels.

The resultant EOP curve increases above capture levels of 90%, but decreases at capture levels between 60 and 90% when the reduction in turbine losses dominates the total EOP. At capture levels below 60%, the increasing EOP of compression becomes significant and EOP increases again until a minimum capture level of 40% is reached. To conclude this chapter, Figure 5-20 depicts this EOP relationship (taken from the curves in Figure 5-19) together with the relative change in exported electricity output potential corresponding to capture level operation, including the output potential at full bypass of the capture unit with only a small penalty for continued solvent pumping.

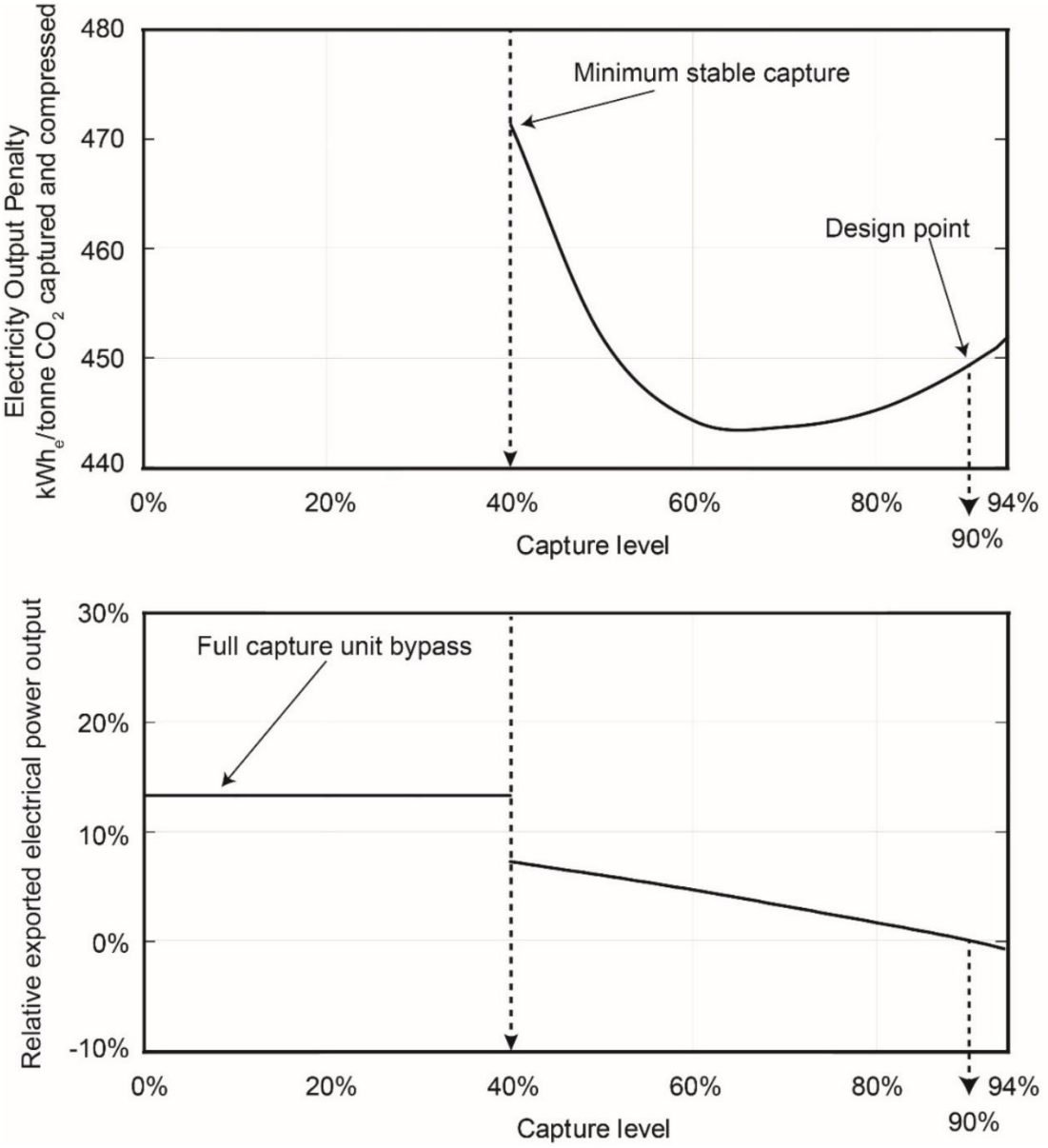

Figure 5-20 The variation in Electricity Output Penalty with capture levels ranging from a minimum capture level of 40% to a maximum of 94%, limited by compressor capability (top). This relationship represents the plant described Chapter 5. The corresponding relative change in exported electricity output potential for off-design point capture level operation is shown (bottom)

6 Optimal operation of CO_2 capture on NGCC plant in low carbon electricity markets

This chapter brings together the concepts described in the preceding chapters to present decision diagrams for optimal capture level operation on the illustrative NGCC plant with post-combustion capture presented in Chapter 5. Diagrams describing both optimal operation, and the relative financial benefit of this operation are presented. The chapter concludes with a discussion on the impacts of this operation to plant operators and to wider society.

6.1 Decision diagrams for optimal capture plant operation of post-combustion capture plant case studies

A set of plant operating decision diagrams are presented in the following section, illustrating the financial implications of optimal capture on the NGCC simulated in Chapter 5. The decision diagrams cover a market space defined by a range of low carbon financial incentives on the x-axis, and wholesale electricity prices on the y-axis. Diagrams are developed under the three different electricity market scenarios considered in this thesis, as described in Chapter 4, namely the “Carbon price” scenario, “Proportional subsidy” scenario and “Counterfactual subsidy” scenario (summarised in Table 4.1).

In the “Carbon price” case study, decision diagrams are based on the balance between the market electricity price and the CO_2 price. Electricity prices ranging from 0 to 200 £/MWh_e and CO_2 prices ranging from 0 to 200 £/tCO_2 are considered. The other two case studies that incorporate a subsidy for zero carbon electricity balance the wholesale market electricity price along-side the premium price paid for zero carbon electricity. Here prices of 0 to 200 £/MWh_e are considered for both wholesale and premium electricity prices. For these latter case studies, the CO_2 price is assumed to be zero, to illustrate the impact of each policy clearly.

Two scenarios are presented for the “Counterfactual Subsidy” case study: a higher value where the ELV is equal to 450 $kgCO_2$/kWh representing near term carbon budgets and a second lower value equal to 100 $kgCO_2$/kWh representing future potential very low carbon electricity systems.

Under each of these market scenarios, there will be an optimal operating regime for each market node represented in the diagrams. This optimal operation corresponds to the previously derived optima described in Equations 4-10 to 4-13.

Operating options in the decision diagrams include operating the plant with capture at optimal capture levels, operating the plant with a capture plant bypass and turning the power plant off when market conditions imply a SRNCF of zero or below. These diagrams build on decision diagrams presented in Chalmers (2010) where options for capture plant on/off and bypass were presented. The decision diagrams demonstrate the financial implications of optimal capture level operation, providing potential values for flexible operation of the integrated NGCC power plant with CO_2 capture.

The operating option which will maximise SRNCF in the each of the given market conditions (i.e. optimal operation) are shown in Figures 6.2-6.5 (A). The real-time (£/hr) financial implications of optimised capture level operation are provided as contour lines for both absolute and additional cash flow at optimal operation in Figures 6.2-6.5 (B). These latter figures present overlays to the original optimal operation decision diagrams, showing cash flow at 90% capture, cash flow at optimal capture, and the relative difference between the two, for each electricity market scenario

To undertake techno-economic analysis of NGCC plant capture level variation, further assumptions of plant operational and cost characteristics are provided in Table 6-1. Energetic values are derived from the simulation described in Chapter 5. Variable costs for the base NGCC plant and the MEA capture plant are taken from NETL (2015), Exhibit 5-18. The power islands are assumed to operate at full load with a constant fuel input.

A natural gas fuel price of 2 p/kWh$_{th}$ is assumed for the contour lines representing financial implications of optimal operation.

Table 6-1 Operating parameters used in techno-economic analysis

Parameter	Units	b) NGCC
Rate of energetic input from fuel ($\boldsymbol{MW_{th}}$)	MW_{th}	1547
Base plant efficiency ($\boldsymbol{\eta_{base}}$)	-	0.605
Fuel specific emissions factor ($\boldsymbol{\epsilon}$)	tCO_2/MWh_{th}	0.202
Energy penalty of ancillary equipment at bypass ($\boldsymbol{anc}$)	%-points	0.121
Variable costs of base plant ($\boldsymbol{vc_{base}}$)	£/MWh_e	1.3
Variable costs of capture plant ($\boldsymbol{vc_{cap}}$)	£/tCO_2	2

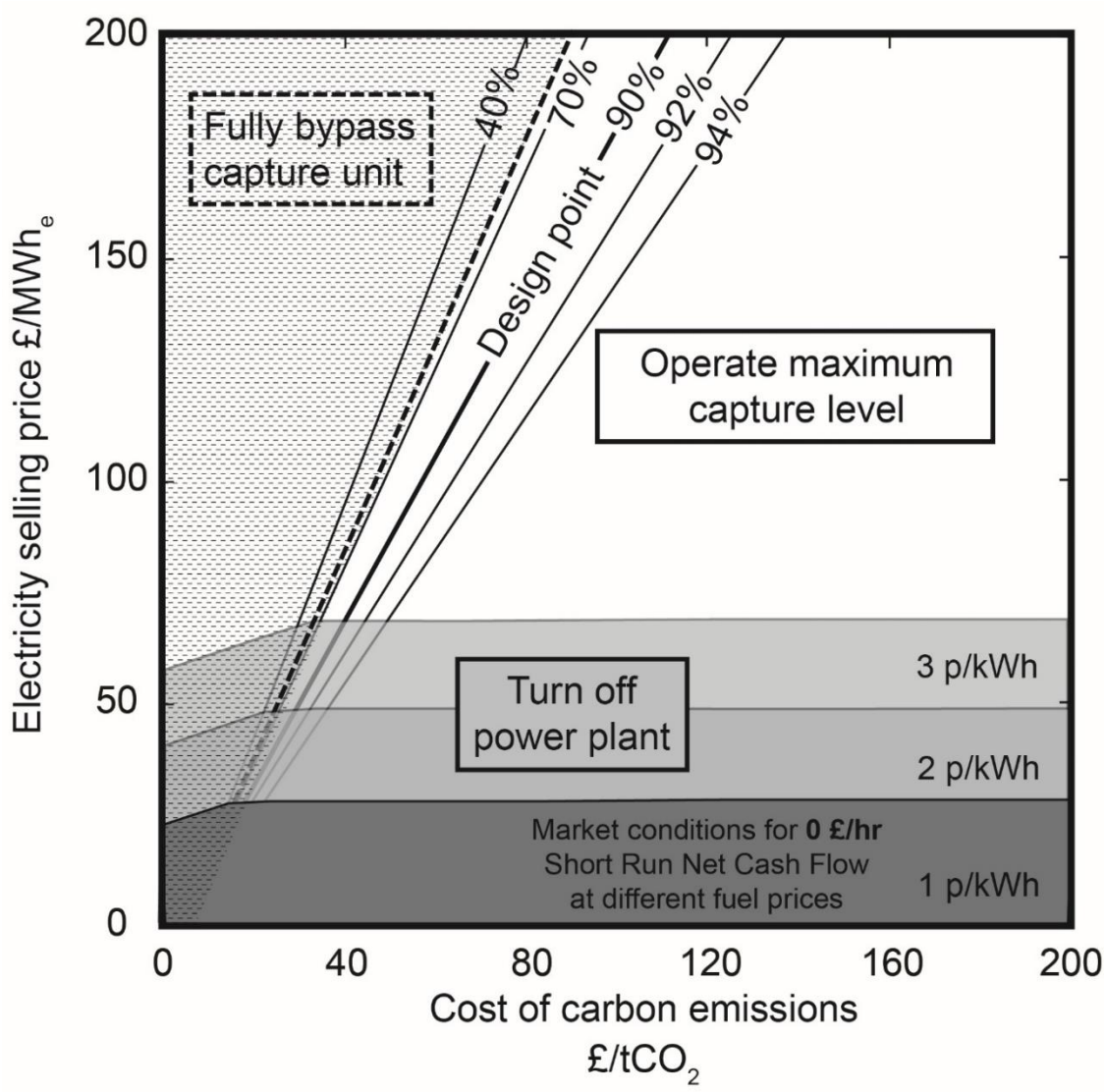

Figure 6-1 (A). Optimal capture operation for the Carbon Price case study

Integrated NGCC post-combustion capture plant operating decision diagram for an electricity market with a carbon price only. Contour lines represent the optimum operating capture levels that maximise SRNCF at the corresponding electricity selling price and CO_2 price conditions. The hatched region indicates price conditions where plant bypass is the optimal operating option. Shaded regions indicate price conditions where the SRNCF of the plant is zero or negative, at a given fuel price, and thus where a power plant must stop operating or experience negative cash flow.

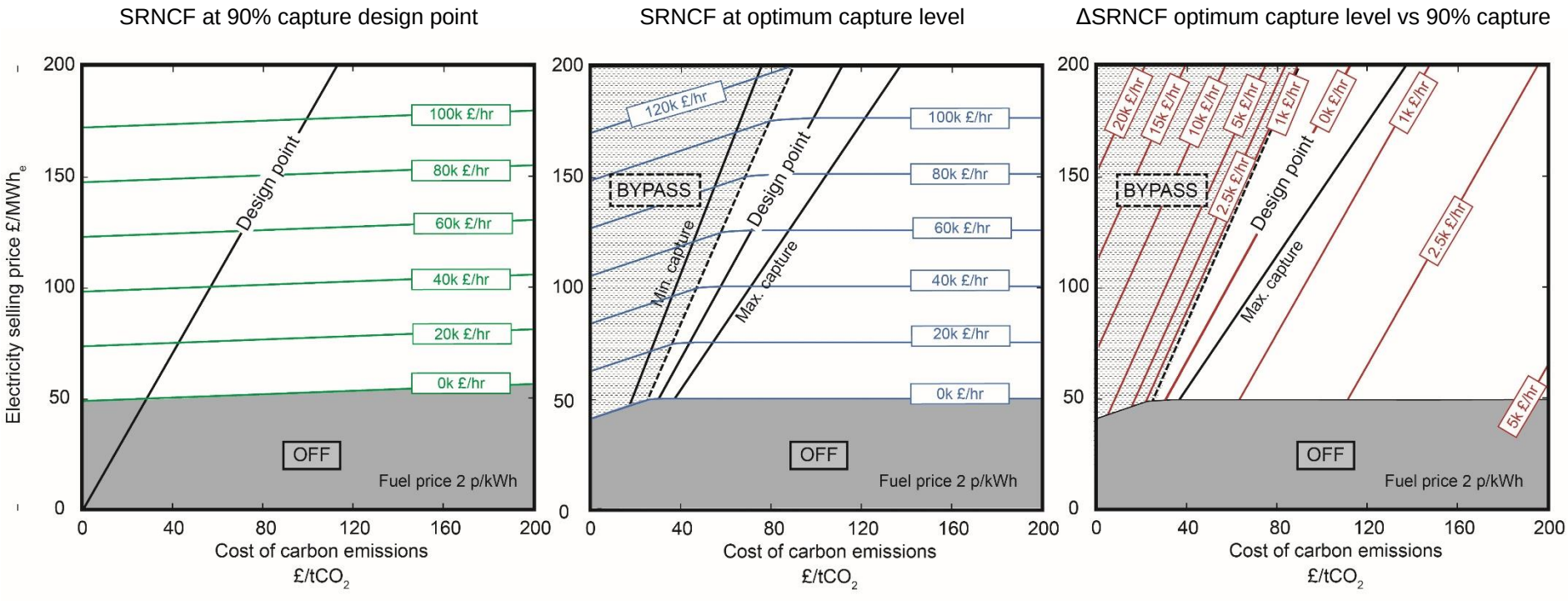

Figure 6-1 (B) Short Run Net Cash Flow (SRNCF) implications for the Carbon Price case study

Short Run Net Cash Flow (SRNCF) contours for NGCC plant operating with post-combustion capture in an electricity market with a carbon price only, under given electricity and CO_2 price conditions. SRNCF achieved maintaining a set capture level of 90% (left), SRNCF achieved operating the capture plant optimally as shown in Figure 6-1 (A) (centre), additional SRNCF achievable by operating in the optimal conditions compared with maintaining a set capture level of 90% under all market price conditions (right) illustrating the difference between the first two diagrams.

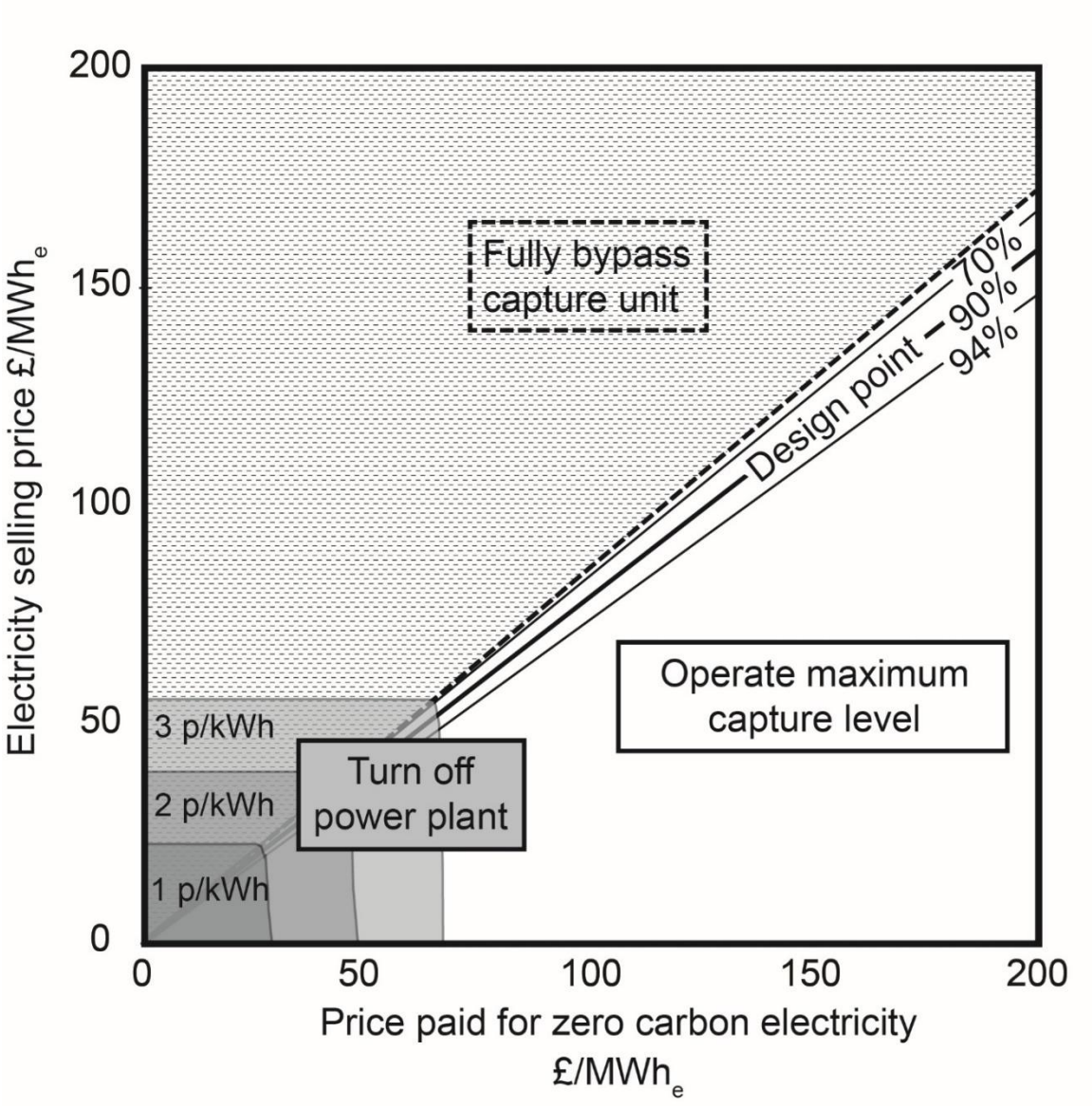

Figure 6-2 (A) Optimal capture operation for the Proportional Subsidy case study

Integrated NGCC post-combustion capture plant operating decision diagram for an electricity market paying a subsidy for zero carbon electricity directly proportional to the capture level. There is no carbon price considered (0 £/tCO_2) in this diagram. Contour lines represent the optimum operating capture levels that maximise SRNCF at the corresponding electricity selling price and the zero-carbon electricity subsidy price. The hatched region indicates price conditions where plant bypass is the optimal operating option. Shaded regions indicate price conditions where the SRNCF of the plant is zero or negative, at a given fuel price, and thus where a power plant must stop operating or experience negative cash flow

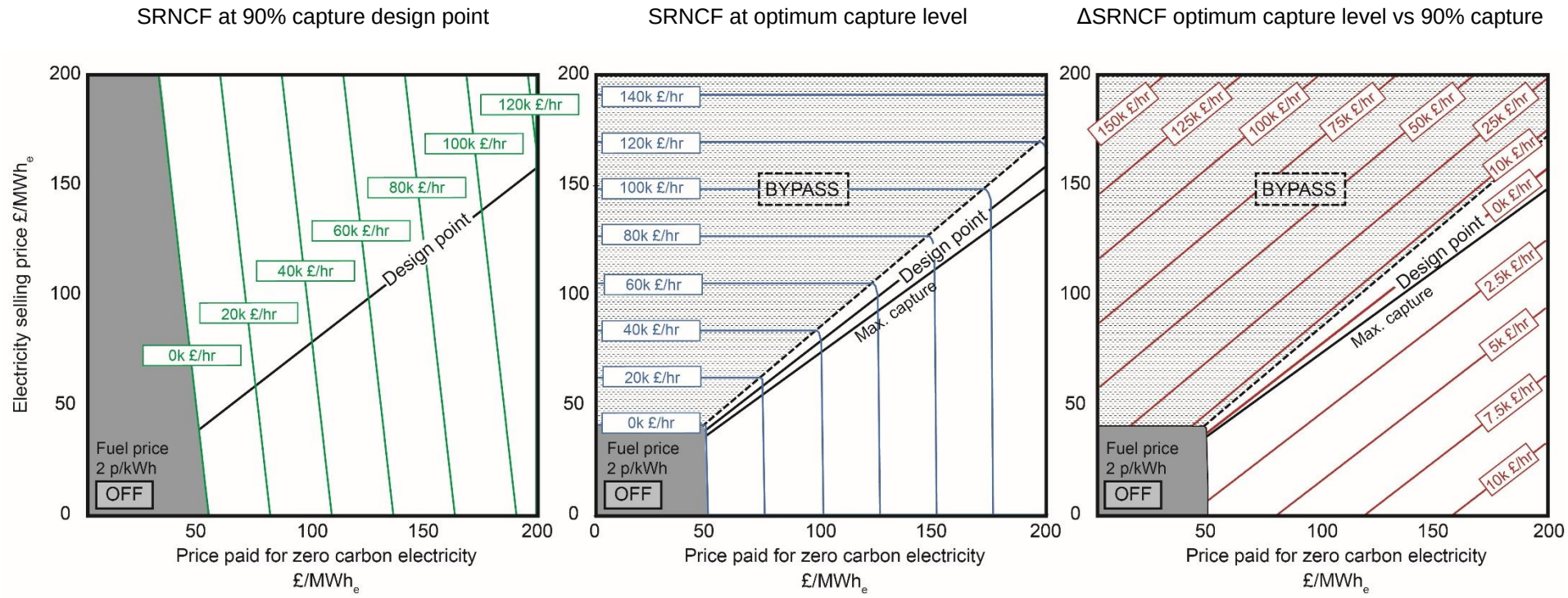

Figure 6-2 (B) Short Run Net Cash Flow (SRNCF) implications for the Proportional Subsidy case study

Short Run Net Cash Flow (SRNCF) contours for NGCC plant operating with post-combustion capture in an electricity market with proportional capture subsidy, under given electricity and subsidy price conditions. SRNCF achieved maintaining a set capture level of 90% (left), SRNCF achieved operating the capture plant optimally as shown in Figure 6-2 (A) (centre), additional SRNCF achievable by operating in the optimal conditions compared with maintaining a set capture level of 90% under all market price conditions (right) illustrating the difference between the first two diagrams. There is no carbon price considered (0 £/tCO_2) in this diagram.

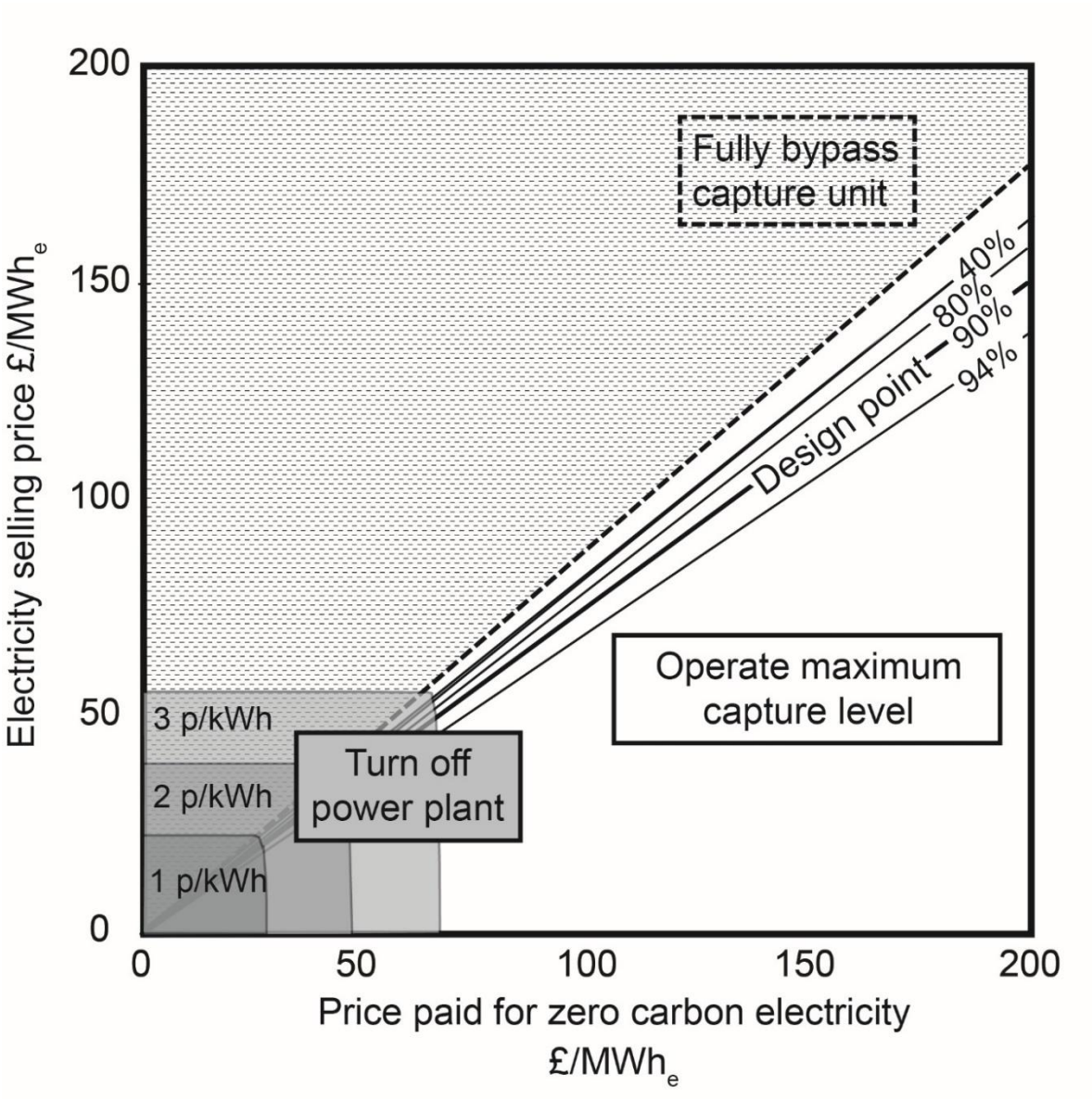

Figure 6-3 (A). Optimal capture operation for the Counterfactual Subsidy case study for an ELV of 450 kg/kWh$_e$

Integrated NGCC post-combustion capture plant operating decision diagram for an electricity market paying a subsidy for zero carbon electricity, based on a counterfactual CO_2 emission intensity of 450 kg/kWh$_e$. There is no carbon price considered (0 £/tCO_2) in this diagram. Contour lines represent the optimum operating capture levels that maximise SRNCF at the corresponding electricity selling price and the zero-carbon electricity subsidy price. The hatched region indicates price conditions where plant bypass is the optimal operating option. Shaded regions indicate price conditions where the SRNCF of the plant is zero or negative, at a given fuel price, and thus where a power plant must stop operating or experience negative cash flow.

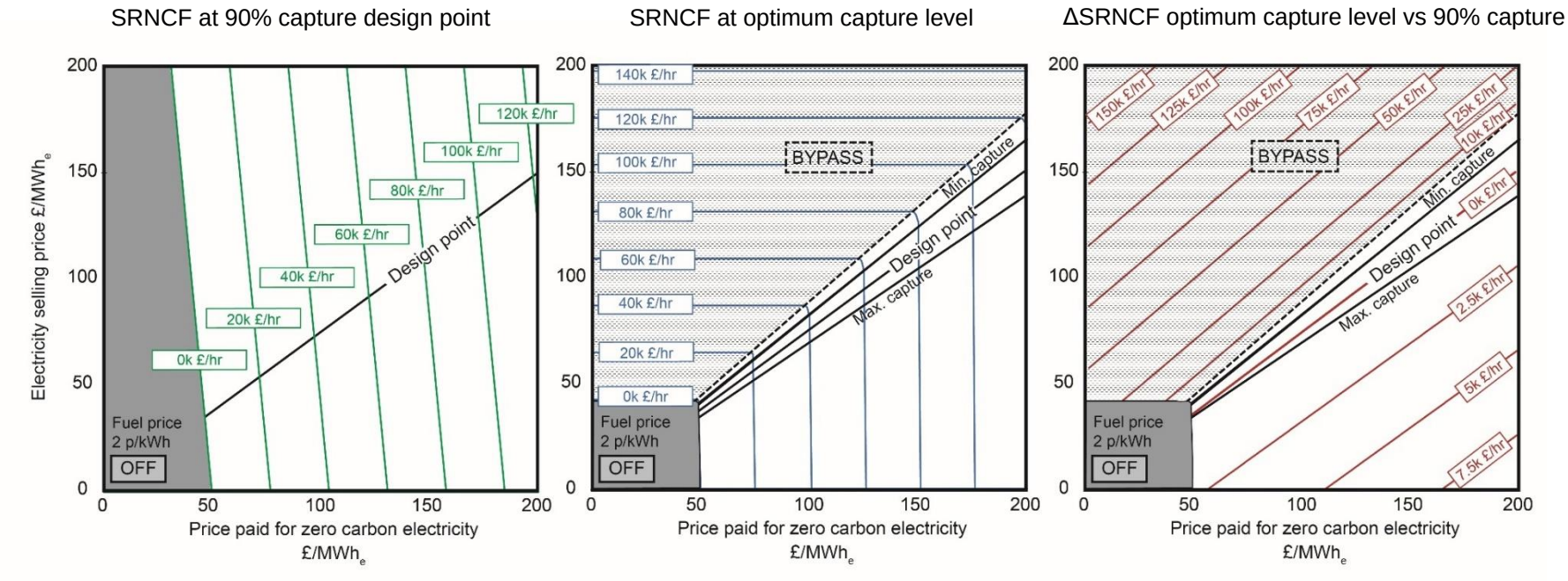

Figure 6-3 (B) Short Run Net Cash Flow (SRNCF) implications for the Counterfactual Subsidy case study for an ELV of 450 kg/kWh$_e$

Short Run Net Cash Flow (SRNCF) contours for NGCC plant operating with post-combustion capture given electricity and subsidy price conditions, in an electricity market with a subsidy based on a counterfactual CO_2 emission intensity of 450 kg/kWh$_e$. *S*RNCF achieved maintaining a set capture level of 90% (left), SRNCF achieved operating the capture plant optimally as shown in Figure 6-3 (A) (centre), additional SRNCF achievable by operating in the optimal conditions compared with maintaining a set capture level of 90% under all market price conditions (right) illustrating the difference between the first two diagrams. Natural gas fuel price of 2 p/kWhth is assumed and there is no carbon price considered (0 £/tCO_2) in this diagram

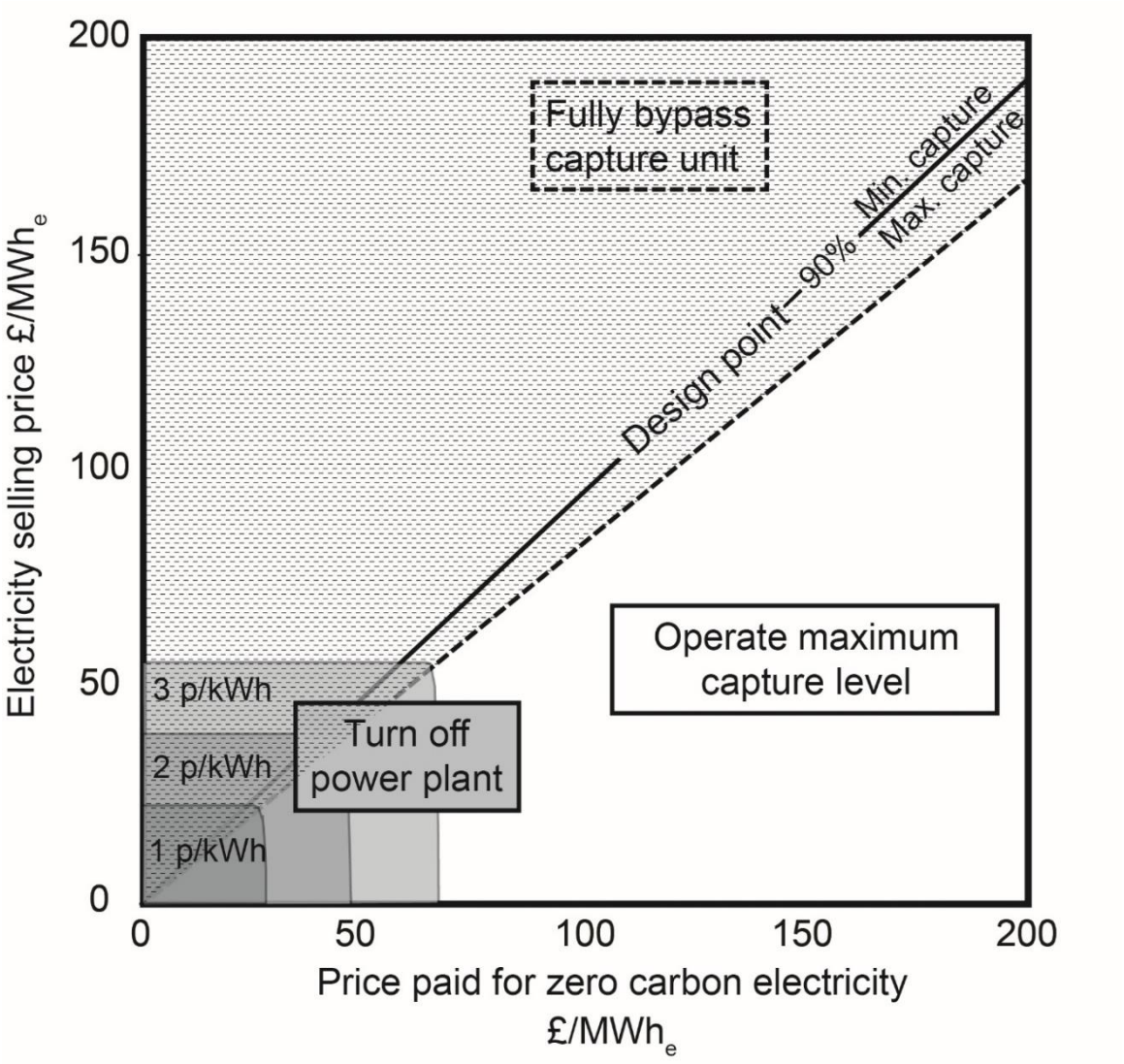

Figure 6-4 (A) Optimal capture operation for the Counterfactual Subsidy case study for an ELV of 100 kg/kWh$_e$

Integrated NGCC post-combustion capture plant operating decision diagram for an electricity market paying a subsidy for zero carbon electricity, based on a counterfactual CO_2 emission intensity of 100 kg/kWh$_e$. There is no carbon price considered (0 £/tCO2) in this diagram. Contour lines represent the optimum operating capture levels that maximise SRNCF at the corresponding electricity selling price and the zero-carbon electricity subsidy price. The hatched region indicates price conditions where plant bypass is the optimal operating option. Shaded regions indicate price conditions where the SRNCF of the plant is zero or negative, at a given fuel price, and thus where a power plant must stop operating or experience negative cash flow.

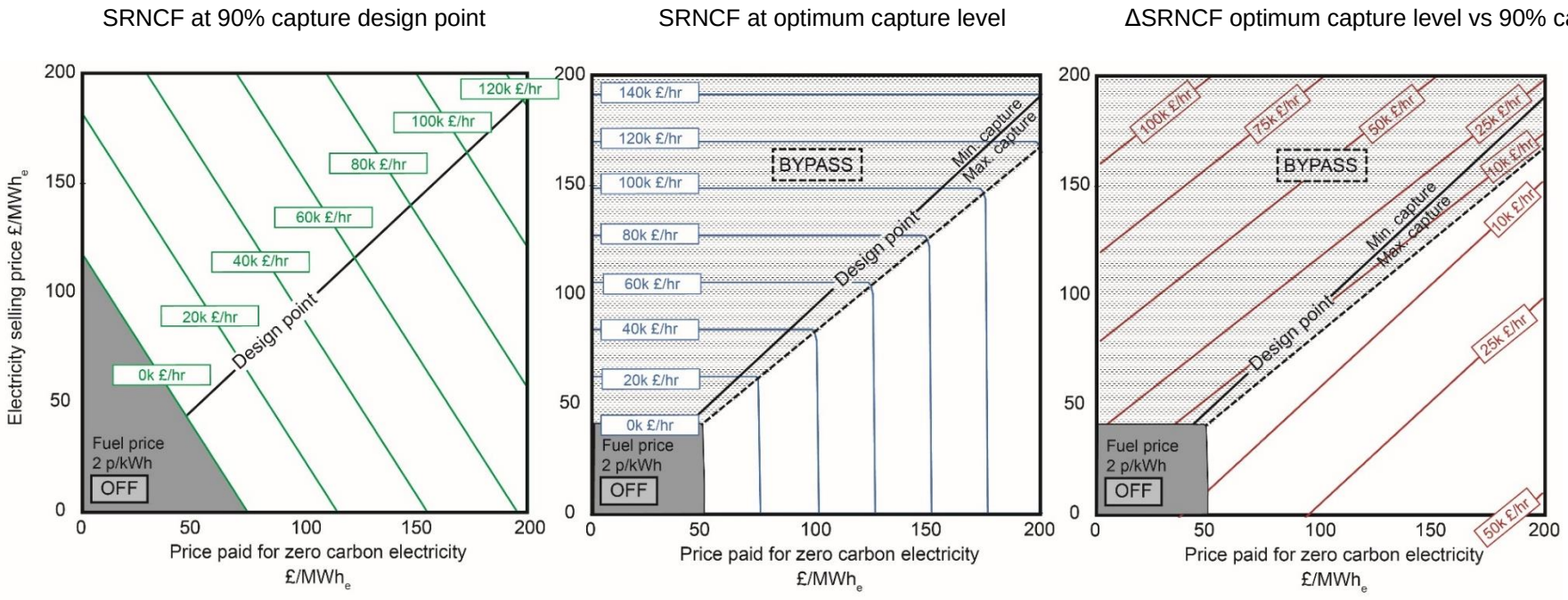

Figure 6-4 (B) Short Run Net Cash Flow (SRNCF) implications for the Counterfactual Subsidy case study for an ELV of 100 kg/kWh$_e$

Short Run Net Cash Flow (SRNCF) contours for NGCC plant operating with post-combustion capture given electricity and subsidy price conditions, in an electricity market with a subsidy based on a counterfactual CO_2 emission intensity of 100 kg/kWh$_e$. SRNCF achieved maintaining a set capture level of 90% (left), SRNCF achieved operating the capture plant optimally as shown in Figure 6-4 (A) (centre), additional SRNCF achievable by operating in the optimal conditions compared with maintaining a set capture level of 90% under all market price conditions (right) illustrating the difference between the first two diagrams. Natural gas fuel price of 2 p/kWh$_{th}$ is assumed and there is no carbon price considered (0 £/tCO_2) in this diagram

Figures 6-1 to 6-4 indicate that within the range of market conditions considered, it is likely to be economically beneficial to operate the capture unit off-design point under certain circumstances for each of the electricity markets. As a general trend, design capture levels are optimum for a limited range of market conditions. There are also limited conditions under which it is optimal to reduce the capture level rather than bypass the plant. When electricity prices are high, or CO_2 prices and zero carbon subsidies low, full plant bypass is shown to return the highest cash flow. Higher capture levels are shown to be preferable when CO_2 abatement incentives (CO_2 prices or subsidies for zero carbon electricity) are high compared with electricity prices. There are also market conditions in all three scenarios under which plant income would be lower than plant SRMC (SRNCF becomes negative) when the financially optimal operation would be to turn the plant off.

Optimal operation and financial implications of this operation are summarised in Table 6-2, where numerical values are given for some possible price points under each of the market scenarios.

The optimum capture level (including plant bypass) and the financial benefit of this operation is unaffected by changes in fuel price, as the fuel input is kept constant with changes in the CO_2 capture process. The hourly financial benefit of flexible operation (the delta increase in SRNCF) is specific to the plant size given in this example. The relative significance of this delta increase in SRNCF compared with total SRNCF at 90% capture is therefore illustrated in Table 6-2 as a percentage, which becomes independent of plant size. However, both values of increased SRNCF are specific to fuel price. The values shown in this analysis would be enhanced at higher fuel prices and diminished at lower fuel prices, but the optimum operation conditions would remain the same, except for the turn off condition. In Table 6-2, as in Figures 6-1 to 6-4, a natural gas price of 2 p/kWh$_{th}$ is assumed.

Although the optimum operating scenarios and relative financial gains from this methodology are not affected by fuel prices when fuel input is constant, the overall net cash flow of the plant would increase or decrease with fuel price, as can be seen in the variable on/off condition of the plants as shown in Figures 6-1 to 6-4. This has implications for a zero-carbon subsidy on carbon capture technologies, since if fuel prices change without proportional changes in a subsidy, plant revenue would decrease by the same amount regardless of the options shown here. Plant capital and associated financing costs may be paid off more slowly, and the plant may

potentially move down system merit orders, reducing the load factor and challenging plant finances.

The general trends illustrated in Table 6-2 and Figures 6-1 to 6-4 illustrate that as electricity prices, or subsidy payments, increase, and as CO_2 prices decrease, the total plant SRNCF will increase. Therefore, delta increases in SRNCF from operating optimally will be, relative to total plant SRNCF, proportionally more significant at lower electricity prices, for lower subsidy payments, and for higher CO_2 prices. This is skewed slightly by the fact that at higher electricity prices, the potential for increasing SRNCF by operating flexibly is also higher, by exporting more electricity to the wholesale market for sale at these prices. Although in some cases the increase in SRNCF may be relatively small, it is important to note that this increase will affect profit at the margin, and by extension the Internal Rate of Return, and so the effective LCOE.

Each market scenario has different implications for the operating patterns of the NGCC plant operating post-combustion capture. The implications for each case study are set out below.

Table 6-2 Summary of optimum capture operation for the illustrative integrated NGCC capture plant and corresponding financial implications for likely price points in different low carbon electricity market case studies, as presented in Figures 6-1 to 6-4. A fuel price of 2 p/kWh$_{th}$ is assumed in these values.

Case study	CO_2 price/ zero carbon subsidy	Whole sale market electricity price								
		50 £/MWh$_e$			100 £/MWh$_e$			150 £/MWh$_e$		
		Optimum capture condition	Additional SRNCF £'000/hr	Additional SRNCF/ SRNCF$_{90}$ %	Optimum capture condition	Additional SRNCF £'000/hr	Additional SRNCF/ SRNCF$_{90}$ %	Optimum capture condition	Additional SRNCF £'000/hr	Additional SRNCF/ SRNCF$_{90\%}$
Carbon price	20 £/tCO_2	Bypass	1.7	2.7	Bypass	7.9	0.19	Bypass	14.2	0.2
	50 £/tCO_2	Turn off			77%	0.1	0.00	Bypass	5.7	0.1
	120 £/tCO_2	Turn off			94%	0.8	0.02	94%	0.5	0.01
Proportional subsidy	50 £/MWh$_e$	Bypass	7.3	5.77	Bypass	50.0	9.4	Bypass	92.6	9.9
	100 £/MWh$_e$	94%	0.8	0.02	Bypass	13.6	0.33	Bypass	56.2	1.27
	150 £/MWh$_e$	94%	2.1	0.03	94%	0.5	0.01	Bypass	19.8	0.24
Counterfactual subsidy: 450 kg/MWh	50 £/MWh$_e$	Bypass	7.3	1.96	Bypass	50.5	7.01	Bypass	93.8	8.8
	100 £/MWh$_e$	94%	0.6	0.01	Bypass	13.6	0.31	Bypass	56.8	1.19
	150 £/MWh$_e$	94%	1.6	0.02	94%	0.2	0.00	Bypass	19.8	0.23
Counterfactual subsidy: 100 kg/MWh	50 £/MWh$_e$	Bypass	7.3	1.96	Bypass	38.4	1.98	Bypass	69.5	1.99
	100 £/MWh$_e$	94%	5.4	0.19	Bypass	13.6	0.31	Bypass	44.6	0.75
	150 £/MWh$_e$	94%	11.3	0.21	94%	5.1	0.07	Bypass	19.8	0.23

6.2 Implications of optimal capture level operation for plant finance

The results from each market scenario indicate that operating flexible capture can lead to increased revenue for the NGCC integrated with post-combustion capture plant considered in this work. Notwithstanding considerations of increased costs in operating off-design point, plant operators will likely be incentivised to vary plant operating capture levels.

To quantify the impact of optimal capture level operation under the different market case studies, a set of price duration curves was taken from Poyry (2011). The price duration curves are illustrated in Figure 6.5 and provide illustrative wholesale electricity prices as a proportion of the year under different renewable penetration scenarios corresponding to 2010, 2020 and 2030. These scenarios correspond to the system profiles shown in Figure 2.3.

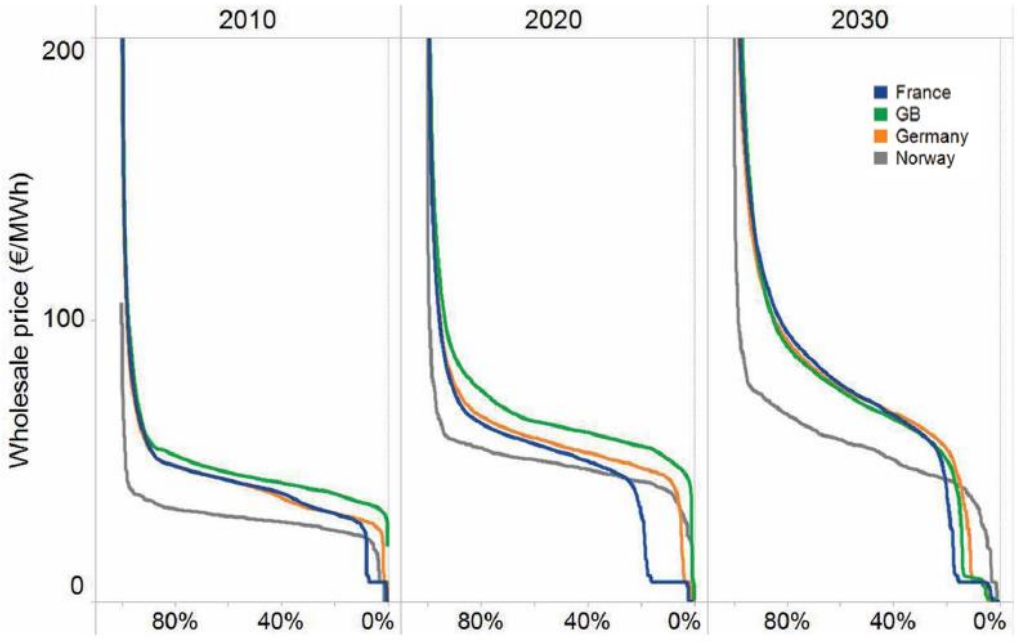

Figure 6-5 Price duration curves showing hourly prices stacked highest to lowest for different electricity system scenarios, relating to different system portfolios as depicted in Figure 2.3. Poyry (2011).

Price points from the GB curves in Figure 6-5 are given in Table 6.3. Poyry's analysis considered electricity prices in Euro rather than pound. Due to uncertainties in conversion rates, this illustrative analysis converts their prices to pounds on a 1:1 basis.

Table 6-3 Wholesale electricity prices, and their duration per year under GB energy system portfolio scenarios for 2010, 2020 and 2030 (extracted from Poyry, 2011)

Wholesale electricity price £/MWh	2010		2020		2030	
	Cumulative hours at or above price	Hours at price	Cumulative hours at or above price	Hours at price	Cumulative hours at or above price	Hours at price
0	8760	0	8760	57	8377	820
10	8760	29	8703	0	7557	72
20	8731	39	8703	38	7485	64
30	8692	2591	8665	35	7421	147
40	6101	3795	8629	563	7275	303
50	2306	1523	8067	2404	6972	922
60	784	252	5663	3221	6049	1771
70	532	154	2441	1121	4278	1400
80	378	62	1321	520	2878	1065
90	316	103	801	250	1813	536
100	214	48	551	119	1277	279
110	165	34	432	75	999	226
120	132	27	357	78	773	147
130	104	27	279	69	626	76
140	77	12	210	36	549	77
150	65	8	174	31	472	45
160	58	8	143	28	427	40
170	50	8	114	25	387	33
180	42	10	89	25	354	55
190	31	29	64	25	299	69
200	2	2	38	38	230	230

Using these price points and durations, it is possible to quantify annual financial benefits of optimal capture operation for each low CO_2 electricity market scenario.

The additional financial benefit of operating the capture plant optimally is quantified based on the annual difference in plant SRNCF operating at optimal capture, compared with a fixed 90% design point operation, described by Equation 6.1.

$$Additional\ SRNCF = SRNCF_{(opt)} - SRNCF_{(90\%\ capture)} \quad (6.1)$$

The SRNCF for each market case study is calculated using the parametric equations defined in Chapter 4 (Equations 4-6 to 4-7) operating optimal capture or bypass based on the given market conditions (Equations 4-8 to 4-13). Table 6-4 presents the

subsequent cumulative additional income from operating with optimal capture, over the course of the price duration curves from Poyry (2011) set out in Table 6-3.

Table 6-4 Additional annual income from operating optimal capture levels in GB energy system portfolio scenarios for 2010, 2020 and 2030 (extracted from Poyry, 2011) at illustrative carbon incentive price points for each low carbon market case study

Case study	**CO_2 price/ zero carbon subsidy**	**Annual benefit of flexible operation £m/yr**					
		2010	**2020**	**2030**	**2010**	**2020**	**2030**
Carbon price	20 £/tCO_2	8	30	39	**Plus carbon price of £50/tCO_2**		
	50 £/tCO_2	1	4	7			
	120 £/tCO_2	2	8	6			
Proportional subsidy	50 £/MWhe	31	150	227	20	70	142
	100 £/MWhe	11	29	66	9	24	48
	150 £/MWhe	7	21	34	7	23	30
Counterfactual subsidy: 450 kg/MWh	50 £/MWhe	31	151	230	20	72	144
	100 £/MWhe	11	28	66	8	23	48
	150 £/MWhe	6	18	32	6	19	28
Counterfactual subsidy: 100 kg/MWh	50 £/MWhe	24	120	178	14	51	101
	100 £/MWhe	18	52	71	16	47	53
	150 £/MWhe	25	83	76	26	85	72

This result indicates that flexible operation through variation of capture levels can be valuable in the order of millions of pounds per year for all the market scenarios presented in this work, under even conservative price assumptions. The value of optimal capture level operation increases in energy systems with higher renewable penetration, as indicated in the increased annual benefit in the 2010, 2020 and 2030 scenarios. Conversely, the value of variable capture decreases with carbon price, as the penalty of venting additional CO_2 increases. In the same way, the value of flexibility is reduced in the Counterfactual Subsidy 100kg/MWh case compared with the 450kg/MWh case, as in a tightly limited system where CO_2 premiums are paid only for very low CO_2 emissions, and so less of the electricity will be eligible for subsidies during capture plant turndown.

6.3 Discussion and analysis of optimal capture level operation in low carbon electricity market case studies

6.3.1 Carbon price case study

The carbon price case study represents a liberalised electricity market constrained by a market CO_2 price, which also varies in value. Electricity prices must be sufficient to cover operating costs of electricity generation including CO_2 emissions; at low electricity prices with higher carbon prices, the cost of operating the plant, even with bypass, will be prohibitive. Current average wholesale electricity prices will not cover the short run marginal costs (SRMC) for a NGCC post-combustion capture plant to operate in a market with a medium to high carbon price.

When the ratio of electricity price to CO_2 price is high, it will be valuable to reduce the capture level and produce more electricity to sell at these prices. At medium carbon prices (assumed here at £50/tCO_2), when electricity prices spike to 100-150 £/MWh, marginally reduced CO_2 capture levels will achieve the highest financial gain, providing small increases in SRNCF. In contrast, when the ratio electricity price/CO_2 price is low at very high CO_2 prices, it may be valuable to increase capture levels, although the gain in SRNCF is likely to be small.

The decision diagram implies that for a current middling market electricity price of £50/MWh and CO_2 price of £20/tCO_2, the NGCC plant would be operating at or near the design point capture level of 90%, although at close to its marginal cost depending on fuel price. However, as the gradient for optimum operation is steep along the electricity selling price axis, an increase in electricity price of less than £10/MWh would incentivise significantly lower capture levels. It is this reason that several additional million pounds per year would be gained under optimal operation when operating in this lower carbon price market. Additionally, this high sensitivity to price increases implies that, for the illustrative plant considered in this work, the price of variable operation in the carbon price market is low, and as such, likely to be competitive with other providers of grid flexibility. For example, short run marginal costs of OCGT or similar peaking plant are typically several times higher than £10/MWh (IEA, 2017).

Significant increases in SRNCF can be seen when electricity prices are very high, especially when carbon prices are low. Flexible operation would therefore be most valuable to plant operators under these conditions

6.3.2 Proportional subsidy case study

The proportional subsidy scenario assumes that CO_2 prices are not developing and instead zero carbon energy is subsidised proportional to the capture level percentage of the total electricity exported. At higher capture levels the amount of money paid through subsidy increases and at lower capture levels, it decreases.

At a market electricity price of £50/MWh_e, a subsidy of £60/MWh_e would be required to incentivise capture levels of around 90% for a coal plant in the absence of any other market CO_2 price. Where a carbon price also existed in addition to the subsidy, the subsidy price to incentivise 90% capture would decrease slightly with increasing CO_2 prices accordingly.

CO_2 capture level turn down is incentivised until the subsidy is equal to the price of electricity plus the costs of variable CO_2 capture, after which bypass becomes the condition to maximise plant SRNCF. This effectively leads to an arbitrage between market electricity prices and zero carbon subsidy prices, which dictates whether the plant will operate with or without CO_2 capture. The benefit of this bypass operation becomes more significant with increasing electricity price. Conversely, high subsidy/electricity market price ratios quickly incentivise maximum capture, even at likely lower end subsidies (£70/MWh). The conditions under which the design capture level is optimum are therefore very limited, i.e. small variations in electricity price incentivise changes in output and thus flexible operation through varying capture in this market would again be low price.

Compared with the carbon price only case study, larger variations in plant output would be expected from the same shift in electricity price, as the electricity sold will obtain returns from both electricity prices and subsidy prices, and so for a given wholesale electricity price and fuel price, the plant is more likely to cover SMRC and generate power when operating optimally and able to bypass the plant: Where CO_2 prices are assumed to be zero, full bypass of the capture unit will always be optimal where the subsidy prices are equal to or lower than wholesale electricity prices. This effect is however impacted by an additional carbon price cost in this market, as can be seen on the right-hand side columns of Table 6-4, where the value of flexible operation is diminished with a medium carbon price applied.

The value of flexible operation to the generator, as shown in Table 6-4, is higher than for the carbon price only case study. This is because operating at design point implies

a fixed price income for 90% of output, regardless of market movements. By operating flexibly the plant is exposed to the peaks in the electricity market it would otherwise not be able to access, which was not true of the carbon price only case study. In this way, the additional value of flexibility reduces with higher priced subsidies.

However, the nature of this case study implies that the money paid is not related to the CO_2 emissions intensity of the plant, i.e. a more CO_2 intensive plant (e.g. coal-fired) operating the same capture level would receive the same subsidy ratio as the NGCC plant. These results lead to significant flaws in this market arrangement. Instead a subsidy that accounts for reductions in CO_2 in definitions of clean electricity is proposed in the counterfactual scenario.

6.3.3 Counterfactual subsidy case study

The counterfactual subsidy scenario represents a market where existing electricity prices and CO_2 prices are not sufficient, and further intervention for incentivising low carbon electricity is required in the form of a subsidy. In this case, the subsidy is designed to recognise the total CO_2 emissions from a given plant by considering an emission limit standard. In this way, the subsidy paid for zero carbon electricity is based upon identical criteria for all plant regardless of capture level, and more representative of a market carbon price.

If the ELV is decreased to very low levels, plant designed for 90% capture operating with a fixed subsidy may no longer be able to operate profitably. At this point, because the optimal capture level is so high, the plant cannot meet this capture level without exceeding very high energy penalties, and it becomes preferable to bypass, as the cost of capture (required to gain significant income from the ELV) is not covered by the energetic penalty. Where plant begin operating above capture level for a high proportion of total operating hours, design capture level plant upgrades may be desirable.

As with the proportional subsidy scenario, the plant receives income from both the electricity market and subsidies, so plant SRMC will be met at lower electricity prices, provided fuel prices are not high. However, for equivalent electricity and fuel prices, a slightly higher subsidy price is required than for the proportional subsidy for the “Turn off/Turn on” conditions as this counterfactual subsidy electricity market will define a smaller proportion of electricity as zero carbon in this coal plant example, basing the definition on CO_2 emissions as well as electricity generated.

Higher capture levels are incentivised at medium subsidy/electricity price ratios, for a small increase in SRNCF. This becomes exacerbated when the ELV become more restricted, shown in the ELV 100 kg/MWh case, as less electricity generated will be eligible for subsidy without higher capture levels. The nature of the swing condition between subsidy and electricity price ratios implies that there are very limited conditions under which variable capture levels are optimal. Instead, either maximum capture or bypass will see the highest cash flows.

Lower capture levels are less likely to be incentivised if bypass is permitted below the ELV, with average emissions over time meeting the ELV by operating at higher capture for sufficient periods. Where the ELV is low compared with plant emission factors without capture, design point capture may never be optimal as not enough electricity will be eligible for sale. Therefore, if the plant can enter the wholesale electricity market through bypass, it will be incentivised to do so except at high subsidy prices when maximum capture becomes the optimal operating condition.

A bypass condition becomes preferable once the plant emits CO_2 to the extent that the sales of electricity eligible for the zero-carbon subsidy do not cover the variable costs and energy penalty of CO_2 capture at the given subsidy/electricity price ratio. In the example where the ELV is assumed to be 450 kg/MWh, this economic cross over to bypass operation is reached when market electricity prices are approximately 90% of subsidy price paid. However, for a CO_2 price higher than £0/tonne, the bypass condition would be more expensive and lower capture levels instead incentivised.

Like the proportional subsidy case, the additional value of flexible operation is higher than in the carbon price only case, as flexible operation enables access to markets that were otherwise limited. The 450 kg/MWh example sees very similar values to the proportional subsidy as the CO_2 intensity of the gas plant is close to this ELV, and therefore the counterfactual is effectively proportional in this circumstance. However as the counterfactual ELV is reduced to 100 kg/MWh the value of flexible capture decreases as the emissions intensities of the plant are properly considered in the pricing incentive.

6.4 Implications of downstream operation

A condition of this work is that the power plant must be able to use the additional steam diverted back to the steam turbine from the capture unit at lower capture levels or bypass to generate the additional electricity output, and the requirement for

increased steam extraction from the steam turbine at higher capture levels does not reduce steam flow below minimum stable load. The transport option, pipeline or otherwise, must be able to handle variable flow of CO_2 and the storage site must also be able to manage variable flows of CO_2 from one of its feed plants.

It is likely in systems operating with carbon capture, that downstream operations will need to handle some variable flow of CO_2 even at fixed operating capture levels, since CO_2 capture on NGCC is unlikely to be baseload, especially in medium to long term scenarios. Additionally, and regardless of plant merit order, there will be plant trips and outages, similar to current power plant behaviour, which will reduce CO_2 flow rates as the plant turns off and on. Downstream infrastructure will need to have mechanisms to manage this variability and therefore it is assumed in this paper that this can be utilised for maximising value to both plant operators and society. Recent FEED studies on large scale capture plants (IEAGHG 2013) illustrate that downstream transport and storage would be able to manage variable flow by use of recompression in transport pipelines and variable diameter wells in the storage site. Furthermore, in the case of medium penetration CCS plant it is likely there will be transport and storage hubs which will buffer the behaviour of any one plant's flow rate output.

However, where large changes in CO_2 flow rate are not feasible and bypassing the capture plant regularly is deemed infeasible, this work illustrates that there is nonetheless modest financial opportunity for smaller, more manageable flow rate changes in smaller variations in CO_2 capture levels.

7 Conclusions

This thesis presents an analysis of the flexible operation of CO_2 capture on a Natural Gas Combined Cycle (NGCC) power plant. The techno-economic potential for varying CO_2 capture, as reduced or enhanced capture levels or as a full bypass of the CO_2 capture process, was assessed. A simulation of an integrated post-combustion CO_2 capture NGCC power plant was developed and the specific relationship between CO_2 capture level and an electricity output penalty of capture was presented. A CO_2 capture level optimisation function was developed and applied to different low carbon market case studies, where the value of this optimal operation was quantified under different electricity system portfolio pricing scenarios.

7.1 Integrated post-combustion NGCC power plant simulation

To provide an illustrative example of the energetic response to variable CO_2 capture on NGCC power plant, a standard MEA based post-combustion CO_2 capture unit operating with a combined cycle natural gas fired power plant was simulated in Aspen Plus. This model builds on previous published simulations that explore the behavior of flexible post-combustion on NGCC, as it comprises a fully integrated plant including the steam cycle, capture unit and compression train, with consideration given to off-design performance of turbines, key heat exchangers, the absorption loop and the steam delivery line as well as compressor operation. This simulation enables detailed assessment of off-design operation and the development of a nuanced relationship between CO_2 capture levels and the specific electricity output penalty (EOP) of CO_2 capture.

The simulation results indicate that rate based NRTL electrolyte modelling of the MEA system provides a reasonable correlation with post combustion capture pilot plant operating with NGCC. This is a useful finding as the data used to develop the simulation in Aspen Plus originates from sources with higher CO_2 concentrations. Simple correlations for off-design behavior of heat exchangers using overall heat exchange coefficients, and the use of Stodola's rule of cones to estimate turbine performance were found to be sufficiently accurate to generate results with insignificant error margins on the total specific EOP of CO_2 capture.

7.2 Variation in electricity output penalty with capture level

The simulation output of the integrated plant with continuous variations in capture level was presented, providing a relationship between power exported and CO_2 capture levels. This builds on the current literature where previously either the only impact of variable capture level on single units has been published (e.g. reboiler duty or compressor performance) or first order approximations for integrated plant with single point high and low capture levels have been proposed. Specific EOP, that is the EOP per kg CO_2 captured and compressed, increases above the design point due to associated increases in solvent flow rate in the stripper and reduced efficiency in the compressor. The EOP was found to increase at capture levels above the 90% design point, then decrease between the 90% capture design point and 60% capture in response to reductions in turbine losses, before increasing significantly below 60% capture, as compressor recycle streams were introduced to prevent surge in the compressor, with an associated high energy penalty.

The CO_2 compression system was found to potentially limit the level to which CO_2 capture levels can be increased, as the swallowing capacity was reached in the compressor used in this work above 94% capture. CO_2 capture level turn down was limited to 40% by hydrodynamics in the absorber and stripper columns.

Variable stripper pressure operation in the capture plant was found to provide a more energetically efficient method of capture level turn down, with fixed stripper pressure operation energetically favorable when operating capture levels above the design point. While the reboiler duty remains the key factor in the EOP as it varies with capture level, the design of the steam extraction line and the design and configuration of the compressor train are also likely to be influential.

7.2 Optimal operation of CO_2 capture in low carbon electricity markets

By developing a cost function for the short run operating income of an NGCC plant with CO_2 capture as a function of CO_2 capture level, analytical parametric solutions for optimal operation were described that maximised income through varying the capture level. Optimal capture plant operations include capture plant bypass as an additional binary option. The analytical solutions account for the EOP of capture and are specific to a given low carbon electricity market price structure. Three low carbon pricing case studies are examined in this work: A Carbon Price case, and two further scenarios where zero-carbon electricity is eligible for a premium tariff, and where the

system is constrained by an Emission Limit Value (ELV) are considered. Previous studies have computed optimal capture behaviour with respect to electricity system wide price signals, but this work presents the novel concept specific analytical relationships between EOP and capture level that can be considered in response to the real time market conditions.

The optimum capture level depends on the ratio between carbon capture incentives (carbon price, premium electricity price difference) and electricity prices, with high carbon prices or subsidies incentivising high capture levels and high market electricity prices incentivising lower capture levels.

The EOP at a given capture level, and the gradient of this EOP are shown to be key to optimising capture level operation. The rate of change of EOP with respect to capture level is significant because it provides an indication of the magnitude of the impact of moving from the current operating conditions.

7.3 The value of optimal capture level flexible operation

The potential for revenues from flexible operation of CO_2 capture plant under each indicative case study are described and quantified. Decision diagrams are presented for the different low carbon market cases described above. These diagrams enable visual evaluation of optimum operation and can provide information for use by plant operators who can act accordingly to maximize plant revenue in response to market price signals.

The real-time cash impact of the optimal operation was shown on overlying contours describing the corresponding absolute and additional income.

In each market case study, flexible operation capture levels were shown to provide the potential for additional cash flow under a range of market conditions. Where a carbon price provided an incentive for CO_2 capture, the market conditions where lower capture levels were optimal was relatively wide, moving to an optimal bypass condition after 60% capture, where the EOP began to increase due to additional compression penalties. For markets with subsidies paid for low carbon electricity, the potential for continuous CO_2 capture level variation was more limited, instead incentivising switches between bypass and maximum capture.

Therefore, while variation of capture level could be beneficial in a limited range of cases, it is likely that plant operators would consider maximum capture or bypass options predominantly, regardless of low carbon market design.

Finally, the value of flexible operation in different electricity system scenarios was assessed using price duration curves for electricity systems with varying amounts of renewable penetration. The value of flexible operation was shown to be millions of pounds per year for all the market scenarios presented in this work, under even conservative price assumptions, with the value increasing in energy systems with higher renewable penetration. The value of capture level reduced with increases in carbon price, as the penalty of venting additional CO_2 increases. Flexible operation of CO_2 capture is found to be most valuable in the electricity market case studies which pay subsidy for low carbon electricity only marginally higher than average electricity prices. In these circumstances, potentially hundreds of millions of additional pounds per year can be achieved by enabling the plant to bypass the CO_2 capture unit and access higher wholesale electricity prices.

7.4 Additional work

There several areas of work that could either improve or build upon the concepts presented in this thesis. While its findings are insightful for plant designers, operators, and policy makers it is acknowledged that NGCC plant model is only simulative and detailed pilot plant data reflecting these off-design operating conditions is limited. Future pilot scale data sets that could validate the future assumptions of electricity output penalty relationships would provide more fidelity and confidence in the plant model. Additionally, plant design variations would provide important insight into the implications of these findings. Interesting variations would include more complex post-combustion capture unit designs with more novel CO_2 capture technologies (see Section 3.3.2), and alternative the capture processes pre-combustion and oxy-combustion. Applying the methodology described in this thesis to the range of capture technologies would give an interesting assessment of the potential value of flexibility between the different methods, and of CCS in general.

The flexible operation in this thesis explores options for venting CO_2. Applying the same assessment to internal energy storage technologies such as solvent storage would provide a different insight into the options for flexibility in very low CO_2 constrained systems. In future low carbon markets venting could be limited through

legislation rather than carbon price stimulus only. In this circumstance, internal energy storage would be the more interesting option for flexible operation.

The quasi-steady state analysis in this work doesn't provide dynamic information on response times, latencies or efficiencies associated with the transitions between optimal capture level operation. While previous work has shown post-combustion capture units are able to move between the optimal conditions described in this work in with response rates that would enable accessing the half hourly electricity market prices used in this analysis (see Sections 3.4.3 and 5.1.3.5), these are limited in number and do not provide detailed relationships between response time and efficiency implications. An integrated dynamic model would be required to properly assess whether the optimal capture operating conditions could be accessed without latency or efficiency penalty, as assumed in this thesis.

Finally, it is recognised that the current overall emissions analysis does not consider upstream emissions associated with extraction and transport of natural gas, which could be significant in highly constrained low carbon systems or in unconventional gas extraction scenarios. The downstream impacts of varying capture level are also not accounted for. A better lifecycle assessment of flexible operation of CO_2 capture on NGCC is an important additional area of work to inform any recommendations made based on techno-economic conclusions alone.

References

Abu-Zahra, M.R., Schneiders, L.H., Niederer, J.P., Feron, P.H. and Versteeg, G.F., 2007. CO2 capture from power plants: Part I. A parametric study of the technical performance based on monoethanolamine. *International Journal of Greenhouse gas control*, 1(1), pp.37-46.

Abu-Zahra, M.R., Niederer, J.P., Feron, P.H. and Versteeg, G.F., 2007. CO_2 capture from power plants. Part II. A parametric study of the economical performance based on mono-ethanolamine. *International Journal of Greenhouse Gas Control*, 1(2), pp.135–142.

Alhajaj, A., Mac Dowell, N. and Shah, N., 2016. A techno-economic analysis of post-combustion CO_2 capture and compression applied to a combined cycle gas turbine: Part I. A parametric study of the key technical performance indicators. *International Journal of Greenhouse Gas Control*, 44, pp.26–41.

Allen, M.R. et al., 2009. Warming caused by cumulative carbon emissions towards the trillionth tonne. *Nature*, 458(7242), pp.1163–1166.

Amann, J.M.G. and Bouallou, C., 2009. CO_2 capture from power stations running with natural gas (NGCC) and pulverized coal (PC): Assessment of a new chemical solvent based on aqueous solutions of N-methyldiethanolamine + triethylene tetramine. *Energy Procedia*, 1(1), pp.909–916.

Amrollahi, Z., Ertesvåg, I.S. and Bolland, O., 2011. Optimized process configurations of post-combustion CO2 capture for natural-gas-fired power plant—exergy analysis. *International Journal of Greenhouse Gas Control*, 5(6), pp.1393-1405..

Amrollahi, Z., Ystad, P.A.M., Ertesvåg, I.S. and Bolland, O., 2012. Optimized process configurations of post-combustion CO2 capture for natural-gas-fired power plant–Power plant efficiency analysis. *International Journal of Greenhouse Gas Control*, 8, pp.1-11..

Arce, A., Mac Dowell, N., Shah, N. and Vega, L.F., 2012. Flexible operation of solvent regeneration systems for CO2 capture processes using advanced control techniques: Towards operational cost minimisation. *International Journal of Greenhouse Gas Control*, 11, pp.236-250.

Ball, M., 2008. Integrated Carbon Capture Sequestration Demonstration - Boundary Dam Power Station. In: *Seventh Annual Conference on Carbon Capture and Sequestration.* Pittsburgh

Barton, J.P. and Infield, D.G., 2004. Energy Storage and Its Use With Intermittent Renewable Energy. *IEEE Transactions on Energy Conversion*, 19(2), pp.441–448.

Bass, R.J., Malalasekera, W., Willmot, P. and Versteeg, H.K., 2011. The impact of variable demand upon the performance of a combined cycle gas turbine (CCGT) power plant. *Energy*, 36(4), pp.1956-1965.

Bernier, E., Maréchal, F. and Samson, R., 2010. Multi-objective design optimization of a natural gas-combined cycle with carbon dioxide capture in a life cycle perspective. *Energy*, 35(2), pp.1121–1128.

Biliyok, C., Canepa, R. and Hanak, D.P., 2015. Investigation of Alternative

Strategies for Integrating Post-combustion CO_2 Capture to a Natural Gas Combined Cycle Power Plant. *Energy & Fuels*, 29(7), pp.4624–4633.

Biliyok, C. and Yeung, H., 2013. Evaluation of natural gas combined cycle power plant for post-combustion CO_2 capture integration. *International Journal of Greenhouse Gas Control*, 19, pp.396–405.

Birol, F., 2015. World energy outlook 2015. Organisation for Economic Co-Operation and Development (OECD): Paris, France.

Boot-Handford, M.E., Abanades, J.C., Anthony, E.J., Blunt, M.J., Brandani, S., Mac Dowell, N., Fernández, J.R., Ferrari, M.C., Gross, R., Hallett, J.P. and Haszeldine, R.S., 2014. Carbon capture and storage update. *Energy & Environmental Science*, 7(1), pp.130-189.

Botero, C., Finkenrath, M., Bartlett, M., Chu, R., Choi, G. and Chinn, D., 2009. Redesign, optimization, and economic evaluation of a natural gas combined cycle with the best integrated technology CO2 capture. *Energy Procedia*, 1(1), pp.3835-3842.

British Petroleum, 2014. BP statistical review of world energy June 2014. In World Petroleum Congress, Moscow. (Vol. 16, p. 2014).

Brouwer, A.S., van den Broek, M., Seebregts, A. and Faaij, A., 2015. Operational flexibility and economics of power plants in future low-carbon power systems. *Applied Energy*, 156, pp.107-128.

Bui, M., Gunawan, I., Verheyen, V., Feron, P., Meuleman, E. and Adeloju, S., 2014. Dynamic modelling and optimisation of flexible operation in post-combustion CO_2 capture plants—A review. *Computers & Chemical Engineering*, 61, pp.245-265.

Bui, M., Gunawan, I., Verheyen, V., Feron, P. and Meuleman, E., 2016. Flexible operation of CSIRO's post-combustion CO2 capture pilot plant at the AGL Loy Yang power station. International Journal of Greenhouse Gas Control, 48, pp.188-203.Ceccarelli, N. et al., 2014. Flexibility of Low-CO_2 Gas Power Plants: Integration of the CO_2 Capture Unit with CCGT Operation. *Energy Procedia*, 63, pp.1703–1726.

Cengel, Y. and Ghajar, A., 2015. *Heat and Mass Transfer, Fundamentals & Application* 5th ed., McGraw-Hill.

Chalmers, H., Leach, M., Lucquiaud, M. and Gibbins, J., 2009. Valuing flexible operation of power plants with CO_2 capture. *Energy Procedia*, 1(1), pp.4289-4296.

Chalmers, H., Lucquiaud, M., Gibbins, J. and Leach, M., 2009. Flexible operation of coal fired power plants with postcombustion capture of carbon dioxide. *Journal of Environmental Engineering*, 135(6), pp.449-458.

Chalmers, H. and Gibbins, J., 2007. Initial evaluation of the impact of post-combustion capture of carbon dioxide on supercritical pulverised coal power plant part load performance. *Fuel*, 86, pp.2109-2123.

Cohen, S.M., Rochelle, G.T. and Webber, M.E., 2013. Optimal CO_2 Capture Operation in an Advanced Electric Grid. *Energy Procedia*, 37, pp.2585–2594.

Cohen, S.M., Rochelle, G.T. and Webber, M.E., 2012. Optimizing post-combustion CO_2 capture in response to volatile electricity prices. *International Journal of Greenhouse Gas Control*, 8, pp.180–195.

Cory, K.S., Couture, T. and Kreycik, C., 2009. Feed-in tariff policy: design, implementation, and RPS policy interactions. Colorado, USA: National Renewable Energy Laboratory.

Coussy, P. and Raynal, L., 2014. CO $_2$ Capture Rate Sensitivity *Versus* Purchase of CO $_2$ Quotas. Optimizing Investment Choice for Electricity Sector. *Oil & Gas Science and Technology – Revue d'IFP Energies nouvelles*, 69(5), pp.785–791.

Davis, J. and Rochelle, G., 2009. Thermal degradation of monoethanolamine at stripper conditions. *Energy Procedia*, 1(1), pp.327–333.

DECC, 2013. *Electricity Generation Costs 2013*.

Delarue, E., Martens, P. and D'haeseleer, W., 2012. Market opportunities for power plants with post-combustion carbon capture. *International Journal of Greenhouse Gas Control*, 6, pp.12–20.

Mac Dowell, N. and Shah, N., 2013. Identification of the cost-optimal degree of CO_2 capture: An optimisation study using dynamic process models. *International Journal of Greenhouse Gas Control*, 13, pp.44–58.

Ela, E., Kirby, B., Navid, N. and Smith, J.C., 2012, July. Effective ancillary services market designs on high wind power penetration systems. In *IEEE Power and Energy Society General Meeting* (pp. 1-8). San Diego, California: IEEE.

ElKady, A.M., Evulet, A., Brand, A., Ursin, T.P. and Lynghjem, A., 2008, January. Exhaust gas recirculation in DLN F-class gas turbines for post-combustion CO_2 capture. In *ASME Turbo Expo 2008: Power for Land, Sea, and Air* (pp. 847-854). American Society of Mechanical Engineers.

Evulet, A.T., ELKady, A.M., Branda, A.R. and Chinn, D., 2009. On the performance and operability of GE's dry low NOx combustors utilizing exhaust gas recirculation for postcombustion carbon capture. *Energy Procedia*, 1(1), pp.3809-3816.

Fitzgerald, F.D., Hume, S.A., McGough, G. and Damen, K., 2014. Ferrybridge CCPilot100+ operating experience and final test results. *Energy Procedia*, 63, pp.6239-6251.

GE Power, 2015. *9F.03/.04/.05 Gas turbine fact sheet.*

Gibbins, J.R. and Crane, R.I., 2004. Preliminary assessment of electricity costs for existing pulverized fuel plant retrofitted with an advanced supercritical boiler and turbine and solvent CO2 capture. *Proceedings of the Institution of Mechanical Engineers, Part A: Journal of Power and Energy*, 218(7), pp.551–555.

Goff, G.S. and Rochelle, G.T., 2004. Monoethanolamine Degradation: O_2 Mass Transfer Effects under CO_2 Capture Conditions. *Industrial & Engineering Chemistry Research*, 43(20), pp.6400–6408.

González, A., Sanchez, E., Santaló, J.G., Gibbins, J. and Lucquiaud, M., 2014. On the integration of sequential supplementary firing in natural gas combined cycle for CO_2-Enhanced Oil Recovery: A techno-economic analysis for Mexico. *Energy Procedia*, 63, pp.7558-7567.

Green, R., 2008. Carbon Tax or Carbon Permits: The Impact on Generators Risks. *The Energy Journal*, 29(3).

Hamborg, E.S., Smith, V., Cents, T., Brigman, N., Falk-Pedersen, O., De Cazenove, T., Chhaganlal, M., Feste, J.K., Ullestad, Ø., Ulvatn, H. and Gorset, O., 2014. Results from MEA testing at the CO_2 Technology Centre Mongstad. Part II: Verification of baseline results. *Energy Procedia*, 63, pp.5994-6011..

Hanak, D.P., Biliyok, C. and Manovic, V., 2015. Evaluation and Modeling of Part-Load Performance of Coal-Fired Power Plant with Postcombustion CO_2 Capture. *Energy & Fuels*, 29(6), pp.3833–3844.

He, Z. and Ricardez-Sandoval, L.A., 2016. Dynamic modelling of a commercial-scale CO_2 capture plant integrated with a natural gas combined cycle (NGCC) power plant. *International Journal of Greenhouse Gas Control*, 55, pp.23–35.

Ho, M.T. and Wiley, D.E., 2016. Flexible strategies to facilitate carbon capture deployment at pulverised coal power plants. *International Journal of Greenhouse Gas Control,* 48, pp.290-299.

Holttinen, H., Robitaille, A., Orths, A., Pineda, I., Lange, B., Carlini, E.M., O'Malley, M., Dillon, J., Tande, J.O., Estanqueiro, A. and Gomez-Lazaro, E., 2013, October. Summary of experiences and studies for Wind Integration–IEA Wind Task 25. In *Proceedings of WIW2013 workshop London* (pp. 22-24).

Hu, Y., Xu, G., Xu, C. and Yang, Y., 2017. Thermodynamic analysis and techno-economic evaluation of an integrated natural gas combined cycle (NGCC) power plant with post-combustion CO_2 capture. *Applied Thermal Engineering*, *111*, pp.308-316.

IEAGHG, 2003. *Potential for improvement in gasification combined cycle power generation with CO_2 capture.* PH4/19.

IEAGHG, 2004. *Improvement in Power Generation with Post-Combustion Capture of CO_2.* PH4/33

IEAGHG, 2012a. *CO_2 Capture At Gas Fired Power Plant,* 2012/8.

IEAGHG, 2012b. *Operating Flexibility of Power Plants with CCS,* 2012/6.

IEAGHG, 2013. *UK FEED Studies 2011 – A Summary,* 2013/12.

Alie, C., Douglas, P. and Croiset, E., 2008. Scoping study on operating flexibility of power plants with CO_2 capture. *IEAGHG*

Intergovernmental Panel on Climate Change, 2006. *2006 IPCC guidelines for national greenhouse gas inventories*.

Intergovernmental Panel on Climate Change, 2015. *Climate change 2014: Mitigation of climate change* (Vol. 3). Cambridge University Press.

International Energy Agency, 2014. *Energy Technology Perspectives 2014: Harnessing Electricity's Potential*. OECD Publishing.

International Energy Agency, 2017. *Energy Technology Perspectives 2017*. OECD Publishing.

Irlam, L., 2015. The costs of CCS and other low-carbon technologies in the United States: 2015 update. *Report. Global Carbon Capture and Storage Institute Canberra, Australia*.

Jordal, K., Ystad, P.A.M., Anantharaman, R., Chikukwa, A. and Bolland, O., 2012. Design-point and part-load considerations for natural gas combined cycle plants with post combustion capture. *International Journal of Greenhouse Gas*

Control, *11*, pp.271-282.

Joskow, P.L., 2011. Comparing the costs of intermittent and dispatchable electricity generating technologies. *American Economic Review*, 101(3), pp.238–241.

Karimi, M., Hillestad, M. and Svendsen, H.F., 2012. Natural gas combined cycle power plant integrated to capture plant. *Energy and Fuels*, 26(3), pp.1805–1813.

Khalilpour, R., 2014. Flexible operation scheduling of a power plant integrated with PCC processes under market dynamics. *Industrial and Engineering Chemistry Research*, 53(19), pp.8132–8146.

Kirschen, D.S., Ma, J., Silva, V. and Belhomme, R., 2011, July. Optimizing the flexibility of a portfolio of generating plants to deal with wind generation. In *Power and Energy Society General Meeting, 2011 IEEE* (pp. 1-7). IEEE.

Knopf, F.C., 2012. Coal-Fired Conventional Utility Plants with CO_2 Capture (Design and Off-Design Steam Turbine Performance). In *Modeling, Analysis and Optimization of Process and Energy Systems*. John Wiley & Sons, pp. 397–418.

Léonard, G., Toye, D. and Heyen, G., 2014. Experimental study and kinetic model of monoethanolamine oxidative and thermal degradation for post-combustion CO_2 capture. *International Journal of Greenhouse Gas Control*, 30, pp.171–178.

Li, H., Haugen, G., Ditaranto, M., Berstad, D. and Jordal, K., 2011. Impacts of exhaust gas recirculation (EGR) on the natural gas combined cycle integrated with chemical absorption CO_2 capture technology. *Energy Procedia*, 4, pp.1411–1418.

Liebenthal, U. and Kather, A., 2011, May. Design and off-design behaviour of a CO2 compressor for a post-combustion CO_2 capture process. In *5th international conference on clean coal technologies, Saragoza, Spain* (pp. 8-12).

Lindqvist, K., Jordal, K., Haugen, G., Hoff, K.A. and Anantharaman, R., 2014. Integration aspects of reactive absorption for post-combustion CO_2 capture from NGCC (natural gas combined cycle) power plants. *Energy*, *78*, pp.758-

Lucquiaud, M. and Gibbins, J., 2009a. Retrofitting CO_2 capture ready fossil plants with post-combustion capture. Part 1: requirements for supercritical pulverized coal plants using solvent-based flue gas scrubbing. *Proceedings of the Institution of Mechanical Engineers, Part A: Journal of Power and Energy*, *223*(3), pp.213-226.

Lucquiaud, M., Patel, P., Chalmers, H. and Gibbins, J., 2009b. Retrofitting CO_2 capture ready fossil plants with post-combustion capture. Part 2: requirements for natural gas combined cycle plants using solvent-based flue gas scrubbing. *Proceedings of the Institution of Mechanical Engineers, Part A: Journal of Power and Energy*, *223*(3), pp.227-238.

Lucquiaud, M. and Gibbins, J., 2011. On the integration of CO_2 capture with coal-fired power plants: A methodology to assess and optimise solvent-based post-combustion capture systems. *Chemical Engineering Research and Design*, 89(9), pp.1553–1571.

Luo, X. and Wang, M., 2015. Optimal operation of MEA-based post-combustion carbon capture for natural gas combined cycle power plants under different market conditions. *International Journal of Greenhouse Gas Control*, 48,

pp.312–320.

Luo, X., Wang, M. and Chen, J., 2015. Heat integration of natural gas combined cycle power plant integrated with post-combustion CO_2 capture and compression. *Fuel*, 151, pp.110–117.

Metz, B., Davidson, O., De Coninck, H.C., Loos, M. and Meyer, L.A., 2005. IPCC, 2005: IPCC special report on carbon dioxide capture and storage. Prepared by Working Group III of the Intergovernmental Panel on Climate Change. *Cambridge, United Kingdom and New York, NY, USA*, *442*.

MHI, 2002. *Flue Gas CO_2 Capture Technology.*

Moller, B., Genrup, M. and Assadi, M., 2007. On the off-design of a natural gas-fired combined cycle with CO_2 capture. *Energy*, 32(4), pp.353–359.

Montañés, R.M., Korpås, M., Nord, L.O. and Jaehnert, S., 2016. Identifying operational requirements for flexible CCS power plant in future energy systems. *Energy Procedia*, *86*, pp.22-31.

Moon, H. and Zarrouk, S.J., 2014. Efficiency of Geothermal Power Plants : a Worldwide Review. *Geothermics*, 51, pp.142–153.

Mores, P.L., Godoy, E., Mussati, S.F. and Scenna, N.J., 2014. A NGCC power plant with a CO_2 post-combustion capture option. Optimal economics for different generation/capture goals. *Chemical Engineering Research and Design*, *92*(7), pp.1329-1353.

NETL et al., 2015. Cost and Performance Baseline for Fossil Energy Plants Volume 1a: Bituminous Coal (PC) and Natural Gas to Electricity Revision 3. National Energy Technology Laboratory Report, DOE/NETL-2015/1723.

Notz, R., Mangalapally, H.P. and Hasse, H., 2012. Post combustion CO_2 capture by reactive absorption: Pilot plant description and results of systematic studies with MEA. *International Journal of Greenhouse Gas Control*, 6, pp.84–112.

Nuclear Energy Agency, 2009. *Technical and Economic Aspects of Load Following with Nuclear Power Plants*.

Oates, D.L., Versteeg, P., Hittinger, E. and Jaramillo, P., 2014. Profitability of CCS with flue gas bypass and solvent storage. *International Journal of Greenhouse Gas Control*, *27*, pp.279-288.

Oexmann, J., 2011. *Post-combustion CO_2 capture: energetic evaluation of chemical absorption processes in coal-fired steam power plants*. Technische Universität Hamburg.

Parliamentary Office on Science & Technology, 2015. *TRENDS IN ENERGY*.

Poyry, 2011. *The challenges of intermittency in North West European power markets.*

Rao, A.B. and Rubin, E.S., 2002. A technical, economic, and environmental assessment of amine-based CO_2 capture technology for power plant greenhouse gas control. *Environmental science & technology*, 36(20), pp.4467–75.

Rao, A.B. and Rubin, E.S., 2006. Identifying cost-effective CO_2 control levels for amine-based CO_2 capture systems. *Industrial and Engineering Chemistry*

Reddy, S., Scherffius, J., Freguia, S. and Roberts, C., 2003, May. Fluor's Econamine FG Plus SM Technology. In *Proceedings of the second annual*

conference on carbon sequestration (pp. 5-8).

Rezazadeh, F. et al., 2016. Performance evaluation and optimisation of post combustion CO_2 capture processes for natural gas applications at pilot scale via a verified rate-based model. *International Journal of Greenhouse Gas Control*, 53, pp.243–253.

Roeder, V. and Kather, A., 2014. Part Load Behaviour of Power Plants with a Retrofitted Post-combustion CO_2 Capture Process. *Energy Procedia*, 51, pp.207–216.

Romeo, L.M., Bolea, I. and Escosa, J.M., 2008. Integration of power plant and amine scrubbing to reduce CO_2 capture costs. *Applied Thermal Engineering*, 28(8–9), pp.1039–1046.

Sanchez Fernandez, E., del Rio Saez, M., Chalmers, H., Khakharia, P., Goetheer, E.L.V., Gibbins, J. and Lucquiaud, M., 2016. Operational flexibility options in power plants with integrated post-combustion capture. *International Journal of Greenhouse Gas Control*, 48, pp.275–289.

Sanpasertparnich, T., Idem, R., Bolea, I. and Tontiwachwuthikul, P., 2010. Integration of post-combustion capture and storage into a pulverized coal-fired power plant. *International Journal of Greenhouse Gas Control*, *4*(3), pp.499-510.

Serth, R. and Lestina, T., 2014. *Process heat transfer principles, applications and rules of thumb*, Oxford: Elsevier Academic Press.

Sipo¨cz, N. and Assadi, M., 2010. Combined Cycles With CO_2 Capture: Two Alternatives for System Integration. *Journal of Engineering for Gas Turbines and Power*, 132(6), p.061701.

Sipöcz, N., Tobiesen, A. and Assadi, M., 2011. Integrated modelling and simulation of a 400 MW NGCC power plant with CO_2 capture. *Energy Procedia*, 4, pp.1941–1948.

Stultz, S.C. & Kitto, J.B., 2005. *Steam its generation and use* (41st ed.) The Babcock & Wilcox Company.

Teeter, P. and Sandberg, J., 2017. Constraining or enabling green capability development? How policy uncertainty affects organizational responses to flexible environmental regulations. *British Journal of Management*, *28*(4), pp.649-665.

Della Valle, A.P., 1988. Short-run versus long-run marginal cost pricing. *Energy Economics*, 10(4), pp.283–286.

Walker, A., Cox, E., Loughhead, J. and Roberts, D.J., 2014. Counting the cost: the economic and social costs of electricity shortfalls in the UK. *Royal Academy of Engineering. London*.

Wiley, D.E., Ho, M.T. and Donde, L., 2011. Technical and economic opportunities for flexible CO2 capture at Australian black coal fired power plants. *Energy Procedia*, 4, pp.1893–1900.

Winterbone, D.E. and Turan, A., 2015. Engine Cycles and their Efficiencies. In *Advanced Thermodynamics for Engineers*. Elsevier, pp. 35–59.

Yucekaya, A., 2013. Bidding of price taker power generators in the deregulated Turkish power market. *Renewable and Sustainable Energy Reviews*, 22,

pp.506–514.

Zaman, M. and Lee, J.H., 2015. Optimization of the various modes of flexible operation for post-combustion CO_2 capture plant. *Computers & Chemical Engineering*, 75, pp.14–27.

Ziaii, S. and Cohen, S., 2009. Dynamic operation of amine scrubbing in response to electricity demand and pricing. *Energy Procedia*, 1(1), pp.4047–4053.

Ziaii, S., Rochelle, G.T. and Edgar, T.F., 2009. Dynamic Modeling to Minimize Energy Use for CO_2 Capture in Power Plants by Aqueous Monoethanolamine. *Industrial & Engineering Chemistry Research*, 48(13), pp.6105–6111.

Ziaii, S., Rochelle, G.T. and Edgar, T.F., 2011. Optimum design and control of amine scrubbing in response to electricity and CO_2 prices. *Energy Procedia*, 4, pp.1683–1690.

Appendix A: Summary of physical property methods for Aspen Plus rate-based model of the CO_2 capture process by MEA.

This Appendix provides a summary of the MEA rate-based model used in this work, detailed in Aspen Tech 2012. Wherever data is described as referenced, detail for each source is provided in the reference list of Aspen Tech (2012).

Physical property models:

The unsymmetrical electrolyte NRTL property method (ENRTL-RK) is used to compute liquid properties and the PC-SAFT equation of state used for vapour properties. The PC-SAFT parameters of MEA are regressed from vapor pressure data, heat of vaporization data, liquid heat capacity data and liquid density data as referenced.

Henry's constants are specified for solutes CO_2, H_2S, N_2, O_2, CH_4, C_2H_6, and C_3H_8, with water and MEA. Henry's constant parameters are either obtained from referenced literature or retrieved from the Aspen Databank. The activity coefficient basis for the Henry's components are calculated based on infinite-dilution condition in pure water.

Characteristic volume parameters for H_2O uses Brelvi-O'Connell Model, parameters for CO_2 are obtained from literature, CH_4 and C_2H_6 are regressed from binary H_2O VLE data, all other components default to their critical volume.

The electrolyte NRTL model specifies all molecule-molecule binary parameters and electrolyte-electrolyte binary parameters as zero. All molecule-electrolyte binary parameters are defaulted to (8, -4), with average values of the parameters referenced. The non-randomness factor is fixed at 0.2. Interaction parameters are determined from regression with VLE data, excess enthalpy data, heat capacity data, absorption heat data, and speciation concentration data.

Dielectric constants of nonaqueous solvents are calculated as:

$$\varepsilon(T) = A + B\left(\frac{1}{T} - \frac{1}{C}\right)$$

With parameters A, B and C for MEA taken as 35.76, 14836.0 and 273.15.

Transport property models:

The aqueous phase Gibbs free energy, the heat of formation and infinite dilution at 25C and the heat capacity at infinite dilution are regressed from VLE data, absorption heat data, heat capacity data, and speciation concentration data as referenced. Additional transport properties are modelled as detailed below.

Property	Model
Liquid molar volume	Clarke model (VAQCLK) with the quadratic mixing rule for solvents. Interaction parameters from experimental density data as referenced
Liquid viscosity	Jones-Dole electrolyte correction model (MUL2JONS) with the mass fraction based Aspen liquid mixture viscosity model for the solvent. Interaction parameters taken from experimental viscosity data as referenced.
Liquid surface tension	Onsager-Samaras model (SIG2ONSG)
Thermal conductivity	Riedel electrolyte correction model (KL2RDL)
Binary diffusivity	Nernst-Hartley model (DL1NST) with mixture viscosity weighted by mass fraction

Column modelling methods:

Process/property	**Method**
Interfacial area	Bravo (1985)
Mass transfer	Bravo (1985)
Heat transfer	Chilton and Colburn
Flooding	Wallis
Hold up	Stichlmair (1989)
Flow model	Plug flow VPlug

Appendix B: Definition files for Aspen Plus simulation

STEAM CYCLE

```
DYNAMICS
   DYNAMICS RESULTS=ON

IN-UNITS MET ENERGY=kJ ENTHALPY='J/kg' ENTROPY='J/kmol-K'  &
       MASS-FLOW='tonne/hr' ENTHALPY-FLO=kW FORCE=Newton  &
       MOLE-HEAT-CA='kJ/kmol-K' HEAT-TRANS-C='Watt/sqm-K'  &
       PRESSURE=bar TEMPERATURE=C DELTA-T=C  &
       MOLE-ENTHALP='kJ/kmol' MASS-ENTHALP='kJ/kg'  &
       MOLE-ENTROPY='J/kmol-K' MASS-ENTROPY='J/kg-K'  &
       MASS-HEAT-CA='kJ/kg-K' UA='J/sec-K' HEAT=kJ PDROP=bar  &
       VOL-HEAT-CAP='kJ/cum-K' HEAT-FLUX='Watt/m'  &
       INVERSE-PRES='1/bar' INVERSE-HT-C='sqm-K/Watt'  &
       VOL-ENTHALPY='kJ/cum'

DEF-STREAMS CONVEN ALL

SIM-OPTIONS MASS-BAL-CHE=YES PARADIGM=SM

DATABANKS 'APV80 PURE27' / 'APV80 AQUEOUS' / 'APV80 SOLIDS' /  &
       'APV80 INORGANIC' / NOASPENPCD

PROP-SOURCES 'APV80 PURE27' / 'APV80 AQUEOUS' / 'APV80 SOLIDS' &
       / 'APV80 INORGANIC'

COMPONENTS
   H2O H2O /
   N2 N2 /
   O2 O2 /
   CO2 CO2 /
   AR AR /
   CH4 CH4 /
   C2H6 C2H6 /
   C3H8 C3H8 /
   NBUTANE C4H10-1 /
   NPENTANE C5H12-1

SOLVE
   RUN-MODE MODE=SIM

INIT-VAR-ATT
   INITIALIZE VNAME="DE-SH-MX.BLK.PCC-STM4_VAPOR_FRACTION"  &
      VALUE=1. PHYS-QTY=DIMENSIONLES ENABLED=NO
   INITIALIZE VNAME="STODOLA.BLK.PARAMETER_1" VALUE=27020347.8  &
      PHYS-QTY=DIMENSIONLES ENABLED=NO

SPECGROUPS
   SPEC-GROUP NAME=DESH ENABLED=NO
   SPEC-CHANGE NAME=DESH SPEC=CONST VAR=  &
      "DE-SH-MX.BLK.PCC-STM4_VAPOR_FRACTION"
   SPEC-CHANGE NAME=DESH SPEC=CALC VAR= "DE-SH-SP.BLK.DE-SH_MASS"
   SPEC-GROUP NAME=STODLP ENABLED=NO
   SPEC-CHANGE NAME=STODLP SPEC=CONST VAR=  &
      "STODOLA.BLK.PARAMETER_1"
   SPEC-CHANGE NAME=STODLP SPEC=CALC VAR= "LPTV.P_O"

FLOWSHEET
   BLOCK HPS3 IN=GT-FG HPS2O OUT=FG2 HPS3O
   BLOCK RH2 IN=FG2 RH1O OUT=FG3 RH2O
   BLOCK HPS2 IN=FG3 HPS1O OUT=FG4 HPS2O
   BLOCK RH1 IN=FG4 RH1I OUT=FG5 RH1O
   BLOCK HPS1 IN=FG5 HPBO OUT=FG6 HPS1O
```

```
   BLOCK HPB IN=FG6 HPE2O OUT=FG7 HPBO
   BLOCK HPE2 IN=FG7 HPE1O OUT=FG8 HPE2O
   BLOCK IPS IN=FG8 IPBO OUT=FG9 IPSO
   BLOCK LPS IN=FG9 LPBO OUT=FG10 LPSO
   BLOCK HPE1 IN=FG10 HPE1IN OUT=FG11 HPE1O
   BLOCK IPB IN=FG11 IPBI OUT=FG12 IPBO
   BLOCK IPE IN=FG12 IPEI OUT=FG13 IPEO
   BLOCK LPB IN=FG13 LPBI OUT=FG14 LPBO
   BLOCK LPE IN=FG14 LPEI-RTN OUT=FG15 LPEO
   BLOCK IP-PUMP IN=IP-PUMPI OUT=IPEI W-IPPUMP
   BLOCK HP-PUMP IN=HP-PUMPI OUT=HP-PUMPO W-HPPUMP
   BLOCK IP-SPLT IN=IPEO OUT=IPBI HP-PUMPI PRH-IN
   BLOCK LP-SPLT IN=LP-PUMPO OUT=IP-PUMPI LPBI
   BLOCK LP-PUMP IN=LPEO OUT=LP-PUMPO W-LPPUMP
   BLOCK HPT IN=HPT-IN OUT=HPT-OUT WORK1
   BLOCK HPTV IN=HPS3O OUT=HPTV-O
   BLOCK IPT IN=IPT-IN WORK1 OUT=IPT-OUT WORK2
   BLOCK IPTV IN=RH2O OUT=IPT-IN
   BLOCK LPT IN=LPT-IN WORK2 OUT=LPT-OUT W-ST
   BLOCK RH-MIX IN=IPSO RH-RTN OUT=RH1I
   BLOCK RHV IN=HPT-OUT OUT=RH-RTN
   BLOCK LPTV IN=LPTV-IN OUT=LPT-IN
   BLOCK PCC-MIX IN=LPSO HPIP-BYP IPT-OUT OUT=PCC-STM1
   BLOCK DE-SH-MX IN=PCC-STM3 DE-SH OUT=PCC-STM4
   BLOCK DE-SH-V IN=PCC-STM2 OUT=PCC-STM3
   BLOCK DE-SH-SP IN=HP-PUMPO OUT=HPE1IN DE-SH
   BLOCK CONDENSO IN=COND-IN CWIN OUT=COND-OUT CWOUT
   BLOCK PCC IN=PCC-STM4 OUT=PCC-RTN1
   BLOCK CND-PUMP IN=COND-OUT OUT=CD-PMP-O W-CPUMP
   BLOCK PCC-PUMP IN=PCC-RTN1 OUT=PCC-RTN2
   BLOCK PCC-MX IN=CD-PMP-O PCC-RTN2 OUT=LPEI-RTN
   BLOCK FUEL-PHH IN=PRH-IN OUT=PRH-OUT
   BLOCK COND-MIX IN=LPT-OUT DEAE-STM PRH-RTN OUT=COND-IN
   BLOCK HPT-SPLT IN=HPTV-O OUT=HPT-IN HPT-DVT
   BLOCK GT-COMP IN=AIR-AMBI OUT=GT1 GTCOMP-W
   BLOCK GT-TURB IN=GT2 GTCOMP-W OUT=GT-FG W-GT
   BLOCK GT-COMB IN=GT1 FUEL-NG OUT=GT2
   BLOCK FUEL-PHC IN=FUEL-NG0 OUT=FUEL-NG
   BLOCK PRH-V IN=PRH-OUT OUT=PRH-RTN
   BLOCK PCC-DVT IN=PCC-STM1 OUT=PCC-STM2 LPTV-IN
   BLOCK B1 IN=W-2GT W-1ST OUT=W-GROSS
   BLOCK B2 IN=W-CPUMP W-IPPUMP W-HPPUMP W-LPPUMP S4 OUT= &
      W-PUMP
   BLOCK 2GTS IN=W-GT OUT=W-2GT
   BLOCK 1ST IN=W-ST OUT=W-1ST
   BLOCK CW-PUMP IN=CW0 OUT=CWIN S4
   BLOCK 2HRSGS IN=W-PUMP OUT=W-2PUMP

PROPERTIES PR-BM FREE-WATER=STEAMNBS

STREAM AIR-AMBI
   SUBSTREAM MIXED TEMP=9. PRES=1.013 MASS-FLOW=2365.
   MOLE-FRAC H2O 0.0094 / N2 0.7739 / O2 0.2074 / CO2  &
      0.0004 / AR 0.0089

STREAM CW0
   SUBSTREAM MIXED TEMP=15. PRES=1.013 MASS-FLOW=41720.
   MASS-FRAC H2O 1.

STREAM CWIN
   SUBSTREAM MIXED TEMP=15. PRES=3.06 MASS-FLOW=41720.
   MASS-FRAC H2O 1.

STREAM DEAE-STM
   SUBSTREAM MIXED TEMP=600. PRES=170. MASS-FLOW=3.8
   MOLE-FRAC H2O 1.

STREAM FG2
   SUBSTREAM MIXED TEMP=626.7 PRES=1.044
   MOLE-FLOW H2O 7532.797 / N2 63451.53 / O2 10079.06 /  &
      CO2 3635.592 / AR 729.3649 / CH4 1.4295E-023 / C2H6  &
      0. / C3H8 0. / NBUTANE 0. / NPENTANE 0.
```

```
STREAM FG3
   SUBSTREAM MIXED TEMP=609.6 PRES=1.041
   MOLE-FLOW H2O 7532.797 / N2 63451.53 / O2 10079.06 /  &
      CO2 3635.592 / AR 729.3649 / CH4 1.4295E-023 / C2H6  &
      0. / C3H8 0. / NBUTANE 0. / NPENTANE 0.

STREAM FG4
   SUBSTREAM MIXED TEMP=591.9 PRES=1.039
   MOLE-FLOW H2O 7532.797 / N2 63451.53 / O2 10079.06 /  &
      CO2 3635.592 / AR 729.3649 / CH4 1.4295E-023 / C2H6  &
      0. / C3H8 0. / NBUTANE 0. / NPENTANE 0.

STREAM FG5
   SUBSTREAM MIXED TEMP=548. PRES=1.037
   MOLE-FLOW H2O 7532.797 / N2 63451.53 / O2 10079.06 /  &
      CO2 3635.592 / AR 729.3649 / CH4 1.4295E-023 / C2H6  &
      0. / C3H8 0. / NBUTANE 0. / NPENTANE 0.

STREAM FG6
   SUBSTREAM MIXED TEMP=462.4 PRES=1.034
   MOLE-FLOW H2O 7532.797 / N2 63451.53 / O2 10079.06 /  &
      CO2 3635.592 / AR 729.3649 / CH4 1.4295E-023 / C2H6  &
      0. / C3H8 0. / NBUTANE 0. / NPENTANE 0.

STREAM FG7
   SUBSTREAM MIXED TEMP=370.97 PRES=1.034
   MOLE-FLOW H2O 7532.797 / N2 63451.53 / O2 10079.06 /  &
      CO2 3635.592 / AR 729.3649 / CH4 1.4295E-023 / C2H6  &
      0. / C3H8 0. / NBUTANE 0. / NPENTANE 0.

STREAM FG8
   SUBSTREAM MIXED TEMP=340.6 PRES=1.032
   MOLE-FLOW H2O 7532.797 / N2 63451.53 / O2 10079.06 /  &
      CO2 3635.592 / AR 729.3649 / CH4 1.4295E-023 / C2H6  &
      0. / C3H8 0. / NBUTANE 0. / NPENTANE 0.

STREAM FG9
   SUBSTREAM MIXED TEMP=337.6 PRES=1.027
   MOLE-FLOW H2O 7532.797 / N2 63451.53 / O2 10079.06 /  &
      CO2 3635.592 / AR 729.3649 / CH4 1.4295E-023 / C2H6  &
      0. / C3H8 0. / NBUTANE 0. / NPENTANE 0.

STREAM FG10
   SUBSTREAM MIXED TEMP=332.8 PRES=1.025
   MOLE-FLOW H2O 7532.797 / N2 63451.53 / O2 10079.06 /  &
      CO2 3635.592 / AR 729.3649 / CH4 1.4295E-023 / C2H6  &
      0. / C3H8 0. / NBUTANE 0. / NPENTANE 0.

STREAM FG11
   SUBSTREAM MIXED TEMP=294.7 PRES=1.022
   MOLE-FLOW H2O 7532.797 / N2 63451.53 / O2 10079.06 /  &
      CO2 3635.592 / AR 729.3649 / CH4 1.4295E-023 / C2H6  &
      0. / C3H8 0. / NBUTANE 0. / NPENTANE 0.

STREAM FG12
   SUBSTREAM MIXED TEMP=268.8 PRES=1.02
   MOLE-FLOW H2O 7532.797 / N2 63451.53 / O2 10079.06 /  &
      CO2 3635.592 / AR 729.3649 / CH4 1.4295E-023 / C2H6  &
      0. / C3H8 0. / NBUTANE 0. / NPENTANE 0.

STREAM FG13
   SUBSTREAM MIXED TEMP=185.5 PRES=1.018
   MOLE-FLOW H2O 7532.797 / N2 63451.53 / O2 10079.06 /  &
      CO2 3635.592 / AR 729.3649 / CH4 1.4295E-023 / C2H6  &
      0. / C3H8 0. / NBUTANE 0. / NPENTANE 0.

STREAM FG14
   SUBSTREAM MIXED TEMP=151.8 PRES=1.015
   MOLE-FLOW H2O 7532.797 / N2 63451.53 / O2 10079.06 /  &
      CO2 3635.592 / AR 729.3649 / CH4 1.4295E-023 / C2H6  &
      0. / C3H8 0. / NBUTANE 0. / NPENTANE 0.

STREAM FUEL-NG
```

```
   SUBSTREAM MIXED TEMP=116.7 PRES=30.43 MASS-FLOW=59.86
   MOLE-FRAC N2 0.0089 / CO2 0.02 / CH4 0.89 / C2H6 0.07 / &
      C3H8 0.01 / NBUTANE 0.001 / NPENTANE 0.0001

STREAM FUEL-NG0
   SUBSTREAM MIXED TEMP=9. PRES=30.43 MASS-FLOW=59.86
   MOLE-FRAC N2 0.0089 / CO2 0.02 / CH4 0.89 / C2H6 0.07 / &
      C3H8 0.01 / NBUTANE 0.001 / NPENTANE 0.0001

STREAM GT-FG
   SUBSTREAM MIXED TEMP=639.8 PRES=1.046 MASS-FLOW=2424.86
   MOLE-FLOW H2O 7532.797 / N2 63451.53 / O2 10079.06 /  &
      CO2 3635.592 / AR 729.3649 / CH4 1.4295E-023 / C2H6  &
      0. / C3H8 0. / NBUTANE 0. / NPENTANE 0.

STREAM HPBO
   SUBSTREAM MIXED PRES=178.7 VFRAC=1. MASS-FLOW=314.4
   MASS-FRAC H2O 1.

STREAM HPE1IN
   SUBSTREAM MIXED TEMP=258.5 PRES=184.1 MASS-FLOW=314.4
   MASS-FRAC H2O 1.

STREAM HPE1O
   SUBSTREAM MIXED TEMP=320.7 PRES=181. MASS-FLOW=314.4
   MASS-FRAC H2O 1.

STREAM HPIP-BYP
   SUBSTREAM MIXED TEMP=266.8 PRES=3.75 MASS-FLOW=6.51
   MOLE-FRAC H2O 1.

STREAM HPS1O
   SUBSTREAM MIXED TEMP=501.7 PRES=174.3 MASS-FLOW=314.4
   MASS-FRAC H2O 1.

STREAM HPT-IN
   SUBSTREAM MIXED TEMP=600. PRES=170. MASS-FLOW=304.1
   MOLE-FRAC H2O 1.

STREAM IPBI
   SUBSTREAM MIXED TEMP=253.9 PRES=43.85 MASS-FLOW=40.71
   MASS-FRAC H2O 1.

STREAM IPBO
   SUBSTREAM MIXED PRES=43.85 VFRAC=1. MASS-FLOW=40.71
   MASS-FRAC H2O 1.

STREAM IPT-IN
   SUBSTREAM MIXED TEMP=600.2 PRES=40.02 MASS-FLOW=344.81
   MOLE-FRAC H2O 1.

STREAM LPEI-RTN
   SUBSTREAM MIXED TEMP=40.4 PRES=3.989 MASS-FLOW=442.
   MASS-FRAC H2O 1.

STREAM LPT-IN
   SUBSTREAM MIXED TEMP=266.8 PRES=3.75 MASS-FLOW=204.5
   MOLE-FRAC H2O 1.

STREAM RH1I
   SUBSTREAM MIXED TEMP=384.1 PRES=43.63 MASS-FLOW=344.81
   MASS-FRAC H2O 1.

DEF-STREAMS WORK GTCOMP-W

DEF-STREAMS WORK S4

DEF-STREAMS WORK W-1ST

DEF-STREAMS WORK W-2GT

DEF-STREAMS WORK W-2PUMP
```

```
DEF-STREAMS WORK W-CPUMP

DEF-STREAMS WORK W-GROSS

DEF-STREAMS WORK W-GT

DEF-STREAMS WORK W-HPPUMP

DEF-STREAMS WORK W-IPPUMP

DEF-STREAMS WORK W-LPPUMP

DEF-STREAMS WORK W-PUMP

DEF-STREAMS WORK W-ST

DEF-STREAMS WORK WORK1

DEF-STREAMS WORK WORK2

BLOCK B1 MIXER

BLOCK B2 MIXER

BLOCK COND-MIX MIXER
   PARAM
   PROPERTIES STEAMNBS FREE-WATER=STEAMNBS SOLU-WATER=3  &
      TRUE-COMPS=YES

BLOCK DE-SH-MX MIXER
   PARAM
   PROPERTIES STEAMNBS FREE-WATER=STEAMNBS SOLU-WATER=3  &
      TRUE-COMPS=YES

BLOCK PCC-MIX MIXER
   PARAM
   PROPERTIES STEAMNBS FREE-WATER=STEAMNBS SOLU-WATER=3  &
      TRUE-COMPS=YES

BLOCK PCC-MX MIXER
   PARAM
   PROPERTIES STEAMNBS FREE-WATER=STEAMNBS SOLU-WATER=3  &
      TRUE-COMPS=YES

BLOCK RH-MIX MIXER
   PARAM
   PROPERTIES STEAMNBS FREE-WATER=STEAMNBS SOLU-WATER=3  &
      TRUE-COMPS=YES

BLOCK DE-SH-SP FSPLIT
   MASS-FLOW DE-SH 32.48
   PROPERTIES STEAMNBS FREE-WATER=STEAMNBS SOLU-WATER=3  &
      TRUE-COMPS=YES

BLOCK HPT-SPLT FSPLIT
   MASS-FLOW HPT-DVT 10.3
   PROPERTIES STEAMNBS FREE-WATER=STEAMNBS SOLU-WATER=3  &
      TRUE-COMPS=YES

BLOCK IP-SPLT FSPLIT
   MASS-FLOW IPBI 40.71 / PRH-IN 15.01
   PROPERTIES STEAMNBS FREE-WATER=STEAMNBS SOLU-WATER=3  &
      TRUE-COMPS=YES

BLOCK LP-SPLT FSPLIT
   PARAM NPHASE=2
   MASS-FLOW LPBI 40.23
   PROPERTIES STEAMNBS FREE-WATER=STEAMNBS SOLU-WATER=3  &
      TRUE-COMPS=YES
   BLOCK-OPTION FREE-WATER=NO

BLOCK PCC-DVT FSPLIT
   FRAC PCC-STM2 0.8
```

```
BLOCK FUEL-PHC HEATER
   PARAM TEMP=116.7 PRES=30.43

BLOCK FUEL-PHH HEATER
   PARAM PRES=41.5 DUTY=4202.2
   PROPERTIES STEAMNBS FREE-WATER=STEAMNBS SOLU-WATER=3  &
      TRUE-COMPS=YES

BLOCK PCC HEATER
   PARAM TEMP=56.98 PRES=3.34
   PROPERTIES STEAMNBS FREE-WATER=STEAMNBS SOLU-WATER=3  &
      TRUE-COMPS=YES

BLOCK CONDENSO HEATX
   PARAM CALC-TYPE=SIMULATION AREA=12245.4432 <sqm>  &
      PRES-COLD=1.656 U-OPTION=POWER-LAW F-OPTION=CONSTANT  &
      CALC-METHOD=SHORTCUT
   FEEDS HOT=COND-IN COLD=CWIN
   OUTLETS-HOT COND-OUT
   OUTLETS-COLD CWOUT
   HEAT-TR-COEF REF-SIDE=HOT-COLD MOLE-HRFLOW=22753.51  &
      MOLE-CRFLOW=2315810. REF-VALUE=2000.
   PROPERTIES STEAMNBS FREE-WATER=STEAMNBS SOLU-WATER=3  &
      TRUE-COMPS=YES / STEAMNBS FREE-WATER=STEAMNBS  &
      SOLU-WATER=3 TRUE-COMPS=YES
   HOT-SIDE DP-OPTION=CONSTANT
   COLD-SIDE DP-OPTION=CONSTANT

BLOCK HPB HEATX
   PARAM VFRAC-COLD=1. CALC-TYPE=DESIGN U-OPTION=PHASE  &
      F-OPTION=CONSTANT CALC-METHOD=SHORTCUT
   FEEDS HOT=FG6 COLD=HPE2O
   OUTLETS-HOT FG7
   OUTLETS-COLD HPBO
   PROPERTIES PR-BM FREE-WATER=STEAMNBS SOLU-WATER=3  &
      TRUE-COMPS=YES / STEAMNBS FREE-WATER=STEAMNBS  &
      SOLU-WATER=3 TRUE-COMPS=YES
   HOT-SIDE DP-OPTION=CONSTANT
   COLD-SIDE DP-OPTION=CONSTANT

BLOCK HPE1 HEATX
   PARAM T-COLD=320.7 CALC-TYPE=DESIGN PRES-HOT=1.022  &
      PRES-COLD=181. U-OPTION=PHASE F-OPTION=CONSTANT  &
      CALC-METHOD=SHORTCUT
   FEEDS HOT=FG10 COLD=HPE1IN
   OUTLETS-HOT FG11
   OUTLETS-COLD HPE1O
   PROPERTIES PR-BM FREE-WATER=STEAMNBS SOLU-WATER=3  &
      TRUE-COMPS=YES / STEAMNBS FREE-WATER=STEAMNBS  &
      SOLU-WATER=3 TRUE-COMPS=YES
   HOT-SIDE DP-OPTION=CONSTANT
   COLD-SIDE DP-OPTION=CONSTANT

BLOCK HPE2 HEATX
   PARAM T-COLD=355.4 CALC-TYPE=DESIGN PRES-HOT=1.032  &
      PRES-COLD=178.7 U-OPTION=PHASE F-OPTION=CONSTANT  &
      CALC-METHOD=SHORTCUT
   FEEDS HOT=FG7 COLD=HPE1O
   OUTLETS-HOT FG8
   OUTLETS-COLD HPE2O
   PROPERTIES PR-BM FREE-WATER=STEAMNBS SOLU-WATER=3  &
      TRUE-COMPS=YES / STEAMNBS FREE-WATER=STEAMNBS  &
      SOLU-WATER=3 TRUE-COMPS=YES
   HOT-SIDE DP-OPTION=CONSTANT
   COLD-SIDE DP-OPTION=CONSTANT

BLOCK HPS1 HEATX
   PARAM T-COLD=501.7 CALC-TYPE=DESIGN PRES-HOT=1.034  &
      PRES-COLD=174.3 U-OPTION=PHASE F-OPTION=CONSTANT  &
      CALC-METHOD=SHORTCUT
   FEEDS HOT=FG5 COLD=HPBO
   OUTLETS-HOT FG6
```

```
   OUTLETS-COLD HPS1O
   PROPERTIES PR-BM FREE-WATER=STEAMNBS SOLU-WATER=3 &
      TRUE-COMPS=YES / STEAMNBS FREE-WATER=STEAMNBS &
      SOLU-WATER=3 TRUE-COMPS=YES
   HOT-SIDE DP-OPTION=CONSTANT
   COLD-SIDE DP-OPTION=CONSTANT DPPARMOPT=YES

BLOCK HPS2 HEATX
   PARAM T-COLD=557.1 CALC-TYPE=DESIGN PRES-HOT=1.039 &
      PRES-COLD=173.5 U-OPTION=PHASE F-OPTION=CONSTANT &
      CALC-METHOD=SHORTCUT
   FEEDS HOT=FG3 COLD=HPS1O
   OUTLETS-HOT FG4
   OUTLETS-COLD HPS2O
   PROPERTIES PR-BM FREE-WATER=STEAMNBS SOLU-WATER=3 &
      TRUE-COMPS=YES / STEAMNBS FREE-WATER=STEAMNBS &
      SOLU-WATER=3 TRUE-COMPS=YES
   HOT-SIDE DP-OPTION=CONSTANT
   COLD-SIDE DP-OPTION=CONSTANT

BLOCK HPS3 HEATX
   PARAM T-COLD=600.9 CALC-TYPE=DESIGN PRES-HOT=1.044 &
      PRES-COLD=172.7 U-OPTION=PHASE F-OPTION=CONSTANT &
      CALC-METHOD=SHORTCUT
   FEEDS HOT=GT-FG COLD=HPS2O
   OUTLETS-HOT FG2
   OUTLETS-COLD HPS3O
   PROPERTIES PR-BM FREE-WATER=STEAMNBS SOLU-WATER=3 &
      TRUE-COMPS=YES / STEAMNBS FREE-WATER=STEAMNBS &
      SOLU-WATER=3 TRUE-COMPS=YES
   HOT-SIDE DP-OPTION=CONSTANT
   COLD-SIDE DP-OPTION=CONSTANT

BLOCK IPB HEATX
   PARAM VFRAC-COLD=1. CALC-TYPE=DESIGN PRES-HOT=1.02 &
      U-OPTION=PHASE F-OPTION=CONSTANT CALC-METHOD=SHORTCUT
   FEEDS HOT=FG11 COLD=IPBI
   OUTLETS-HOT FG12
   OUTLETS-COLD IPBO
   PROPERTIES PR-BM FREE-WATER=STEAMNBS SOLU-WATER=3 &
      TRUE-COMPS=YES / STEAMNBS FREE-WATER=STEAMNBS &
      SOLU-WATER=3 TRUE-COMPS=YES
   HOT-SIDE DP-OPTION=CONSTANT
   COLD-SIDE DP-OPTION=CONSTANT

BLOCK IPE HEATX
   PARAM T-COLD=253.9 CALC-TYPE=DESIGN PRES-HOT=1.018 &
      PRES-COLD=43.85 U-OPTION=PHASE F-OPTION=CONSTANT &
      CALC-METHOD=SHORTCUT
   FEEDS HOT=FG12 COLD=IPEI
   OUTLETS-HOT FG13
   OUTLETS-COLD IPEO
   PROPERTIES PR-BM FREE-WATER=STEAMNBS SOLU-WATER=3 &
      TRUE-COMPS=YES / STEAMNBS FREE-WATER=STEAMNBS &
      SOLU-WATER=3 TRUE-COMPS=YES
   HOT-SIDE DP-OPTION=CONSTANT
   COLD-SIDE DP-OPTION=CONSTANT

BLOCK IPS HEATX
   PARAM T-COLD=317.9 CALC-TYPE=DESIGN PRES-HOT=1.027 &
      PRES-COLD=43.63 U-OPTION=PHASE F-OPTION=CONSTANT &
      CALC-METHOD=SHORTCUT
   FEEDS HOT=FG8 COLD=IPBO
   OUTLETS-HOT FG9
   OUTLETS-COLD IPSO
   PROPERTIES PR-BM FREE-WATER=STEAMNBS SOLU-WATER=3 &
      TRUE-COMPS=YES / STEAMNBS FREE-WATER=STEAMNBS &
      SOLU-WATER=3 TRUE-COMPS=YES
   HOT-SIDE DP-OPTION=CONSTANT
   COLD-SIDE DP-OPTION=CONSTANT

BLOCK LPB HEATX
   PARAM VFRAC-COLD=1. CALC-TYPE=DESIGN PRES-HOT=1.015 &
```

```
      U-OPTION=PHASE F-OPTION=CONSTANT CALC-METHOD=SHORTCUT
   FEEDS HOT=FG13 COLD=LPBI
   OUTLETS-HOT FG14
   OUTLETS-COLD LPBO
   PROPERTIES PR-BM FREE-WATER=STEAMNBS SOLU-WATER=3  &
      TRUE-COMPS=YES / STEAMNBS FREE-WATER=STEAMNBS  &
      SOLU-WATER=3 TRUE-COMPS=YES
   HOT-SIDE DP-OPTION=CONSTANT
   COLD-SIDE DP-OPTION=CONSTANT

BLOCK LPE HEATX
   PARAM T-COLD=131.5 CALC-TYPE=DESIGN PRES-HOT=1.013  &
      PRES-COLD=3.8 U-OPTION=POWER-LAW F-OPTION=CONSTANT  &
      CALC-METHOD=SHORTCUT
   FEEDS HOT=FG14 COLD=LPEI-RTN
   OUTLETS-HOT FG15
   OUTLETS-COLD LPEO
   HEAT-TR-COEF REF-SIDE=HOT-COLD MOLE-HRFLOW=82935.59  &
      MOLE-CRFLOW=22503.12 REF-VALUE=50.
   PROPERTIES PR-BM FREE-WATER=STEAMNBS SOLU-WATER=3  &
      TRUE-COMPS=YES / STEAMNBS FREE-WATER=STEAMNBS  &
      SOLU-WATER=3 TRUE-COMPS=YES
   HOT-SIDE DP-OPTION=CONSTANT
   COLD-SIDE DP-OPTION=CONSTANT

BLOCK LPS HEATX
   PARAM T-COLD=297.2 CALC-TYPE=DESIGN PRES-HOT=1.025  &
      PRES-COLD=3.75 U-OPTION=PHASE F-OPTION=CONSTANT  &
      CALC-METHOD=SHORTCUT
   FEEDS HOT=FG9 COLD=LPBO
   OUTLETS-HOT FG10
   OUTLETS-COLD LPSO
   PROPERTIES PR-BM FREE-WATER=STEAMNBS SOLU-WATER=3  &
      TRUE-COMPS=YES / STEAMNBS FREE-WATER=STEAMNBS  &
      SOLU-WATER=3 TRUE-COMPS=YES
   HOT-SIDE DP-OPTION=CONSTANT
   COLD-SIDE DP-OPTION=CONSTANT

BLOCK RH1 HEATX
   PARAM T-COLD=538.5 CALC-TYPE=DESIGN PRES-HOT=1.037  &
      PRES-COLD=41.885 U-OPTION=PHASE F-OPTION=CONSTANT  &
      CALC-METHOD=SHORTCUT
   FEEDS HOT=FG4 COLD=RH1I
   OUTLETS-HOT FG5
   OUTLETS-COLD RH1O
   PROPERTIES PR-BM FREE-WATER=STEAMNBS SOLU-WATER=3  &
      TRUE-COMPS=YES / STEAMNBS FREE-WATER=STEAMNBS  &
      SOLU-WATER=3 TRUE-COMPS=YES
   HOT-SIDE DP-OPTION=CONSTANT
   COLD-SIDE DP-OPTION=CONSTANT

BLOCK RH2 HEATX
   PARAM T-COLD=600.5 CALC-TYPE=DESIGN PRES-HOT=1.041  &
      PRES-COLD=40.77 U-OPTION=PHASE F-OPTION=CONSTANT  &
      CALC-METHOD=SHORTCUT
   FEEDS HOT=FG2 COLD=RH1O
   OUTLETS-HOT FG3
   OUTLETS-COLD RH2O
   PROPERTIES PR-BM FREE-WATER=STEAMNBS SOLU-WATER=3  &
      TRUE-COMPS=YES / STEAMNBS FREE-WATER=STEAMNBS  &
      SOLU-WATER=3 TRUE-COMPS=YES
   HOT-SIDE DP-OPTION=CONSTANT
   COLD-SIDE DP-OPTION=CONSTANT

BLOCK GT-COMB RGIBBS
   PARAM PRES=-0.9 DUTY=0.

BLOCK CND-PUMP PUMP
   PARAM PRES=3.989 EFF=0.6
   PROPERTIES STEAMNBS FREE-WATER=STEAMNBS SOLU-WATER=3  &
      TRUE-COMPS=YES

BLOCK CW-PUMP PUMP
```

```
   PARAM PRES=3.06 EFF=0.6
   PROPERTIES STEAMNBS FREE-WATER=STEAMNBS SOLU-WATER=3  &
      TRUE-COMPS=YES

BLOCK HP-PUMP PUMP
   PARAM PRES=184.1 EFF=0.66
   PROPERTIES STEAMNBS FREE-WATER=STEAMNBS SOLU-WATER=3  &
      TRUE-COMPS=YES

BLOCK IP-PUMP PUMP
   PARAM PRES=45.67 EFF=0.6
   PROPERTIES STEAMNBS FREE-WATER=STEAMNBS SOLU-WATER=3  &
      TRUE-COMPS=YES

BLOCK LP-PUMP PUMP
   PARAM PRES=3.921 EFF=0.6
   PROPERTIES STEAMNBS FREE-WATER=STEAMNBS SOLU-WATER=3  &
      TRUE-COMPS=YES

BLOCK PCC-PUMP PUMP
   PARAM PRES=3.989 EFF=0.6
   PROPERTIES STEAMNBS FREE-WATER=STEAMNBS SOLU-WATER=3  &
      TRUE-COMPS=YES

BLOCK GT-COMP COMPR
   PARAM TYPE=ISENTROPIC PRES=18.583 SEFF=0.85

BLOCK GT-TURB COMPR
   PARAM TYPE=ISENTROPIC PRES=1.046 SEFF=0.8926  &
      MODEL-TYPE=TURBINE

BLOCK HPT COMPR
   PARAM TYPE=ISENTROPIC PRES=45.19 SEFF=0.877  &
      MODEL-TYPE=TURBINE
   PROPERTIES STEAMNBS FREE-WATER=STEAMNBS SOLU-WATER=3  &
      TRUE-COMPS=YES

BLOCK IPT COMPR
   PARAM TYPE=ISENTROPIC PRES=3.75 SEFF=0.9244  &
      MODEL-TYPE=TURBINE
   PROPERTIES STEAMNBS FREE-WATER=STEAMNBS SOLU-WATER=3  &
      TRUE-COMPS=YES

BLOCK LPT COMPR
   PARAM TYPE=ISENTROPIC PRES=0.0264 SEFF=0.9048 NPHASE=2  &
      MODEL-TYPE=TURBINE
   PROPERTIES STEAMNBS FREE-WATER=STEAMNBS SOLU-WATER=3  &
      TRUE-COMPS=YES
   BLOCK-OPTION FREE-WATER=NO

BLOCK 1ST MULT
   PARAM FACTOR=1.

BLOCK 2GTS MULT
   PARAM FACTOR=2.

BLOCK 2HRSGS MULT
   PARAM FACTOR=2.

BLOCK DE-SH-V VALVE
   PARAM P-OUT=3.74
   PROPERTIES STEAMNBS FREE-WATER=STEAMNBS SOLU-WATER=3  &
      TRUE-COMPS=YES

BLOCK HPTV VALVE
   PARAM P-OUT=170.
   PROPERTIES STEAMNBS FREE-WATER=STEAMNBS SOLU-WATER=3  &
      TRUE-COMPS=YES

BLOCK IPTV VALVE
   PARAM P-OUT=40.02
   PROPERTIES STEAMNBS FREE-WATER=STEAMNBS SOLU-WATER=3  &
      TRUE-COMPS=YES
```

```
BLOCK LPTV VALVE
   PARAM P-OUT=3.75
   PROPERTIES STEAMNBS FREE-WATER=STEAMNBS SOLU-WATER=3  &
      TRUE-COMPS=YES

BLOCK PRH-V VALVE
   PARAM P-OUT=0.0381

BLOCK RHV VALVE
   PARAM P-OUT=43.63
   PROPERTIES STEAMNBS FREE-WATER=STEAMNBS SOLU-WATER=3  &
      TRUE-COMPS=YES

DESIGN-SPEC COND-P
   DEFINE SATURATI BLOCK-VAR BLOCK=CONDENSO VARIABLE=DEGSUB-HOT  &
      SENTENCE=PARAM
   SPEC "SATURATI" TO "0"
   TOL-SPEC "0.001"
   VARY BLOCK-VAR BLOCK=LPT VARIABLE=PRES SENTENCE=PARAM
   LIMITS "0.005" "0.02" STEP-SIZE=0.0001 MAX-STEP-SIZ=0.001

DESIGN-SPEC STOD-OUT
   DEFINE KLP PARAMETER 1 PHYS-QTY=DIMENSIONLES UOM="Unitless"  &
      INIT-VAL=21902349.9
   SPEC "KLP" TO "27035906.7"
   TOL-SPEC "5000"
   VARY BLOCK-VAR BLOCK=LPTV VARIABLE=P-OUT SENTENCE=PARAM
   LIMITS "0.5" "3.75" STEP-SIZE=0.1 MAX-STEP-SIZ=0.1

EO-CONV-OPTI

CALCULATOR STODOLA
   DEFINE PLPIN STREAM-VAR STREAM=LPT-IN SUBSTREAM=MIXED  &
      VARIABLE=PRES
   DEFINE DLPIN STREAM-VAR STREAM=LPT-IN SUBSTREAM=MIXED  &
      VARIABLE=MASS-DENSITY
   DEFINE PLPOUT STREAM-VAR STREAM=LPT-OUT SUBSTREAM=MIXED  &
      VARIABLE=PRES
   DEFINE MLPIN STREAM-VAR STREAM=LPT-IN SUBSTREAM=MIXED  &
      VARIABLE=MASS-FLOW
   DEFINE KLP PARAMETER 1 PHYS-QTY=DIMENSIONLES UOM="Unitless"
C Stodolas constant for LP steam turbine
F     A = PLPIN * DLPIN
F     B = (PLPOUT ** 2) * DLPIN / PLPIN
F     KLP = (MLPIN ** 2) / (A - B)
C Stodolas constant for IP steam turbine
C      A2 = PIPIN * DIPIN
C      B2 = (PIPOUT ** 2) * DIPIN / PIPIN
C      KIP = (MIPIN ** 2) / (A2 - B2)
C Stodolas constant for HP steam turbine
C      A3 = PHPIN * DHPIN
C      B3 = (PHPOUT ** 2) * DHPIN / PHPIN
C      KHP = (MHPIN ** 2) / (A3 - B3)
   READ-VARS DLPIN PLPOUT MLPIN PLPIN
   WRITE-VARS KLP

STREAM-REPOR MOLEFLOW
```

CAPTURE PLANT AND COMPRESSION TRAIN

```
IN-UNITS SI ENERGY=kcal ENTHALPY-FLO=kW POWER=kW PRESSURE=bar  &
      TEMPERATURE=C DELTA-T=C ELEC-POWER=kW WORK=kJ  &
      PDROP-PER-HT='mbar/m' PDROP=bar INVERSE-PRES='1/bar'

DEF-STREAMS CONVEN ALL

DIAGNOSTICS
   HISTORY STREAM-LEVEL=4
   TERMINAL STREAM-LEVEL=4
```

```
SIM-OPTIONS MASS-BAL-CHE=YES FLASH-TOL=0.0001 NPHASE=2  &
      ATM-PRES=1.013250000 PARADIGM=SM GAMUS-BASIS=AQUEOUS

DATABANKS 'APV80 PURE22' / 'APV80 AQUEOUS' / 'APV80 SOLIDS' /  &
      'APV80 INORGANIC' / 'APV80 PURE20' / NOASPENPCD

PROP-SOURCES 'APV80 PURE22' / 'APV80 AQUEOUS' / 'APV80 SOLIDS' &
       / 'APV80 INORGANIC' / 'APV80 PURE20'

COMPONENTS
   H2O H2O /
   N2 N2 /
   O2 O2 /
   CO2 CO2 /
   AR AR /
   MEA C2H7NO /
   MEAH+ C2H8NO+ /
   MEACOO- C3H6NO3- /
   HCO3- HCO3- /
   CO3-2 CO3-2 /
   H3O+ H3O+ /
   OH- OH- /
   H2S H2S /
   HS- HS- /
   S-2 S-2

ADA-SETUP
   ADA-SETUP PROCEDURE=REL9

HENRY-COMPS MEA CO2 N2 O2 H2S

SOLVE
   RUN-MODE MODE=SIM

CHEMISTRY MEA
   STOIC 1 H2O -2. / H3O+ 1. / OH- 1.
   STOIC 2 CO2 -1. / H2O -2. / HCO3- 1. / H3O+ 1.
   STOIC 3 HCO3- -1. / H2O -1. / CO3-2 1. / H3O+ 1.
   STOIC 4 MEAH+ -1. / H2O -1. / MEA 1. / H3O+ 1.
   STOIC 5 MEACOO- -1. / H2O -1. / MEA 1. / HCO3- 1.
   K-STOIC 1 A=132.89888 B=-13445.9 C=-22.4773
   K-STOIC 2 A=231.465439 B=-12092.1 C=-36.7816
   K-STOIC 3 A=216.05043 B=-12431.7 C=-35.4819
   K-STOIC 4 A=-3.038325 B=-7008.357 D=-0.0031348
   K-STOIC 5 A=-0.52135 B=-2545.53

FLOWSHEET COMP
   BLOCK C-VALVE IN=CO2-3 OUT=CO2-4
   BLOCK CO2SPLIT IN=CO2-6 OUT=CO2-7 SURGE

FLOWSHEET PCC
   BLOCK PUMP-2 IN=LEAN-1B OUT=LEAN-1 WLEANP
   BLOCK REBOILER IN=STEAM-4 BOTTOM-1 OUT=RBCOND-1 BOTTOM-2
   BLOCK B-DRUM IN=BOTTOM-2 OUT=BOILUP LEAN-1B
   BLOCK STRIPPER IN=BOILUP REFLUX RICH-3 OUT=CO2-1 BOTTOM-1
   BLOCK PUMP IN=RICH-1 WRICH OUT=RICH-2 WRICHP
   BLOCK ABSORBER IN=LEAN-4 FGAS-7 OUT=FGAS-9 RICH-1
   BLOCK WASH IN=FGAS-9 WMAKE OUT=FGAS-10 KOWASH CD-10
   BLOCK LRHX IN=LEAN-1 RICH-2 OUT=LEAN-2 RICH-3
   BLOCK C-DRUM IN=CO2-2 OUT=CO2-3 REFLUX
   BLOCK COOLER2 IN=LEAN-2 KOWASH OUT=LEAN-3 CD-9
   BLOCK BLOWER IN=FGAS-6 OUT=FGAS-8 WFAN
   BLOCK PC-COND IN=CO2-1 OUT=CO2-2 CD-8
   BLOCK DCC IN=FGAS-8 OUT=FGAS-7 WASTE
   BLOCK PCCSPLIT IN=FGAS-1 OUT=FGAS-2 FGAS-6
   BLOCK D-2X IN=FGAS-10 OUT=FGAS-11
   BLOCK S-DRUM IN=WCO2-4 SURGE OUT=CO2-5 KOWATER7

FLOWSHEET SC
   BLOCK AUXILIAR IN=WCONDP WFAN WRICHP WLEANP WWCOMPT OUT= &
      WAUX-1
   BLOCK PCHEAT-2 IN=STEAM-1 OUT=STEAM-3
```

```
   BLOCK FSSPLIT IN=STEAM-3 OUT=STEAM-5 STEAM-4
   BLOCK PC-PUMP IN=RBCOND-1 OUT=RBCOND-2 WCONDP
   BLOCK AUX-2X IN=WAUX-1 OUT=AUX
   BLOCK CWDUTY IN=CD-5 CD-4 CD-3 CD-2 CD-1 CD-10 CD-9  &
      CD-8 CD-6 OUT=CD-TOTAL
   BLOCK B1 IN=CO2-4 OUT=WCO2-4
   BLOCK B2 IN=WCOMPT OUT=WWCOMPT
   BLOCK CO2-COMP IN=CO2-5 OUT=CO2-6 KOWATER5 KOWATER4  &
      KOWATER3 KOWATER2 KOWATER1 CD-5 CD-6 CD-4 CD-3 CD-2  &
      CD-1 WCOMPT

PROPERTIES STEAMNBS TRUE-COMPS=YES
   PROPERTIES ELECNRTL PCC HENRY-COMPS=MEA CHEMISTRY=MEA  &
      FREE-WATER=STEAM-TA SOLU-WATER=3 TRUE-COMPS=YES /  &
      PENG-ROB COMP FREE-WATER=STEAM-TA SOLU-WATER=3  &
      TRUE-COMPS=YES
   PROPERTIES STMNBS2

PROP-REPLACE ELECNRTL ELECNRTL
   MODEL VAQCLK 1 1
   MODEL MUL2JONS 1 1 1 2
   MODEL DL1NST 1 1
   MODEL SIG2ONSG 1 -9 1
   MODEL DL0NST 1 1

DEF-STREAMS CONVEN RICH-3

PROP-SET XAPP XAPP SUBSTREAM=MIXED COMPS=CO2 MEA H2O PHASE=L

STREAM BOILUP
   SUBSTREAM MIXED TEMP=120. PRES=1.9 MASS-FLOW=70.
   MOLE-FRAC H2O 1.

STREAM FGAS-1
   SUBSTREAM MIXED TEMP=98. PRES=1. MASS-FLOW=675.
   MOLE-FRAC H2O 0.0882 / N2 0.7427 / O2 0.118 / CO2  &
      0.0426 / AR 0.0085

STREAM LEAN-4
   SUBSTREAM MIXED TEMP=40. PRES=5. MASS-FLOW=740.
   MOLE-FRAC H2O 0.86 / O2 0. / CO2 0.028 / MEA 0.112

STREAM REFLUX
   SUBSTREAM MIXED TEMP=40. PRES=1.87 MASS-FLOW=20.
   MOLE-FRAC H2O 1.

STREAM RICH-3
   SUBSTREAM MIXED TEMP=115. PRES=5. MOLE-FLOW=44.44444444
   MOLE-FRAC H2O 0.8318 / CO2 0.05 / MEA 0.1182

STREAM STEAM-1
   SUBSTREAM MIXED TEMP=234.40559 PRES=3.74027004  &
      MASS-FLOW=141.5
   MOLE-FRAC H2O 1.

STREAM STEAM-4
   SUBSTREAM MIXED TEMP=133.63 PRES=3. MASS-FLOW=76.
   MASS-FRAC H2O 1.

STREAM WMAKE
   SUBSTREAM MIXED TEMP=25. PRES=1. MASS-FLOW=7.
   MOLE-FRAC H2O 1.

STREAM WRICH
   SUBSTREAM MIXED TEMP=25. PRES=1.03 MASS-FLOW=0.
   MOLE-FLOW H2O 0.82699722 / CO2 0.05567925 / MEA  &
      0.11732073

DEF-STREAMS HEAT CD-1

DEF-STREAMS HEAT CD-2

DEF-STREAMS HEAT CD-3
```

```
DEF-STREAMS HEAT CD-4

DEF-STREAMS HEAT CD-5

DEF-STREAMS HEAT CD-6

DEF-STREAMS HEAT CD-8

DEF-STREAMS HEAT CD-9

DEF-STREAMS HEAT CD-10

DEF-STREAMS HEAT CD-TOTAL

DEF-STREAMS WORK AUX

DEF-STREAMS WORK WAUX-1

DEF-STREAMS WORK WCOMPT

DEF-STREAMS WORK WCONDP

DEF-STREAMS WORK WFAN

DEF-STREAMS WORK WLEANP

DEF-STREAMS WORK WRICHP

DEF-STREAMS WORK WWCOMPT

BLOCK AUXILIAR MIXER

BLOCK CWDUTY MIXER

BLOCK CO2SPLIT FSPLIT
   MASS-FLOW SURGE 1E-005

BLOCK FSSPLIT FSPLIT
   FRAC STEAM-4 0.5

BLOCK PCCSPLIT FSPLIT
   FRAC FGAS-2 0.

BLOCK COOLER2 HEATER
   PARAM TEMP=40. PRES=5.

BLOCK PC-COND HEATER
   PARAM TEMP=40. PRES=0.

BLOCK PCHEAT-2 HEATER
   PARAM DEGSUP=0. DPPARM=0.9

BLOCK B-DRUM FLASH2
   PARAM PRES=0. DUTY=0.

BLOCK C-DRUM FLASH2
   PARAM PRES=0. DUTY=0.

BLOCK DCC FLASH2
   PARAM TEMP=33. PRES=1.063

BLOCK S-DRUM FLASH2
   PARAM PRES=0. DUTY=0.

BLOCK WASH FLASH2
   PARAM TEMP=45. PRES=1. <atm>

BLOCK LRHX HEATX
   PARAM CALC-TYPE=SIMULATION AREA=46790.1221 PRES-HOT=5.3  &
      PRES-COLD=0. U-OPTION=POWER-LAW F-OPTION=CONSTANT  &
      CALC-METHOD=SHORTCUT
   FEEDS HOT=LEAN-1 COLD=RICH-2
```

```
    OUTLETS-HOT LEAN-2
    OUTLETS-COLD RICH-3
    HEAT-TR-COEF REF-SIDE=HOT-COLD MASS-HRFLOW=829.8  &
       MASS-CRFLOW=870.7 REF-VALUE=500.
    HOT-SIDE DP-OPTION=CONSTANT DPPARMOPT=NO
    COLD-SIDE DP-OPTION=CONSTANT

BLOCK REBOILER HEATX
    PARAM CALC-TYPE=SIMULATION AREA=12299.8389 PRES-HOT=3.34  &
       U-OPTION=POWER-LAW F-OPTION=CONSTANT CALC-METHOD=SHORTCUT
    FEEDS HOT=STEAM-4 COLD=BOTTOM-1
    OUTLETS-HOT RBCOND-1
    OUTLETS-COLD BOTTOM-2
    HEAT-TR-COEF REF-SIDE=HOT-COLD MASS-HRFLOW=69.4  &
       MASS-CRFLOW=893.7 REF-VALUE=600.
    PROPERTIES STEAMNBS FREE-WATER=STEAM-TA SOLU-WATER=3  &
       TRUE-COMPS=YES / ELECNRTL HENRY-COMPS=MEA CHEMISTRY=MEA  &
       FREE-WATER=STEAM-TA SOLU-WATER=3 TRUE-COMPS=YES
    HOT-SIDE DP-OPTION=CONSTANT
    COLD-SIDE DP-OPTION=CONSTANT

BLOCK ABSORBER RADFRAC
    PARAM NSTAGE=20 ALGORITHM=STANDARD INIT-OPTION=STANDARD  &
       HYDRAULIC=YES
    COL-CONFIG CONDENSER=NONE REBOILER=NONE
    RATESEP-ENAB CALC-MODE=RIG-RATE
    RATESEP-PARA RS-TOL=1E-005 RS-STABLE-IT=25 RS-MAXIT=50
    FEEDS LEAN-4 1 ON-STAGE / FGAS-7 21
    PRODUCTS FGAS-9 1 V / RICH-1 20 L
    P-SPEC 1 1. <atm>
    COL-SPECS DP-COL=.0400000000
    REAC-STAGES 1 20 MEA-REA
    HOLD-UP 1 20 VOL-LHLDP=0.0075
    T-EST 1 48.33160000 / 2 57.85770000 / 3 65.65550000 /  &
       4 70.43480000 / 5 72.59970000 / 6 73.07790000 / 7  &
       72.58460000 / 8 71.53720000 / 9 70.15710000 / 10  &
       68.09110000 / 11 67.01420000 / 12 65.70310000 / 13  &
       64.24200000 / 14 62.69310000 / 15 60.99060000 / 16  &
       59.10670000 / 17 56.97510000 / 18 54.47390000 / 19  &
       51.38320000 / 20 46.95580000
    L-EST 1 .0261394 / 2 .0265378 / 3 .0268442 / 4  &
       .0269903 / 5 .0269988 / 6 .0269227 / 7 .0268034 /  &
       8 .0266654 / 9 .0265212 / 10 .0264298 / 11  &
       .0263293 / 12 .0262264 / 13 .0261240 / 14 .0260200 /  &
       15 .0259134 / 16 .0258018 / 17 .0256801 / 18  &
       .0255394 / 19 .0253626 / 20 .0251261
    V-EST 1 5.16116E-3 / 2 5.55704E-3 / 3 5.99860E-3 / 4  &
       6.35740E-3 / 5 6.55986E-3 / 6 6.62436E-3 / 7  &
       6.60125E-3 / 8 6.53066E-3 / 9 6.43626E-3 / 10  &
       6.33045E-3 / 11 6.27264E-3 / 12 6.20017E-3 / 13  &
       6.12076E-3 / 14 6.03807E-3 / 15 5.95080E-3 / 16  &
       5.85881E-3 / 17 5.76002E-3 / 18 5.64998E-3 / 19  &
       5.52019E-3 / 20 5.35385E-3
    PACK-SIZE 1 1 20 MELLAPAK VENDOR=SULZER PACK-MAT=STANDARD  &
       PACK-SIZE="250Y" PACK-HT=20. P-UPDATE=NO
    PACK-RATE 1 1 20 MELLAPAK VENDOR=SULZER PACK-MAT=STANDARD  &
       PACK-SIZE="250Y" PACK-HT=20. DIAM=19. P-UPDATE=NO
    PACK-RATE2 1 RATE-BASED=YES LIQ-FILM=DISCRXN VAP-FILM=FILM  &
       MTRFC-CORR=BRF-85 INTFA-CORR=BRF-85  &
       HOLDUP-CORR=STICHLMAIR89 FLOW-MODEL=VPLUG AREA-FACTOR=0.8  &
       NLPOINTS=10 LDISCPT=0.001 0.002 0.003 0.004 0.005  &
       0.006 0.007 0.008 0.009 0.01 BASE-STAGE=20
    REPORT HYDRAULIC
    HTLOSS-SEC SECNO=1 1 1 HTLOSS-SEC=1.465355000 / SECNO=2 2  &
       9 HTLOSS-SEC=.5861421000 / SECNO=3 10 10  &
       HTLOSS-SEC=3.516853000 / SECNO=4 11 13  &
       HTLOSS-SEC=1.025749000 / SECNO=5 14 19  &
       HTLOSS-SEC=1.025749000 / SECNO=6 20 20  &
       HTLOSS-SEC=1.465355000

BLOCK STRIPPER RADFRAC
    PARAM NSTAGE=8 ALGORITHM=NONIDEAL INIT-OPTION=STANDARD  &
       HYDRAULIC=YES
```

```
   COL-CONFIG CONDENSER=NONE REBOILER=NONE
   RATESEP-ENAB CALC-MODE=EQUILIBRIUM
   FEEDS BOILUP 8 ON-STAGE / REFLUX 1 ON-STAGE / RICH-3 2  &
      ON-STAGE
   PRODUCTS BOTTOM-1 8 L / CO2-1 1 V
   P-SPEC 1 1.844
   COL-SPECS DP-COL=0.015
   PACK-SIZE 1 1 7 MELLAPAK VENDOR=SULZER PACK-MAT=STANDARD  &
      PACK-SIZE="250Y" PACK-HT=20. P-UPDATE=NO
   PACK-RATE 1 1 7 MELLAPAK VENDOR=SULZER PACK-MAT=STANDARD  &
      PACK-SIZE="250Y" PACK-HT=20. DIAM=8. P-UPDATE=NO
   REPORT HYDRAULIC

BLOCK PC-PUMP PUMP
   PARAM PRES=5.614 EFF=0.85 DEFF=0.996

BLOCK PUMP PUMP
   PARAM PRES=5.3

BLOCK PUMP-2 PUMP
   PARAM PRES=5.6

BLOCK BLOWER COMPR
   PARAM TYPE=ISENTROPIC DELP=158. <mbar> SEFF=0.85 MEFF=0.996

BLOCK CO2-COMP MCOMPR
   PARAM NSTAGE=6 TYPE=ASME-POLYTROPIC
   FEEDS CO2-5 1
   PRODUCTS CO2-6 6 / KOWATER5 5 L / KOWATER4 4 L /  &
      KOWATER3 3 L / KOWATER2 2 L / KOWATER1 1 L /  &
      CD-5 5 / CD-6 6 / CD-4 4 / CD-3 3 / CD-2 2 /  &
      CD-1 1 / WCOMPT GLOBAL
   COMPR-SPECS 1 MEFF=0.99 / 2 MEFF=0.99 / 3 MEFF=0.99 /  &
      4 MEFF=0.99 / 5 MEFF=0.99 / 6 MEFF=0.99
   COOLER-SPECS 1 TEMP=40. PDROP=20. <mbar> / 2 TEMP=40.  &
      PDROP=40. <mbar> / 3 TEMP=40. PDROP=60. <mbar> / 4  &
      TEMP=40. PDROP=80. <mbar> / 5 TEMP=40. PDROP=100. <mbar> / &
      6 TEMP=60. PDROP=120. <mbar>
   PERFOR-PARAM NCURVES=6 NMAP=6 H-FLOW-VAR=VOL-FLOW H-FLOW-UNIT &
      ="cum/sec" HEAD-UNITS="KJ/KG" HEAD-NPOINT=25  &
      EF-FLOW-VAR="VOL-FLOW" EF-FLOW-UNIT="cum/sec"  &
      EFF-NPOINT=13
   STAGE-DATA STAGE=1 ACT-SH-SPEED=9000. <rpm> MAP=1 / STAGE=2  &
      ACT-SH-SPEED=9000. <rpm> MAP=2 / STAGE=3  &
      ACT-SH-SPEED=9000. <rpm> MAP=3 / STAGE=4  &
      ACT-SH-SPEED=9000. <rpm> MAP=4 / STAGE=5  &
      ACT-SH-SPEED=9000. <rpm> MAP=5 / STAGE=6  &
      ACT-SH-SPEED=9000. <rpm> MAP=6
   SHAFT-SPEED MAP=1 CURVE=1 9000. <rpm> / MAP=1 CURVE=2  &
      11700. <rpm> / MAP=1 CURVE=3 6300. <rpm> / MAP=1  &
      CURVE=4 4500. <rpm> / MAP=1 CURVE=5 2700. <rpm> /  &
      MAP=1 CURVE=6 1800. <rpm> / MAP=2 CURVE=1 9000. <rpm> /  &
      MAP=2 CURVE=2 11700. <rpm> / MAP=2 CURVE=3 6300. <rpm> / &
      MAP=2 CURVE=4 4500. <rpm> / MAP=2 CURVE=5 2700. <rpm> /  &
      MAP=2 CURVE=6 1800. <rpm> / MAP=3 CURVE=1 9000. <rpm> /  &
      MAP=3 CURVE=2 11700. <rpm> / MAP=3 CURVE=3 6300. <rpm> / &
      MAP=3 CURVE=4 4500. <rpm> / MAP=3 CURVE=5 2700. <rpm> /  &
      MAP=3 CURVE=6 1800. <rpm> / MAP=4 CURVE=1 9000. <rpm> /  &
      MAP=4 CURVE=2 11700. <rpm> / MAP=4 CURVE=3 6300. <rpm> / &
      MAP=4 CURVE=4 4500. <rpm> / MAP=4 CURVE=5 2700. <rpm> /  &
      MAP=4 CURVE=6 1800. <rpm> / MAP=5 CURVE=1 9000. <rpm> /  &
      MAP=5 CURVE=2 11700. <rpm> / MAP=5 CURVE=3 6300. <rpm> / &
      MAP=5 CURVE=4 4500. <rpm> / MAP=5 CURVE=5 2700. <rpm> /  &
      MAP=5 CURVE=6 1800. <rpm> / MAP=6 CURVE=1 9000. <rpm> /  &
      MAP=6 CURVE=2 11700. <rpm> / MAP=6 CURVE=3 6300. <rpm> / &
      MAP=6 CURVE=4 4500. <rpm> / MAP=6 CURVE=5 2700. <rpm> /  &
      MAP=6 CURVE=6 1800. <rpm>
 PROPERTIES PENG-ROB FREE-WATER=STEAM-TA SOLU-WATER=3  &
      TRUE-COMPS=YES

BLOCK AUX-2X MULT
   PARAM FACTOR=2.
```

```
BLOCK B1 MULT
   PARAM FACTOR=1.

BLOCK B2 MULT
   PARAM FACTOR=1.

BLOCK D-2X MULT
   PARAM FACTOR=2.

BLOCK C-VALVE VALVE
   PARAM P-DROP=0.2

DESIGN-SPEC 90CAP
   DEFINE RCO2 PARAMETER 1 INIT-VAL=0.9
   SPEC "RCO2" TO "0.90"
   TOL-SPEC "0.001"
   VARY STREAM-VAR STREAM=LEAN-4 SUBSTREAM=MIXED  &
      VARIABLE=MASS-FLOW
   LIMITS "500" "1200" STEP-SIZE=0.5 MAX-STEP-SIZ=1.

DESIGN-SPEC LOADBAL
   DEFINE LEANIN PARAMETER 2 INIT-VAL=0.26
   DEFINE LEANOUT PARAMETER 3 INIT-VAL=0.26
   SPEC "LEANOUT" TO "LEANIN"
   TOL-SPEC "0.001"
   VARY BLOCK-VAR BLOCK=STRIPPER VARIABLE=PRES SENTENCE=P-SPEC  &
      ID1=1
   LIMITS "1.75" "2.2" STEP-SIZE=0.01 MAX-STEP-SIZ=0.05

DESIGN-SPEC STEAM
   DEFINE CONDENS STREAM-VAR STREAM=RBCOND-1 SUBSTREAM=MIXED  &
      VARIABLE=VFRAC
   SPEC "CONDENS" TO "0.01"
   TOL-SPEC "0.005"
   VARY STREAM-VAR STREAM=STEAM-1 SUBSTREAM=MIXED  &
      VARIABLE=MASS-FLOW
   LIMITS "50" "400" STEP-SIZE=1.

EO-CONV-OPTI

CALCULATOR LOAD
   DEFINE XCO2 MASS-FLOW STREAM=FGAS-1 SUBSTREAM=MIXED  &
      COMPONENT=CO2
   DEFINE XH2O MASS-FLOW STREAM=FGAS-1 SUBSTREAM=MIXED  &
      COMPONENT=H2O
   DEFINE XN2 MASS-FLOW STREAM=FGAS-1 SUBSTREAM=MIXED  &
      COMPONENT=N2
c Boiler black box model
c Steam flow in ks/s
F     FS = 413.81
c Flue gas calc (FG) error R2=0.9917
c FG = Flue gas kg/s
c XCO2W / XH2OW % weight
c XCO2 / XH2O mass flow kg/s
F     FGAS = 0.8909 * FS + 129.07
F     XCO2W = -0.00002483 * FS * FS + 0.02701 * FS + 13.16
F     XH2OW = -0.000004545 * FS * FS + 0.004945 * FS + 3.038
F     XCO2 = XCO2W / 100 * FGAS
F     XH2O = XH2OW / 100 * FGAS
F     XN2 = (100 - XCO2W - XH2OW) / 100 * FGAS
   WRITE-VARS XCO2 XH2O XN2
   EXECUTE FIRST

CALCULATOR LOADINGS
   DEFINE LEANIN PARAMETER 2 PHYS-QTY=DIMENSIONLES  &
      INIT-VAL=0.2
   DEFINE LEANOUT PARAMETER 3 PHYS-QTY=DIMENSIONLES  &
      INIT-VAL=0.2
   DEFINE CO2I MOLE-FLOW STREAM=LEAN-4 SUBSTREAM=MIXED  &
      COMPONENT=CO2
   DEFINE MEAI MOLE-FLOW STREAM=LEAN-4 SUBSTREAM=MIXED  &
      COMPONENT=MEA
   DEFINE MEAHI MOLE-FLOW STREAM=LEAN-4 SUBSTREAM=MIXED  &
```

```
      COMPONENT=MEAH+
   DEFINE MEACOOI MOLE-FLOW STREAM=LEAN-4 SUBSTREAM=MIXED  &
      COMPONENT=MEACOO-
   DEFINE HCO3I MOLE-FLOW STREAM=LEAN-4 SUBSTREAM=MIXED  &
      COMPONENT=HCO3-
   DEFINE CO32I MOLE-FLOW STREAM=LEAN-4 SUBSTREAM=MIXED  &
      COMPONENT=CO3-2
   DEFINE CO2O MOLE-FLOW STREAM=LEAN-3 SUBSTREAM=MIXED  &
      COMPONENT=CO2
   DEFINE MEAO MOLE-FLOW STREAM=LEAN-3 SUBSTREAM=MIXED  &
      COMPONENT=MEA
   DEFINE MEAHO MOLE-FLOW STREAM=LEAN-3 SUBSTREAM=MIXED  &
      COMPONENT=MEAH+
   DEFINE MEACOOO MOLE-FLOW STREAM=LEAN-3 SUBSTREAM=MIXED  &
      COMPONENT=MEACOO-
   DEFINE HCO3O MOLE-FLOW STREAM=LEAN-3 SUBSTREAM=MIXED  &
      COMPONENT=HCO3-
   DEFINE CO32O MOLE-FLOW STREAM=LEAN-3 SUBSTREAM=MIXED  &
      COMPONENT=CO3-2
   DEFINE AI PARAMETER 10
   DEFINE BI PARAMETER 11
   DEFINE AO PARAMETER 12
   DEFINE BO PARAMETER 13
   DEFINE CO2R MOLE-FLOW STREAM=RICH-1 SUBSTREAM=MIXED  &
      COMPONENT=CO2
   DEFINE MEAR MOLE-FLOW STREAM=RICH-1 SUBSTREAM=MIXED  &
      COMPONENT=MEA
   DEFINE MEAHR MOLE-FLOW STREAM=RICH-1 SUBSTREAM=MIXED  &
      COMPONENT=MEAH+
   DEFINE MEACOOR MOLE-FLOW STREAM=RICH-1 SUBSTREAM=MIXED  &
      COMPONENT=MEACOO-
   DEFINE HCO3OR MOLE-FLOW STREAM=RICH-1 SUBSTREAM=MIXED  &
      COMPONENT=HCO3-
   DEFINE CO32OR MOLE-FLOW STREAM=RICH-1 SUBSTREAM=MIXED  &
      COMPONENT=CO3-2
   DEFINE RICH PARAMETER 14 PHYS-QTY=DIMENSIONLES
   DEFINE AR PARAMETER 15 PHYS-QTY=DIMENSIONLES
   DEFINE BR PARAMETER 16 PHYS-QTY=DIMENSIONLES
F    AI = MEAI + MEAHI + MEACOOI
F    BI = CO2I + HCO3I + CO32I + MEACOOI
F    AO = MEAO + MEAHO + MEACOOO
F    BO = CO2O + HCO3O + CO32O + MEACOOO
F    LEANIN = BI / AI
F    LEANOUT = BO / AO
F    AR = MEAR + MEAHR + MEACOOR
F    BR = CO2R + HCO3R + CO32R + MEACOOR
F    RICH = BR / AR
   READ-VARS CO2I CO2O MEAI MEAO HCO3I HCO3O MEAHI MEACOOI  &
      CO32I MEAHO MEACOOO CO32O CO2R MEAHR MEACOOR MEAR  &
      HCO3OR CO32OR
   WRITE-VARS LEANIN LEANOUT AI BI AO BO RICH BR AR

CALCULATOR RCO2
   DEFINE CO2IN MOLE-FLOW STREAM=FGAS-8 SUBSTREAM=MIXED  &
      COMPONENT=CO2
   DEFINE CO2OUT MOLE-FLOW STREAM=FGAS-9 SUBSTREAM=MIXED  &
      COMPONENT=CO2
   DEFINE RCO2 PARAMETER 1
   DEFINE CO2COMPO MOLE-FLOW STREAM=CO2-7 SUBSTREAM=MIXED  &
      COMPONENT=CO2
   DEFINE RRCO2 PARAMETER 6 PHYS-QTY=DIMENSIONLES
c CO2 recovery calculation
F    RCO2 = 1 - CO2OUT / CO2IN
F    RRCO2 = CO2COMPO / CO2IN
   READ-VARS CO2IN CO2OUT CO2COMPO

CALCULATOR SHAFTS
   DEFINE S1 BLOCK-VAR BLOCK=CO2-COMP VARIABLE=ACT-SH-SPEED  &
      SENTENCE=STAGE-DATA ID1=1
   DEFINE S2 BLOCK-VAR BLOCK=CO2-COMP VARIABLE=ACT-SH-SPEED  &
      SENTENCE=STAGE-DATA ID1=2
   DEFINE S3 BLOCK-VAR BLOCK=CO2-COMP VARIABLE=ACT-SH-SPEED  &
      SENTENCE=STAGE-DATA ID1=3 EO-NAME="ACT-"
```

```
   DEFINE S4 BLOCK-VAR BLOCK=CO2-COMP VARIABLE=ACT-SH-SPEED  &
      SENTENCE=STAGE-DATA ID1=4
   DEFINE S5 BLOCK-VAR BLOCK=CO2-COMP VARIABLE=ACT-SH-SPEED  &
      SENTENCE=STAGE-DATA ID1=5
   DEFINE S6 BLOCK-VAR BLOCK=CO2-COMP VARIABLE=ACT-SH-SPEED  &
      SENTENCE=STAGE-DATA ID1=6
F    S2 = S1
F    S3 = S1
F    S4 = S1
F    S5 = S1
F    S6 = S1
   READ-VARS S1
   WRITE-VARS S2 S3 S4 S5 S6

CALCULATOR WATER
   DEFINE WMAKE STREAM-VAR STREAM=WMAKE SUBSTREAM=MIXED  &
      VARIABLE=MASS-FLOW
   DEFINE WIN MASS-FLOW STREAM=FGAS-6 SUBSTREAM=MIXED  &
      COMPONENT=H2O
   DEFINE WOUT1 MASS-FLOW STREAM=FGAS-10 SUBSTREAM=MIXED  &
      COMPONENT=H2O
   DEFINE WOUT2 MASS-FLOW STREAM=CO2-3 SUBSTREAM=MIXED  &
      COMPONENT=H2O
   DEFINE WOUT3 MASS-FLOW STREAM=WASTE SUBSTREAM=MIXED  &
      COMPONENT=H2O
c water balance
F    WMAKE = WOUT1 + WOUT2 + WOUT3 - WIN
   READ-VARS WIN WOUT1 WOUT2 WOUT3
   WRITE-VARS WMAKE

CONV-OPTIONS
   PARAM TEAR-VAR=YES

CONVERGENCE MEA BROYDEN
   TEAR REFLUX / BOILUP / RICH-3
   PARAM MAXIT=50

REPORT INPUT

STREAM-REPOR MOLEFLOW MASSFRAC PROPERTIES=XAPP

PROPERTY-REP PCES

REACTIONS MEA-REA REAC-DIST
   REAC-DATA 1 DELT=0.0
   REAC-DATA 2 DELT=0.0
   REAC-DATA 3 DELT=0.0
   REAC-DATA 4 KINETIC
   REAC-DATA 5 KINETIC
   REAC-DATA 6 KINETIC
   REAC-DATA 7 KINETIC
   K-STOIC 1 A=-3.038325 B=-7008.357 D=-0.0031348
   K-STOIC 2 A=132.89888 B=-13445.9 C=-22.4773
   K-STOIC 3 A=216.05043 B=-12431.7 C=-35.4819
   RATE-CON 4 PRE-EXP=4.32E+013 ACT-ENERGY=55470913.1
   RATE-CON 5 PRE-EXP=2.38E+017 ACT-ENERGY=1.23305447E+8
   RATE-CON 6 PRE-EXP=97700000000. ACT-ENERGY=4.12642634E+7
   RATE-CON 7 PRE-EXP=2.18E+018 ACT-ENERGY=5.91946531E+7
   STOIC 1 H2O -1. / MEAH+ -1. / MEA 1. / H3O+ 1.
   STOIC 2 H2O -2. / H3O+ 1. / OH- 1.
   STOIC 3 HCO3- -1. / H2O -1. / CO3-2 1. / H3O+ 1.
   STOIC 4 CO2 -1. / OH- -1. / HCO3- 1.
   STOIC 5 HCO3- -1. / CO2 1. / OH- 1.
   STOIC 6 MEA -1. / CO2 -1. / H2O -1. / MEACOO- 1. /  &
      H3O+ 1.
   STOIC 7 MEACOO- -1. / H3O+ -1. / MEA 1. / H2O 1. /  &
      CO2 1.
   POWLAW-EXP 4 CO2 1. / OH- 1.
   POWLAW-EXP 5 HCO3- 1.
   POWLAW-EXP 6 MEA 1. / CO2 1. / H2O 0.
   POWLAW-EXP 7 MEACOO- 1. / H3O+ 1.
```